SOIL EROSION ASSESSMENT IN ALPINE GRASSLANDS USING FALLOUT RADIONUCLIDES: Critical points, solutions and applications

Inauguraldissertation

zur
Erlangung der Würde eines Doktors der Philosophie
vorgelegt der
Philosophisch-Naturwissenschaftlichen Fakultät
der Universität Basel

von

Laura Fausta Arata
Von Italien

Zürich, 2018

Genehmigt von der Philosophisch-Naturwissenschaftlichen Fakultät
auf Antrag von

Prof. Dr. Christine Alewell
Fakultätsverantwortliche / Dissertationsleiterin

Prof. Dr. Markus Egli
Korreferent

Basel, den 13.12.2016

Prof. Dr. Jörg Schibler
Dekan

SUMMARY

Soil erosion processes are one of the main threats to the Alps. They affect slope stability, water budgets, vegetation productivity and the overall biodiversity of the alpine ecosystem. In particular, recent land use and climate changes exacerbated the impact that sheet erosion, a dominant but scarcely visible process, has on alpine grasslands. Yet, the quantitative estimation of the effects of sheet erosion is constrained by the topographic and climatic conditions of the Alps, which hinder the application of conventional assessment techniques. Recently, the use of fallout radionuclides (FRN) as soil erosion tracers showed very promising results in deriving integrated estimates of soil degradation processes affecting alpine soils, over a range of different time scales. Nonetheless, for a correct application of the FRN method, special attention should be paid to three main critical points that are extensively discussed in this thesis, namely: (i) the selection of suitable reference sites; (ii) the selection of the approach (i.e. the traditional approach, the resampling approach, or the repeated sampling approach); and (iii) the selection of the appropriate conversion model.

First, we investigated the suitability of undisturbed reference sites in an alpine valley (Urseren Valley, Canton Uri, Switzerland) for the application of ^{137}Cs, the most commonly used FRN for soil erosion studies. In alpine regions, which are heavily affected by the heterogeneous Chernobyl ^{137}Cs fallout and by high geomorphic and anthropogenic activity, the choice of reference sites is a great challenge. To avoid the uncertainties associated with a wrong selection of reference sites, we have developed and proposed the decision support tool **CheSS**, which allows **Che**cking the **S**uitability of reference **S**ites using a repeated sampling strategy and a decision tree. Comparing the ^{137}Cs inventories of reference sites, which have been sampled in two different periods, enables identifying the sites where no soil disturbance processes have occurred and that can be further used as a stable and reliable basis for the application of the method. Chess also directs particular attention to the analysis of the spatial variability of the ^{137}Cs distribution at the sites. The results of the Chess application to our study area imply that no suitable reference sites could be found.

As a further step, we have tested the application of a ^{137}Cs repeated sampling approach in the Piora Valley (Canton Ticino, Switzerland), where previous studies have failed to identify undisturbed and homogeneous reference sites. The repeated sampling approach facilitates the derivation of short-term soil redistribution rates by comparing the FRN inventories measured at sampling sites in different times, thus

without the need of reference sites. Twelve points located along four transects have been sampled in 2010 and in 2014, and their ^{137}Cs inventory has been compared. The results indicate high soil degradation dynamics, which correspond to a range of yearly soil redistribution rates of 3-36 t ha^{-1}.

At both study areas, the high difficulties associated with the use of ^{137}Cs as tracers (i.e. the extremely high small-scale variability of ^{137}Cs distribution) led us to examine the applicability of $^{239+240}Pu$ (also an artificial FRN), whose presence in the Alps is not connected to the Chernobyl fallout, but mainly to the atmospheric nuclear weapon tests. As a result, its distribution is much more homogeneous compared to ^{137}Cs. $^{239+240}Pu$ is also preferable to ^{137}Cs, because it has a longer half-life and its measurements are more cost- and time-effective. However, the conversion of $^{239+240}Pu$ inventories into soil redistribution rates has been impeded by the fact that the available models are not able to describe the specific behavior of Pu isotopes in the soil, as they are mainly designed for ^{137}Cs.

Consequently, our energy has been directed towards developing a new conversion model, called **MODERN** (**Mo**delling **D**eposition and **E**rosion rates with fallout **R**adio**N**uclides). MODERN is an innovative model based on a single formula that derives both soil erosion and deposition rates. MODERN accurately depicts the soil profile shape of any selected FRN at reference sites and allows the adaptation of the depth profile to simulate the behavior of the FRN under different agro-environmental conditions. A first application of MODERN has been performed on a $^{239+240}Pu$ dataset collected in the Urseren valley. Thanks to its characteristics and its adaptability, MODERN describes the specific depth distribution of Pu isotopes in the soil better than other models. The MODERN code has been developed in Matlab™ and is publically released on the website of our research group. In order to expand its accessibility, the new package *modeRn* has been recently developed using the free and open-source system R. *modeRn* also includes new features that enhance its potential and usability.

This thesis offers a detailed overview of the difficulties associated with the application of FRN in alpine areas. It also presents new, effective, and useful tools that help reduce the sources of uncertainty of the FRN method (CheSS) and promote its application to derive soil redistribution rates at different land use conditions (MODERN). Future studies should focus on using precise and accurate FRN-based estimates to validate large-scale modelling techniques, in order to improve the monitoring and identification of soil erosion risk areas in alpine regions.

TABLE OF CONTENTS

TABLE OF CONTENTS

CHAPTER 1: INTRODUCTION

1.1 Soil erosion in the Alps

The stability of alpine soils is endangered (e.g. Alewell *et al.*, 2015, Bennet *et al.*, 2012, Herman *et al.*, 2013, Mathys *et al.*, 2003, Stoffel and Huggel, 2012). Their vulnerability is determined by different factors. First, the specific topographic and climatic conditions of the Alps limit the development of soil profiles. At steep slopes the runoff continuously transports surface material and compromises the natural process of soil formation (Stanchi *et al.*, 2012). Moreover, due to the typically low temperatures, alpine soils are shallower and less productive in comparison to lowlands (FAO, 2015).

Second, recent land use has strained the already fragile stability of alpine soils. In the last century, alpine grasslands experienced abandonment by both farmers and the local population, as well as the increase of intensive grazing activities (Hinojosa *et al.*, 2016, Stanchi *et al.*, 2013). In particular, remote areas unsuitable for the mechanization of farming were marginalized (Bätzing, 2003). An average of approximately 20% of agricultural land of the Alps (ranging up to 70% in other areas) has been abandoned (MacDonald *et al.*, 2000). The unsustainable management of grassland soils is one of the causes underlying excessive soil loss and the consequent degradation of the soil's physical, chemical, and biological properties (Alewell *et al.*, 2015). As a result, soil losses in the Alps often exceed soil formation, resulting in even shallower and thus less stable soils (Alewell *et al.*, 2015, Morgan, 2009).

Finally, future climate changes might also endanger the stability of alpine soils. In the near future, recurrent extreme events, such as heavy precipitation (snow/rainfall) in mountainous areas, are expected and already observed (Beniston, 2003, Bronstert *et al.*, 2002, Brunetti *et al.*, 2009, Christensen and Christensen, 2003, Christensen and Christensen, 2004, Fuhrer *et al.*, 2006, Kirtman *et al.*, 2013, Parry *et al.*, 2007, Schmidli and Frei, 2005, Stoffel and Huggel, 2012). Those events may trigger shallow landslides and intensify the potential soil erosion risk in the Alps.

Soil degradation in the Alps is the result of different processes that often occur simultaneously and interact with each other (Stanchi *et al.*, 2013). Recent studies show that, above all, sheet erosion is a major degradation process affecting alpine grasslands, as it may cause almost double the soil losses that landslides cause (Meusburger and Alewell, 2008). Sheet erosion is defined as the gradual detachment and transport of single soil grains and aggregates. In the Alps, this is especially enhanced by the reduction of vegetation cover that results from overgrazing and snow processes (snow melting and gliding, wet avalanches)(Meusburger *et al.*, 2014).

Alpine sheet erosion is associated with the irretrievable loss of the basic soil resource and thus has a major impact on water and biogeochemical cycles, biodiversity, and plant primary productivity. In fact, accelerated soil degradation decreases soil fertility and productivity (on-site impacts), making it very hard for re-vegetation processes to take place (Meusburger and Alewell, 2012). Degraded soils are mostly used for grazing activities, which could exacerbate the risks associated with excessive runoff and therefore enhance the possibility of erosion processes (Beniston, 2012). Moreover, sheet erosion increases related environmental pollution and sedimentation problems (off-site impacts), which might affect the overflow of alpine watercourses, leading to an enhanced risk of flooding. Sediments in rivers can also compromise the ecological integrity of the aquatic environment and affect the health, reproduction, and development of aquatic species (Wildhaber *et al.*, 2014). Finally, eroded soils are less stable and more prone to further degradation as a consequence of extreme events, such as landslides and avalanches, which are associated with enormous economic and social costs.

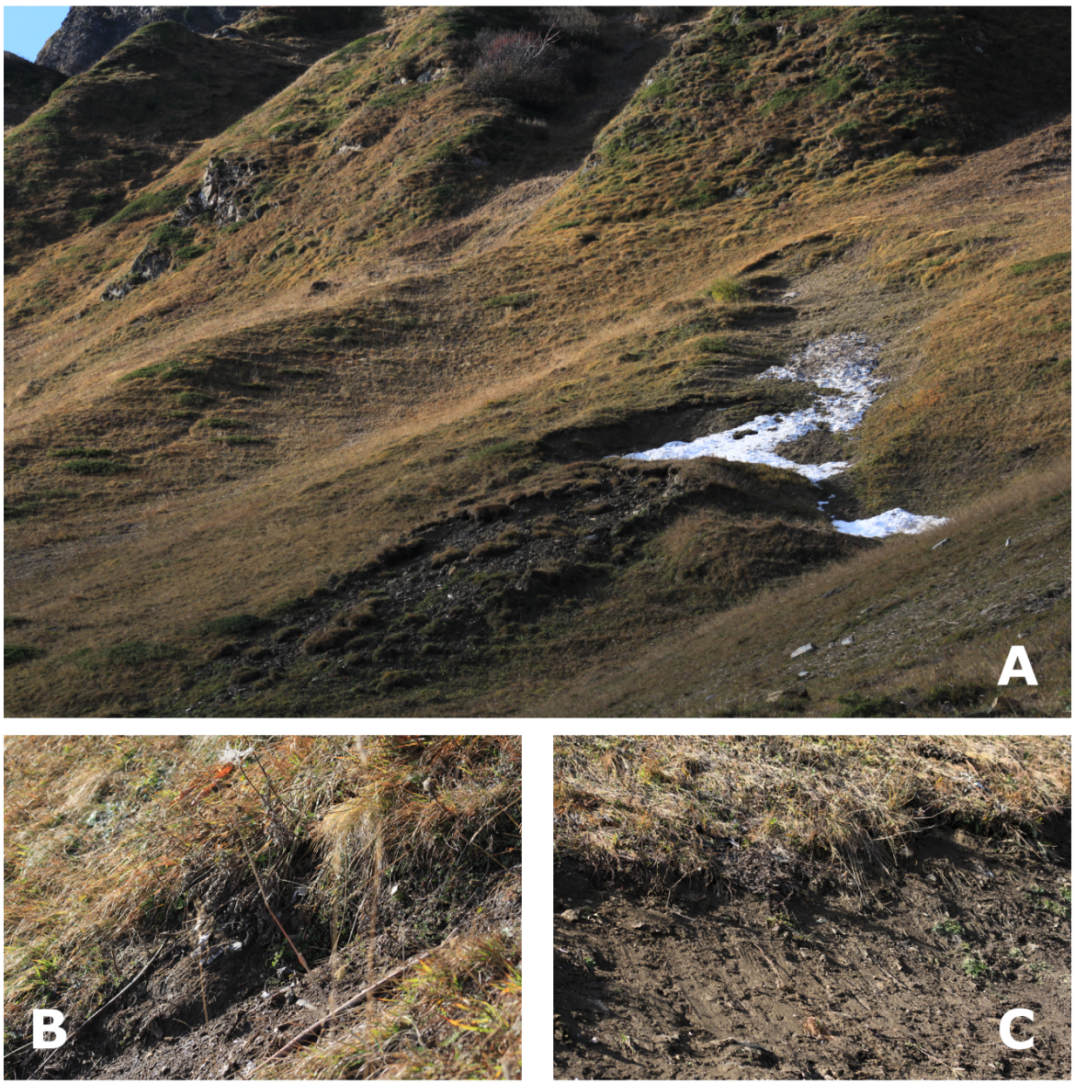

Figure 1-1: Example of an area affected by sheet erosion (A) and details (B and C) in the Piora Valley (Canton Ticino, Switzerland) (October 2013).

To this end, methods to describe and predict the ecosystem stability of alpine systems are necessary (Garcia-Ruiz *et al.*, 1996, Lasanta *et al.*, 2006). Modelling is currently the most popular method for evaluating soil erosion risk (Van Dijk *et al.*, 2005). Soil erosion risk modelling techniques (such as, for example, the Revised Universal Soil Loss Equation (RUSLE) by Wischmeier & Smith, 1978) have the advantage of producing up-scaled maps, which help identify areas with high erosion potential and define specific and efficient resource management practices. To validate the models' outputs, however, information regarding yearly erosion rates is necessary.

In the past years, several efforts have been made to define a methodology to estimate sheet erosion rates in mountainous areas (Alewell *et al.*, 2008, Konz *et al.*, 2012, Meusburger and Alewell, 2014). The inaccessibility and the particularly harsh climatic conditions of alpine slopes hinder the application of techniques conventionally used in lowlands (e.g. sediment traps, rainfall simulations). Moreover, the experimental design of those techniques can irreversibly be damaged by landslides and avalanches (Alewell *et al.*, 2014, 2015, Konz *et al.*, 2012). Conventional methods also have important limitations in terms of the costs involved, their spatial resolution, as well as their potential to provide information regarding long-term soil loss rates (Alewell *et al.*, 2008; Konz *et al.*, 2009; Meusburger and Alewell, 2014). Instead, the application of fallout radionuclides (FRN) as soil tracers shows very promising results and represents the only effective method to estimate sheet erosion in alpine areas (e.g. Alewell *et al.*, 2008, Alewell *et al.*, 2014, Arata *et al.*, 2016b, Konz *et al.*, 2012, Meusburger *et al.*, 2013, Schaub and Alewell, 2009, Schaub *et al.*, 2010, Schimmack *et al.*, 2002, Zollinger *et al.*, 2014).

1.2 The quantification of sheet erosion in the Alps - the FRN method

In the last 50 years, FRN have been widely used as soil tracers to provide estimates of water-induced soil erosion rates under different environmental conditions (e.g. Mabit *et al.*, 2008, Walling, 1997, Zapata, 2002). FRN include artificial radionuclides, such as ^{137}Cs [half-life = 30.2 years], $^{239+240}$Pu (i.e. ^{239}Pu [half-life = 24110 years], and ^{240}Pu [half-life = 6561 years]). These originated from thermonuclear weapon tests in the 1950s-1960s and nuclear power plant accidents (e.g. Chernobyl in 1986 and Fukushima-Daiichi in 2011); geogenic radioisotopes, such as unsupported $^{210}Pb_{ex}$ [half-life = 22.3 years]; and cosmogenic radioisotopes, such as short-lived ^{7}Be [half-life = 53.3 days]. Once deposited on the ground, FRN strongly bind to fine particles on the surface soil and move across the landscape, primarily through physical processes. As such, these radiotracers provide effective tracking of soil and sediment redistribution (Mabit *et al.*, 2014).

There are different approaches to the application of FRN as soil erosion tracers. The traditional approach is based on a spatial comparison in which the inventory (total radionuclide activity per unit area) at a given sampling site is compared to that of a reference site located in a flat area that is undisturbed by erosion and deposition processes (Walling and Quine, 1993). The FRN total inventory measured at the reference site represents the cumulative atmospheric fallout input at the site. One of the main assumptions of the method is that its value did not change following the main fallout, excepting natural decay processes (Zapata, 2002). If the FRN inventory at the sampling site is lower than the reference inventory, the method indicates that the site has experienced erosion processes since the main fallout. On the other hand, if the site presents a greater FRN inventory than the reference site, the site has experienced deposition processes (Mabit *et al.*, 2008) (Figure 1-2, A). Different available conversion models derive quantitative estimates of soil erosion and deposition rates from FRN measurements (Walling *et al.*, 2014). Especially in the case of the application of artificial radionuclides (such as ^{137}Cs and $^{239+240}Pu$), the results of the method are medium- to long-term soil redistribution rates (30-50 years) and express the erosion and deposition processes that have occurred at the sampling sites since the main fallout (which can be set in the1950s-1960s or in 1986, in the areas affected by the Chernobyl fallout).

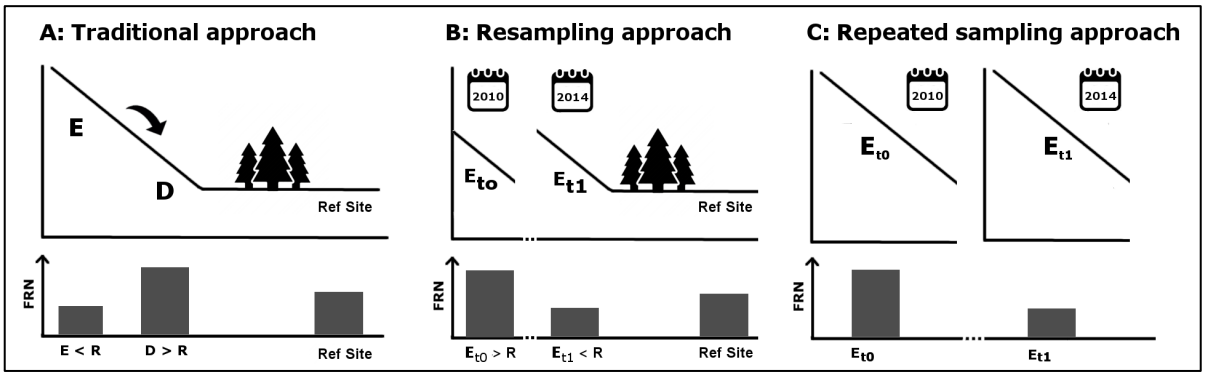

Figure 1-2: A: Concept of the fallout radionuclide (FRN) traditional method, in which the FRN content of a reference site located in a flat and undisturbed area (R) is compared to the FRN content of disturbed sites (E and D). If the FRN at the site under investigation is lower than at the reference site, the site has experienced erosion processes (E), while if the FRN content is greater than at the reference site, the site has experienced deposition processes (D). B: Concept of the resampling approach, in which the FRN inventories in different periods at the sampling sites are compared to the same reference inventory. C: Concept of the repeated sampling approach, in which the same site is sampled at two (or more) different periods, and the FRN content measured in the different campaigns is compared in order to derive soil redistribution rates.

In some cases it is necessary to document changes in rates of soil redistribution within shorter periods, such as, for example, examining the consequences of a particular land use change or investigating the impact of a certain soil conservation measure (e.g. Fornes *et al.*, 2005; Loughran and Balog, 2006; Porto *et al.*, 2014; Tiessen *et al.*, 2009). Consequently, there are two other approaches for using FRN as tracers, which are known as the resampling approach and the repeated sampling approach (for an exhaustive overview of these techniques, see Porto *et al.*, 2014). As with the

resampling approach, the FRN inventories at the sampling sites are measured in different periods and then compared to the same reference inventory (Figure 1-2, B). The estimates derived for the two or more different time windows are then juxtaposed and eventually subtracted to provide a short-term assessment of soil erosion dynamics. On the other hand, the repeated sampling approach is based on a temporal comparison of the FRN inventories measured at the same site at different times (Figure 1-2, C). A big advantage of this approach is that it does not require the selection of reference sites, because the inventory documented by the initial sampling campaign is used as the reference inventory for that point (Porto *et al.*, 2014). Thus, the repeated sampling approach represents a practical option when there are difficulties in finding suitable and undisturbed reference sites.

The main advantages of using FRN for soil erosion assessment in the Alps are the following. First, the method requires a single (or double in the case of the resampling and repeated sampling approaches) field visit to collect the soil samples. Second, prior to FRN measurement, the soil preparation process is relatively simple and fast. The method finally provides an integrated estimate of the total net soil redistribution rate since the time of the main fallout or the first sampling campaign, including all erosion processes by water, wind, and snow during the summer and winter seasons (Meusburger *et al.*, 2014).

Of the different FRN, ^{137}Cs is by far the one most widely used and has been employed to study soil redistribution under different agro-environmental conditions of different scales, ranging from experimental plots to fields of a few hectares, and to small watersheds of several km^2 (Mabit *et al.*, 2008, 2013). It was applied in the Alps for the first time a few years ago (e.g. Konz *et al.*, 2009, Schaub *et al.*, 2010). The presence of ^{137}Cs in the Alps is connected to two main causes. It was first injected into the stratosphere as a result of atmospheric nuclear weapons tests, which mainly took place between 1950 and 1970, and it was homogeneously deposited over Europe during the months following each atmospheric weapon test. Due to their high altitude and precipitation rates, the Alps have been highly contaminated by fallout radionuclides (Chawla *et al.*, 2010). The second main input is the result of the Chernobyl nuclear power plant accident (26 April 1986), when a large amount of radioactivity was released as fuel-containing particles into the environment (Zapata, 2002). At the time, the Alps were partially covered with snow. The very short fallout time window and the snow melting processes caused an unusually high heterogeneity of the initial ^{137}Cs fallout distribution in alpine soils. This heterogeneity compromises the comparison between sites that experienced different fallout inputs, and in particular the application of the traditional and of the resampling approach.

To this end, the suitability of another artificial FRN, $^{239+240}$Pu, to trace erosion processes in the Alps was recently tested and validated (Schimmack *et al.*, 2002, Alewell *et al.*, 2014 The Chernobyl $^{239+240}$Pu fallout was confined to a small area in the proximity of the power plant and did not reach the Alps (Alewell *et al.*, 2014). Consequently, the

presence of $^{239+240}$Pu in alpine soils is principally connected to the nuclear weapons tests, which means that its distribution presents lower small-scale variability in comparison to ^{137}Cs (Alewell *et al.*, 2014). Moreover, the longer half-life and the cost- and time-effective measurements of $^{239+240}$Pu activities make the application of this tracer to the investigation of soil erosion in the Alps more suitable than ^{137}Cs (Alewell *et al.*, 2014).

1.3 Critical points regarding the application of FRN as soil erosion tracers in the Alps

The validity of the FRN method has recently been at the centre of a dispute within the scientific community (Parsons and Foster, 2011, Mabit *et al.*, 2013, Parsons and Foster, 2013). The controversy started with Parsons and Foster (2011), who highlighted the uncertainties associated with the fundamental assumptions of the use of ^{137}Cs as a soil erosion tracer, such as the homogeneous distribution of the ^{137}Cs fallout (Walling and Quine, 1992) and the effectiveness of the mathematical models in terms of converting FRN inventories into soil erosion rates. They have analyzed a number of published ^{137}Cs based studies, in which the method might have been applied improperly or in a careless way; they conclude that "^{137}Cs cannot be used to provide information about rates of soil erosion" (Parsons and Foster, 2011 In their reply, Mabit *et al.*, (2013) agree on the importance of a rigorous application of the tracer, which implies a careful sampling design and a correct choice of the conversion model. However, while discussing each argument brought forth by Parsons and Foster, they present several recent studies where the ^{137}Cs method has been meticulously applied, thus underlining the potential and usefulness of ^{137}Cs, and FRN in general, in assessing soil erosion magnitude.

In agreement with Mabit *et al.* (2013) regarding the validity of the FRN method, this thesis addresses three main key points, which, if thoroughly considered, facilitate the appropriate employment of the FRN technique for soil erosion assessment (at alpine grasslands, but not only there). The three key points are: (i) the selection of stable and suitable reference sites; (ii) the choice of the approach to be applied (i.e. traditional, re-sampling, or repeated sampling; see Figure 1.2); (iii) the choice of the conversion model from which quantitative estimates of soil erosion and deposition rates are derived.

In terms of the first point, the reference sites play a fundamental role in the application of the FRN traditional approach, in which the reference inventory is compared to the inventories of the sampling sites, therefore determining if and how strongly a site has eroded or is accumulating sediments. A close proximity between the reference sites and the area under investigation is required to meet the assumption that both have experienced a similar initial fallout. Reference sites should also be located in flat areas that have neither been affected by soil redistribution

processes or human and animal activities since the main fallout. To take the spatial variability of the FRN fallout into account, multiple reference sites should be selected and the variability between the sites properly taken into consideration (Kirchner, 2013; Mabit *et al.*, 2013; Pennock and Appleby, 2002). In the alpine context, the selection of suitable references sites involves a high degree of uncertainties (Alewell *et al.*, 2014). In the alpine context, the selection of suitable references sites involves a high degree of uncertainties. Finding undisturbed and reliable sites in the geomorphological and anthropogenic highly active slopes of the Alps may be very challenging. Contact with landowners is essential, in order to exclude sites used for ploughing and grazing activities. However, it can be extremely hard to access information about the different land uses the sites have experienced in the past 30-50 years (since the main fallout). In addition, when using ^{137}Cs it is necessary to consider the small-scale variability of its distribution in alpine soils caused by the atmospheric ^{137}Cs Chernobyl fallout. If improper and unreliable reference sites are selected, this may result in major bias.

The second critical point in the application of the FRN method in the Alps is the selection of the approach. If suitable and reliable reference sites are identified, then it is possible to apply the traditional and resampling FRN methods and derive soil redistribution erosion rates over short- (as for the resampling approach), medium- or long-term periods (as for the traditional approach In the case that a significant uncertainty associated with the reference inventory is observed, the repeated sampling approach should be preferred. In fact, the latter does not require any reference sites, as it is based on a temporal comparison of the FRN inventories of sites located at disturbed areas sampled in different periods. This approach returns short-term erosion rates, where the investigated time period (namely the time window between the two sampling campaigns) can be defined on a case specific basis. The repeated sampling approach can be very useful to analyze the effects of a particular land use change (e.g. from cultivated to uncultived and vice versa)(Fornes *et al.*, 2005).

Independently of the selected approach, a quantitative estimate of soil erosion processes through the FRN method involves the conversion of FRN measurements into soil erosion rates using a specific mathematical model (Walling *et al.*, 2014). The complexity of each available model is variegated, depending on the number and type of parameters included in the formula. Theoretical models, such as the Proportional Model (Walling ad Quine, 1990), derive the erosion or deposition rates mainly from the inventory change, namely the difference in the FRN inventory between the sampling site and the reference site. The simplicity and promptness of theoretical models make them an appealing tool to estimate soil losses and gains. However, due to their nature, the scientific validity of empirical relationships is under discussion (Walling *et al.*, 2002). Profile-oriented models include information about the vertical distribution of the FRN in the soil; this distribution is commonly assumed to be

exponential (Walling *et al.*, 2014). The most widely used model is the profile distribution model for uncultivated soils (Walling and Quine, 1990). Process-oriented models, such as the mass balance model and the diffusion migration model (DMM), describe both the vertical distribution and the downward transfer of FRN in the soil (Walling *et al.*, 2002). Their algorithms contain several parameters to derive the conversion relationship, which attempt to express the physical mechanisms affecting the FRN since the main fallout. However, it is very difficult to determine such parameters, and they are often defined empirically.

When choosing the conversion model, different factors play a role, such as the selected FRN, the investigated land use, and the ability of the model to adapt to specific case conditions. The most common and available models have been developed mainly for ^{137}Cs; they were later adapted to other FRNs, with each model being defined for specific land use and process (e.g., erosion or deposition). With regard to $^{239+240}$Pu, the application of most available models to $^{239+240}$Pu inventories may produce significant bias, because ^{137}Cs and $^{239+240}$Pu can have differing depth distribution patterns in soils (attributed to differing time since the main fallout in Chernobyl affected areas and differing sorption behavior in soils)(Chawla *et al.*, 2010). When this PhD project started, few $^{239+240}$Pu based studies had been performed (Schimmack *et al.*, 2002, Hoo *et al.*, 2011, Lal *et al.*, 2013, Alewell *et al.*, 2014). At the time, the conversion of Pu inventories into soil erosion rates was still a challenge.

If (and only if) all of the above described critical points are carefully and successfully tackled, FRN-based soil erosion studies can effectively contribute (i) to understanding the extent of soil degradation processes affecting the stability of alpine soils; (ii) to validating existing soil erosion risk models; and (iii) to identifying sustainable land management practices for the protection of alpine grasslands.

1.4 Aims and outline of the thesis

The principal aim of this thesis is to propose and test different tools for a correct application of the FRN method to assess soil erosion rates at alpine grasslands. The work is subdivided into three main sections, corresponding to the main critical points discussed in Chapter 1.3 (Figure 1-3).

First, a decision support tool to validate the suitability of reference sites is introduced (Chapter 2) and tested at an alpine study area in Switzerland. A preliminary application of the repeated sampling approach at alpine grasslands is then discussed (Chapter 3). Finally, the thesis presents a new and innovative conversion model (MODERN), which enables the derivation of soil redistribution rates from the inventories of any FRN at any land use conditions (Chapter 4). The performance of the model is then tested by converting $^{239+240}$Pu inventories measured at an alpine valley in Switzerland into soil erosion rates (Chapter 5). The application of the new model MODERN is compared to that of other available conversion models.

Furthermore, the development of an R package based on the new conversion model is presented (Chapter 6). The package includes new useful features, such as the possibility to consider the spatial variability of the FRN distribution in the study area. Finally, the major findings of the thesis are discussed and suggestions for future research are proposed (Chapter 7).

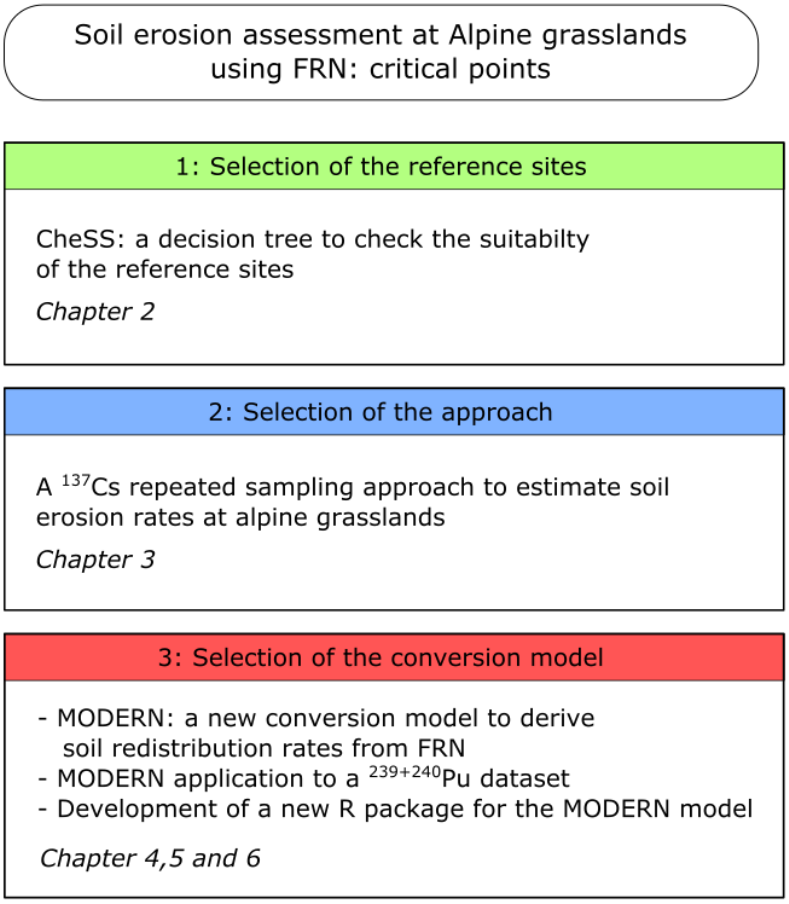

Figure 1-3: Outline of the thesis; the main critical points of the application of the FRN method at alpine grasslands are extensively discussed in the following chapters.

CHAPTER 2: DECISION SUPPORT FOR THE SELECTION OF REFERENCE SITES USING ^{137}CS AS SOIL EROSION TRACER

This chapter is published in *Soil* as: Arata L.[1], Meusburger K.[1], Bürge A.[1], Zehringer M.[2], Ketterer M. E.[3], Mabit L.[4] and Alewell C.[1] ,2017: *Decision support for the selection of reference sites using ^{137}Cs as soil erosion tracer. Soil*, *3*(3), 113-122.

(1) Environmental Geosciences, Department of Environmental Sciences, University of Basel, Switzerland.

(2) State Laboratory Basel-City, Basel, Switzerland,

(3) Chemistry Department, Metropolitan State University of Denver, Colorado, USA,

(4) Soil and Water Management & Crop Nutrition Laboratory, FAO/IAEA Agriculture & Biotechnology Laboratory, Austria.

2.1 Abstract

The classical approach of using ^{137}Cs as a soil erosion tracer is based on the comparison between stable reference sites and sites affected by soil redistribution processes; it enables the derivation of soil erosion and deposition rates. The method is associated with potentially large sources of uncertainty with major parts of this uncertainty being associated with the selection of the reference sites. We propose a decision support tool to Check the Suitability of reference Sites (**CheSS**). Commonly, the variation among ^{137}Cs inventories of spatial replicate reference samples is taken as the sole criterion to decide on the suitability of a reference inventory. Here we propose an extension of this procedure using a repeated sampling approach, in which the reference sites are resampled after a certain time period. Suitable reference sites are expected to present no significant temporal variation in their decay-corrected ^{137}Cs depth profiles. Possible causes of variation are assessed by a decision tree. More specifically, the decision tree tests for (i) uncertainty connected to small-scale variability in ^{137}Cs due to its heterogeneous initial fallout (such as in areas affected by the Chernobyl fallout), (ii) signs of erosion or deposition processes and (iii) artefacts due to the collection, preparation and measurement of the samples; (iv) finally, if none of the above can be assigned, this variation might be attributed to "turbation" processes (e.g. bioturbation, cryoturbation and mechanical turbation, such as avalanches or rockfalls). CheSS was exemplarily applied in one Swiss alpine valley where the apparent temporal variability called into question the suitability of the selected reference sites. In general we suggest the application of CheSS as a first step towards a comprehensible approach to test for the suitability of reference sites.

2.2 Introduction

Soil erosion is a global threat (Lal, 2003). Recent estimated erosion rates range from low rates of 0.001–2 t ha^{-1} yr^{-1} on flat relatively undisturbed lands (Patric, 2002) to high rates under intensive agricultural use of > 50 t ha^{-1} yr^{-1} . In mountainous regions, rates ranging from 1–30 t ha^{-1} yr^{-1} have been reported (e.g. Descroix *et al.* 2003, Frankenberg *et al.* 1995, Konz *et al.*, 2012) where they often exceed the natural process of soil formation (Alewell *et al.*, 2015). The use of the artificial radionuclide ^{137}Cs as soil erosion tracer has been increasing during the last decades, and the method has been applied all over the world with success (e.g. Mabit *et al.*, 2013; Zapata, 2002). The use of ^{137}Cs as soil erosion tracer allows an integrated temporal estimate of the total net soil redistribution rate per year since the time of the main fallout, including all erosion processes by water, wind and snow during summer and winter seasons (Meusburger *et al.*, 2014).

^{137}Cs was released in the atmosphere during nuclear bomb tests and as a consequence of nuclear power plant (NPP) accidents such as Chernobyl in April

1986. It reached the land surface by dry and wet fallouts and once deposited on the ground, it is strongly bound to fine particles at the soil surface. Due to its low vertical migration rates, it moves predominantly in association with fine soil particles through physical processes, and provides an effective track of soil and sediment redistribution processes (IAEA, 2014). The traditional approach in using the ^{137}Cs method is based on the comparison between the inventory (total radionuclide activity per unit area) at a given sampling site and that of a so-called reference site, located in a flat and undisturbed/stable area. The method indicates the occurrence of erosion processes at sites with lower ^{137}Cs inventory as compared to the reference site, and sediment deposition processes at sites with a greater ^{137}Cs inventory (Figure 2-1, A). Specific mathematical conversion models allow then to derive from the latter comparison quantitative estimates of soil erosion and deposition rates (IAEA, 2014).

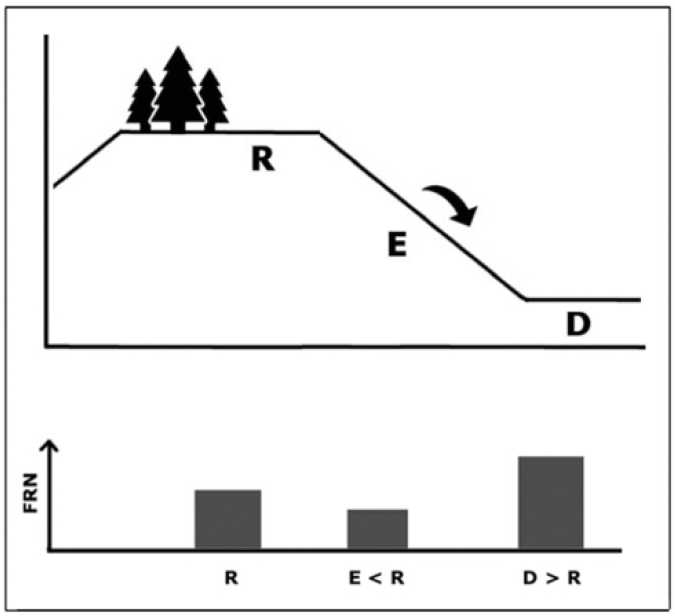

Figure 2-1: Concept of the fallout radionuclide (FRN) traditional method, in which the FRN content of a reference site located in a flat and undisturbed area (R) is compared to the FRN content of disturbed sites (E and D). If the FRN at the site under investigation is lower than at the reference site, the site has experienced erosion processes (E), while if the FRN content is greater than at the reference site, the site has experienced deposition processes (D).

The efficacy of the method relies on an accurate selection of representative reference sites (Mabit *et al.*, 2008; Owens and Walling, 1996, Sutherland,1996). The measured total ^{137}Cs inventory at the reference sites represents the baseline fallout (i.e. reference inventory), a fundamental parameter for the qualitative and quantitative assessment of soil redistribution rates (Loughran *et al.*, 2002). It is used for the comparison with the total ^{137}Cs inventories of the sampling sites, and therefore determines if and how strongly a site is eroding or accumulating sediments. Moreover, the depth profile of the ^{137}Cs distribution in the soil at the reference site plays a very important role, as the shape of this profile is used in the models to convert changes in ^{137}Cs inventory changes to quantitative estimates of soil erosion rates (Walling *et al.*, 2002). Recent studies demonstrated the sensitivity of conversion

models to uncertainties or even biases in the reference inventory (e.g. Arata *et al.*, 2016; Iurian *et al.*, 2014; Kirchner, 2013).

The close proximity of a reference site to the area under investigation is required to meet the assumption that both experienced similar initial fallout. The latter is particularly important if the study area was strongly affected by Chernobyl fallout, which is, aside global fallout from nuclear weapons testing, the major input of ^{137}Cs in many regions of Europe. Because of different geographical situations and meteorological conditions at the time of passage of the radioactive cloud, the contamination associated with Chernobyl fallout was very inhomogeneous (Chawla *et al.*, 2010, Alewell *et al.*, 2014) . Therefore, in some areas a significant small scale variability of ^{137}Cs distribution may be expected and, as already pointed out by Lettner *et al.*, (1999) and Owens and Walling (1996), might impede the comparison between reference and sampling sites. To consider adequately the spatial variability of the FRN fallout, multiple reference sites should be selected and the variability within the sites properly addressed (Kirchner, 2013, Mabit *et al.*, 2013, Pennock and Appleby, 2002). In addition, the reference site should not have experienced any soil erosion or deposition processes since the main ^{137}Cs fallout (which generally requires that it was under continuous vegetation cover such as perennial grass). Different forms of turbation, including animal- or anthropogenic impact and cryoturbation or snow processes may also affect the ^{137}Cs soil depth distribution at the reference site. Finally, the collection of the samples, the preparation process and the gamma analysis might introduce a certain level of uncertainty, which should be carefully considered. For instance, Lettner *et al.* (2000) estimated that the preparation and measuring processes contribute 12.2% to the overall variability of the reference inventory. Guidance in form of independent indicators (e.g. stable isotopes as suggested by Meusburger *et al.*, 2013) for the suitability of reference sites might help to assist with the selection of reference sites.

All in all the suitability or unsuitability of references site is crucial; it may even be the most crucial step in all FRN-based erosion assessments. The general suitability of ^{137}Cs-based erosion assessment has been recently and controversially discussed (Parsons and Forster, 2011, 2013; Mabit et al., 2013). We would like to propose that the FRN community agree on general concepts and sampling strategies to test the suitability of reference sites in order to improve the method and establish trust in this useful erosion assessment method. Up to now, the variability among spatial replicate samples at reference sites has commonly been the sole criterion to decide on the suitability of a reference value. We propose an extended method to Check the Suitability of reference Sites (CheSS) using a repeated sampling strategy and an assessment of the temporal variability of reference sites. The suitability of reference sites for an accurate application of ^{137}Cs as a soil erosion tracer is tested at Urseren Valley (Canton Uri, Swiss Central Alps).

2.3 CheSS (Check the Suitability of reference Sites): a concept to assess the suitability of reference sites for proper application of ^{137}Cs as soil erosion tracer

2.3.1 Repeated sampling strategy and calculation of inventories

The time period for the repeated sampling of reference sites needed for the application of ^{137}Cs as soil erosion tracer will be case specific and depends on the initial small scale spatial variability of the reference inventory. The time span should be of sufficient length to cause an inventory change that is larger than the uncertainty related to the inventory assessment, e.g. larger than 35 %. In our study site, which is affected by anthropogenic disturbance and snow erosion of several millimetres per winter, 2 years can be considered sufficient (Meusburger et al.,2014). Several spatial repetitions following the suggestion of Sutherland (1996) are necessary and should be analysed separately to investigate the small-scale variability in ^{137}Cs in the area. As we detected measurement differences between different detectors (see below), all samples should ideally be measured for ^{137}Cs activity using the same analytical facilities. Finally, ^{137}Cs activity needs to be decay corrected to the same date (either the period of the first sampling campaign or the second) considering the half-life of ^{137}Cs (30.17 years).

The decay corrected ^{137}Cs activities (*act*, Bq kg^{-1}), of each soil layer of the depth profile are converted into inventories (*inv,* Bq m^{-2}) with the following equation:

$$Inv = act \times xm \quad (1)$$

where *xm* is the measured mass depth of fine soil material (<2 mm fraction) (kg m^{-2}) of the respective soil sample. The depth profile of each reference site is then displayed as inventory (Bq m^{-2}) against the depth of each layer (cm). The repeated-sampling inventory change (Inv_{change}) can then be defined as:

$$Inv_{change} = \frac{Inv_{t0} - Inv_{t1}}{Inv_{t0}} \times 100 \quad (2)$$

where t_0 and t_1 are the dates of the first and the second sampling campaigns respectively, Inv_{t1} is the ^{137}Cs inventory (Bq m^{-2}) at t_1, and Inv_{t0} is the ^{137}Cs inventory at *t0*. Positive values of Inv_{change} indicate erosion, whereas negative values stand for deposition.

2.3.2 A decision tree to identify possible pitfalls for the suitability of reference sites

We evaluated the suitability of the reference sites by analysing, in addition to the spatial variability, the temporal variation in the ^{137}Cs inventory. Given the assumption that no additional deposition of ^{137}Cs occurred at the sites during the investigated time window (which is valid worldwide except for the areas affected by

the Fukushima Daiichi fallout), any temporal variation in the ^{137}Cs content should be attributable to different forms of soil disturbance or artefacts in the preparation or measurement of the samples. The potential causes of the spatial and temporal variation in the ^{137}Cs total inventories and depth profiles are examined through a decision tree which includes three main nodes (Fig. 2-2).

Node 1: No significant temporal variation of the ^{137}Cs total inventory

Firstly, the spatial variation in the ^{137}Cs total inventory at each reference site is tested. Ideally, several replicates have been collected. If the coefficient of variation (CV) exceeds 35 % as suggested by Sutherland (1996), this could be a sign of unsuitability of the reference site, but it leaves the possibility of (i) increasing sampling numbers, (ii) analyzing the causes of the spatial variation (see CheSS A to D) and (iii) moving to nodes 2 and 3 in CheSS.

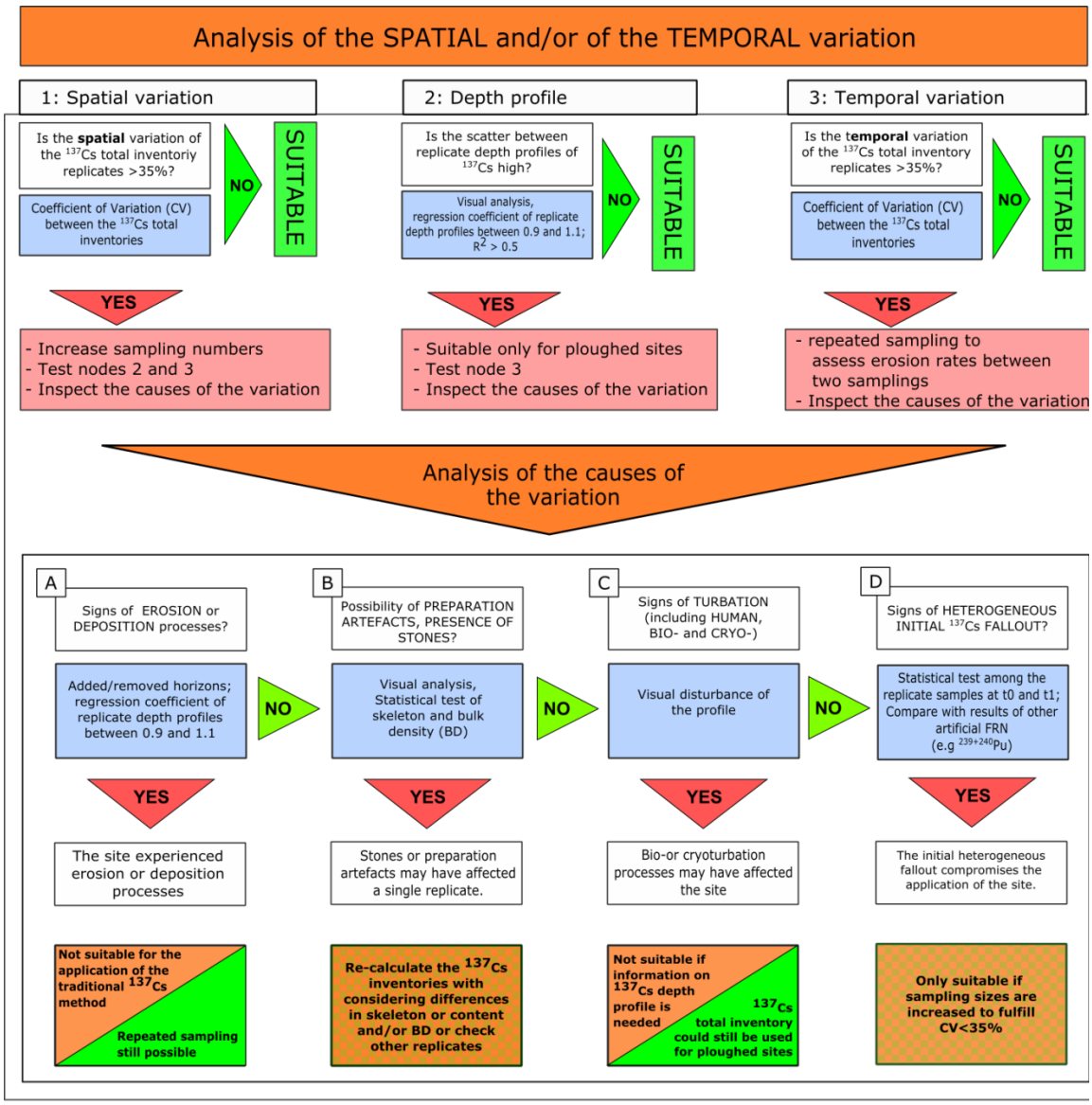

Figure 2-2: The CheSS decision tree to validate the suitability of a reference site for using ^{137}Cs as soil erosion tracer.

Node 2: No significant temporal variation of the ^{137}Cs depth profile

Secondly, whether there is a significant variation between the ^{137}Cs depth profiles measured as spatial or temporal (in t0 and t1) replicates is tested. In theory, at a stable site the shape of the depth profile should not change between replicates. Consequently, a regression between the FRN activity depth profiles collected as spatial or temporal replicates should follow a 1:1 line, and the variability should lie within the range of the observed spatial uncertainty (node 1). A deviation of the linear regression coefficient from the 1:1 line in combination with high residues and low R^2 values (<0.5 R^2) indicates an immediate and significant change in the profile, which is typically caused by anthropogenic disturbance.

For the FRN application at ploughed sites, the reference site might still be considered appropriate if the total inventory is not affected because conversion models used for ploughed sites are less sensitive to the shape of the FRN depth distribution. For unploughed soils, again the analysis of causes A to D might help in understanding the causes of the variability. Alternative options would be to take temporal replicates to evaluate the stability and thus the suitability of the reference site (node 3).

Node 3: Signs of a heterogeneous initial fallout of ^{137}Cs over the area

If the CV of all replicates taken in t0 and t1 is < 35 %, the reference site might be used for the FRN method. The longer the time period between the first and second sampling, the more reliable the yielded assessments. A suitable test for significant differences should confirm or reject the hypothesis of ^{137}Cs total inventory stability over time. If the potential causes of variation (A to D) do not apply, the site is not suitable for the traditional FRN approach, but a repeated sampling approach could still be used to assess soil redistribution rates based on FRN methods (Porto et al., 2014; Kachanoski and de Jong, 1984).

Signs of disturbance associated with erosion and deposition processes (A)

A variation in the ^{137}Cs depth profile may have been caused by soil movement processes affecting the site (Fig. 2-2). If the site experienced a loss of soil due to erosion, we expect to observe a removal of the top soil layers of the profile measured, for instance during the second sampling campaign (Fig. 3; red values below the reference profile). Further, the regression coefficient of the reference site that was affected by erosion will tend to be <0.9 when plotted against a suitable reference profile or (for node 3) the reference profile before the disturbance (Fig. 3). In the case of deposition, a sedimentation layer should be found on the top of the reference depth profile, assuming that no ploughing operations affected the site (Fig. 3; red values above the reference profile). In this case, the regression coefficient will be >1.1. Information on the depth distribution of another FRN might provide additional reliable confirmation. If redistribution processes are confirmed, the site is not suitable as a reference site and another location or a repeated FRN

sampling approach to estimate erosion rates between the two sampling campaign should be considered (Kachanoski and de Jong, 1984).

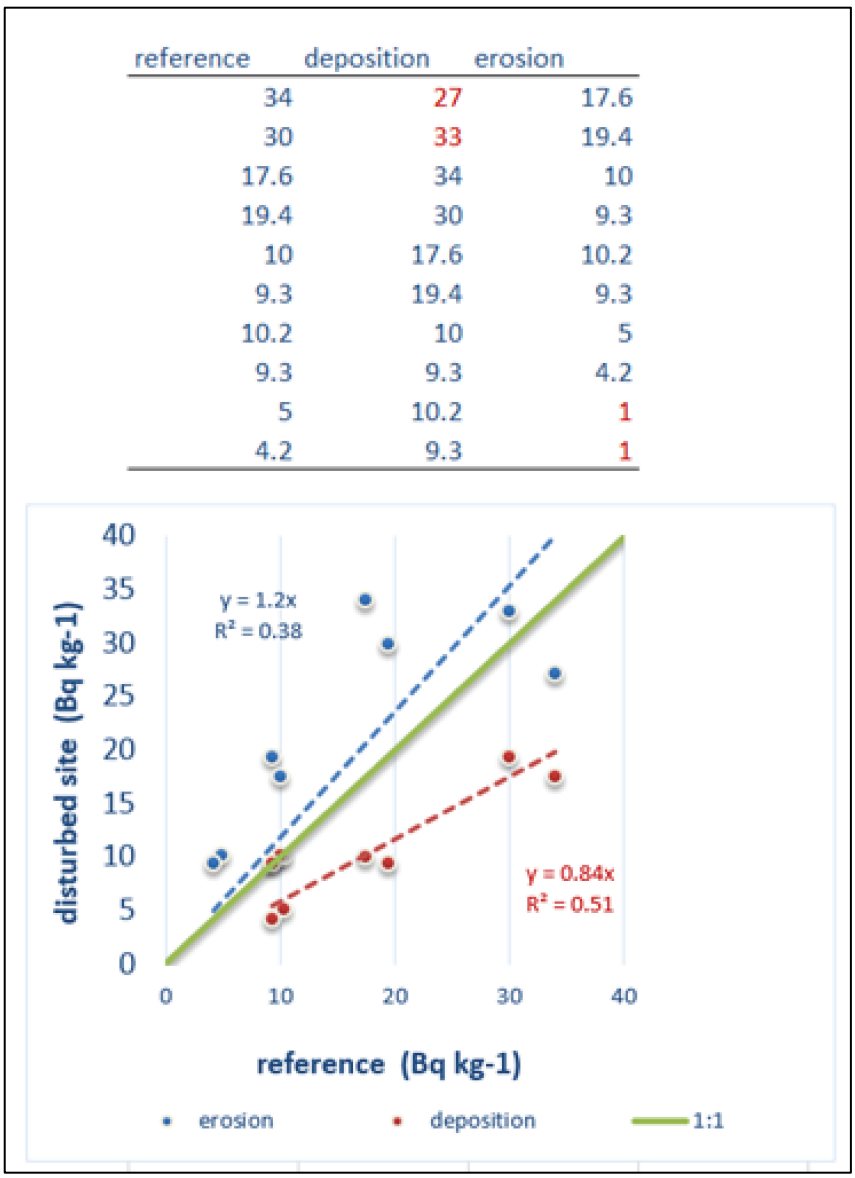

reference	deposition	erosion
34	27	17.6
30	33	19.4
17.6	34	10
19.4	30	9.3
10	17.6	10.2
9.3	19.4	9.3
10.2	10	5
9.3	9.3	4.2
5	10.2	1
4.2	9.3	1

Figure 2-3: Hypothetical signs of sheet erosion (red) and deposition (blue) on a depth profile compared to an undisturbed site.

Sampling or preparation artefacts (B)

One very common artefact which might bias the comparison between the samples collected at *t0* and *t1* is the difference in the skeleton content (the percentage of soil fractions > 2mm) (Figure 2-2, node 5). The presence of stones might determine passways for water and very fine particles and solutes in the soil and thus influence the accumulation and migration of ^{137}Cs through the soil layers. As ^{137}Cs reaches the soil by fallout from the atmosphere, the common shape of the ^{137}Cs distribution along the undisturbed depth profile can be described by an exponential function with the highest ^{137}Cs concentrations located in the uppermost soil layers (Mabit et al., 2008; Walling et al., 2002). This is particularly the case for soils with a low skeleton content (Fig. 4a) since the presence of stones may affect ^{137}Cs depth distribution either

through (i) impeding the ^{137}Cs downward migration (^{137}Cs activity could then be concentrated in the layer above the stone; Fig. 4b) or (ii) creating macropores and micropores, favouring the ^{137}Cs associated with fine particles to "migrate" to deeper layers (Fig. 4c) or causing lateral movement which will induce a lower ^{137}Cs content in our samples. As such, the seemingly spatial or temporal variation in the depth profile might indeed be a spatial variation induced by differences in skeleton content and/or bulk densities. Higher bulk densities will result in higher increment inventories even if ^{137}Cs activities at the layers are comparable. Thus, a thorough control (eventually through a statistical test, such as a paired t-test) of whether skeleton content and bulk densities are comparable between replicates is suggested. Finally, sampling, preparation artefacts and measuring processes may produce various sources of error between different sites and years. The latter is especially the case if different people prepare the samples. An estimation of possible errors might be considered, for example through a simulation of different increment assignment along the profile. If different detectors or different calibration sources and/or geometry are used in the two sampling campaigns, a comparability check of the measurements is advisable. For instance, a subset of samples could be measured with the two different detectors, and any potential discrepancy in the results should be properly reported.

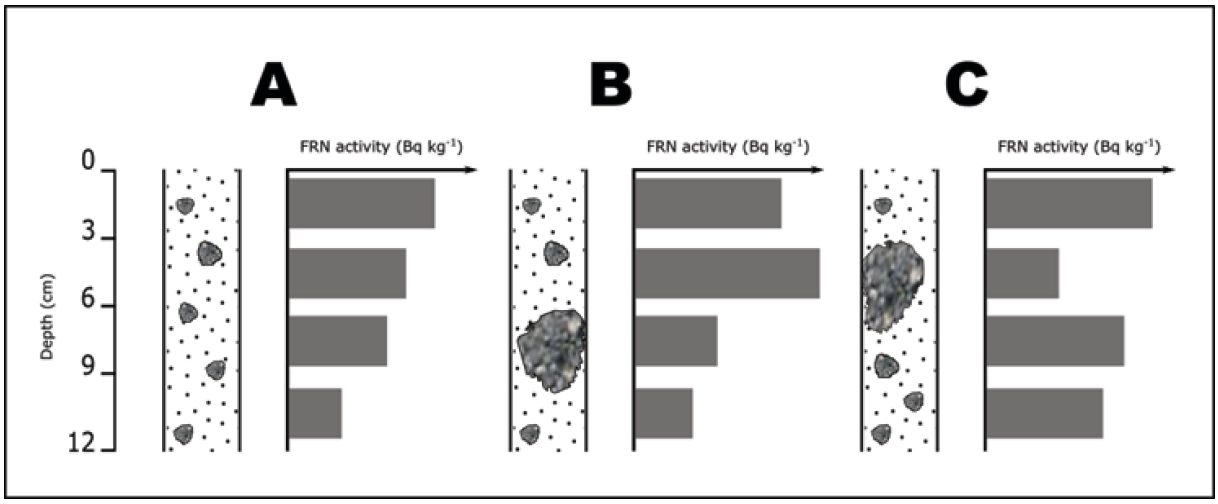

Figure 2-4: Possible influence of stones on the FRN depth distribution.

Signs of soil disturbance (C)

Different forms of disturbance, such as bioturbation, cryoturbation or even human-induced soil perturbation (e.g. tillage, seedbed preparation or digging), might have influenced the ^{137}Cs depth distribution between different sites and t0 and t1 (Fig. 2-4c). Occurrences of turbation are often difficult to identify prior to sampling but might eventually be detected by using other tracing approaches, such as the □13 C depth distribution (Meusburger et al., 2013; Schaub and Alewell, 2009). In the case of turbation, the shape of the depth profile will be highly variable and should not be considered in the estimation of soil redistribution rates for unploughed soils.

Nonetheless, the total inventory of ^{137}Cs at a ploughed site could still be used in combination with simple and basic mathematical conversion models, such as the proportional model (Ritchie and McHenry, 1990; IAEA, 2014), which require information only about the total reference inventory of ^{137}Cs and do not need detailed information about the ^{137}Cs depth distribution.

Signs of a heterogeneous initial fallout of ^{137}Cs over the area (D)

Finally, a significant difference between reference replicates may be caused by high small-scale spatial variability in ^{137}Cs distribution at the site due to heterogeneous initial fallout over the study area (Fig. 2d). In Europe, significant small-scale variability in ^{137}Cs distribution is known to be due to the Chernobyl fallout, which was characterized by high ^{137}Cs deposition associated with few rain events. Compared to nuclear bomb test fallout, the Chernobyl fallout was significantly more heterogeneous (e.g. Alewell et al., 2014). Therefore, in the areas affected by the Chernobyl fallout, sites sampled closely to each other may present very different ^{137}Cs contents. It is therefore necessary to investigate the small-scale spatial variability (e.g. the same scale as distance between reference site replicates) measured at both or at least one sampling campaign by looking at the CV again, as presented in the previous sections, or through a statistical test (for example, the analysis of variance, ANOVA). If the spatial variability is highly significant, the site should not be envisaged as a reference site for the application of the ^{137}Cs method unless the number of samples collected for the determination of the reference baseline is large enough (at least 10) to counterweight the small-scale variability within the site (Mabit et al., 2012; Sutherland, 1996; Kirchner, 2013).

A possible validation of this cause of heterogeneity might be a comparison with the spatial distribution of another FRN, such as $^{239+240}$Pu or ^{210}Pb$_{ex}$ (Porto et al., 2013; Fig. 2d). As the fallout deposition of $^{239+240}$Pu after the Chernobyl accident was confined to a restricted area in the vicinity of the nuclear power plant (Ketterer et al., 2004), the origin of plutonium fallout in the rest of Europe is linked to the past nuclear bomb tests only. Consequently, the Pu fallout distribution was more homogeneous (Alewell et al., 2014; Ketterer et al., 2004; Zollinger et al., 2015). If the $^{239+240}$Pu depth profiles do not vary significantly between the two sampling years, there should be no disturbance (e.g. turbation, erosion) or measurement artefacts. As such, it might be concluded that the heterogeneous deposition of ^{137}Cs at the time of the fall-out prejudices the use of Cs at this site.

2.4 The application of the CheSS decision tree

2.4.1 Study area

To test the methodology described above, we used a dataset from an alpine study area, the Urseren Valley (30 km^2) in Central Switzerland (Canton Uri, Fig. 1), which has an elevation ranging from 1440 to 3200 m a.s.l. At the valley bottom (1442 m a.s.l.), average annual air temperature for the years 1980–2012 is around 4.1 ± 0.7 °C and the mean annual precipitation is 1457 ± 290 mm, with 30% falling as snow (MeteoSwiss, 2013). The U-formed valley is snow-covered from November to April. On the slopes, pasture is the dominant land use, whereas hayfields are prevalent near the valley bottom.

2.4.2 Sampling design

Supportive information was provided by the local landowners to select the reference sites in both valleys. Sites used for ploughing and grazing activities were excluded. A first sampling campaign was undertaken in autumn 2010 for $^{239+240}$Pu and 2013 for ^{137}Cs measurements. Six reference sites (REF1 to REF6) were identified in flat and undisturbed areas along the valley. At each site 3 cores (40 cm depth), collected 1 m apart from each other, were sampled. The cores were cut into 3 cm increments, to derive the ^{137}Cs depth profile. The three cores from each site were bulked to provide one composite sample per site. During the second sampling campaign in spring 2015, all six reference sites were resampled. Considering the typical and high soil redistribution dynamics of the valley of >1cm per year caused by snow-induced soil removal (Meusburger et al., 2014), the period considered is sufficiently long to ensure the possibility to observe changes in the depth profiles if soil erosion and deposition processes affected the area. At each site, we collected three replicates, which were analyzed separately, to investigate the small scale variability of the FRN content. All cores were air-dried (40°C for 72h), sieved (<2 mm) to remove coarse particles and to determine the skeleton content. The bulk density (BD) was also determined.

2.4.3 Measurement of anthropogenic FRN activities and inventories

All soil samples were counted in sealed discs (65 mm diameter, 12 mm height, 32 cm^3) and the measurements were corrected for sample density and potential radioactivity background. The detectors located at the state laboratory Basel-City were calibrated with a reference solution of the same geometry. The reference contained ^{152}Eu and ^{241}Am (2.6 kBq rsp. 7.7 kBq) to calibrate the detectors from 60 to 1765 keV. It was obtained from the Czech Metrology Institute, Prague. This solution was bound in a silicon resin with a density of 1.0. The efficiency functions were corrected for coincidence summing of the ^{152}Eu lines using a Monte Carlo simulation program (Gespecor). The ^{137}Cs was counted at 662 keV with an emission probability of 0.85 and a (detector) resolution of 1.3 to 1.6 keV (FWHM). All measurements and calculations were performed with the gamma software Interwinner 7. The ^{137}Cs activity measurements were all decay-corrected to the year 2015.

To compare the ^{137}Cs results with those obtained with another artificial FRN, all samples were also analyzed for $^{239+240}$Pu activity. The determination of Plutonium isotopes from both valleys and for both sampling years were performed using a Thermo X Series II quadrupole ICP-MS at the Northern Arizona University, USA. Detailed description of the ICP-MS specifications and sample preparation procedure can be found in Alewell *et al.*, 2014. The activities of ^{137}Cs and $^{239+240}$Pu (*act*, Bq kg^{-1}) were converted into inventories (Bq m^{-2}) according to equation (1).

2.4.4 Application of the CheSS decision support tool to the reference sites

Because the ^{137}Cs activity of the samples was measured with different detectors for the two sampling years, we investigated the potential variability between the results obtained from these two detectors. A selected subset of samples (n= 24) was analysed using both detectors (i.e. the one located at the Institute of Physics of the University of Basel and the other located at the State Laboratory Basel-City). The results highlight a high correspondence of the measurements obtained with the two analytical systems (R^2 = 0.97; $p < 0.005$), although the detector of the State Laboratory Basel-City returns slightly lower ^{137}Cs activities (Figure 5). Thus, the ^{137}Cs activities of the samples measured in 2013 were corrected to be comparable to those obtained with the detector of State Laboratory Basel-City (higher efficiency) to allow comparability between the different data sets.

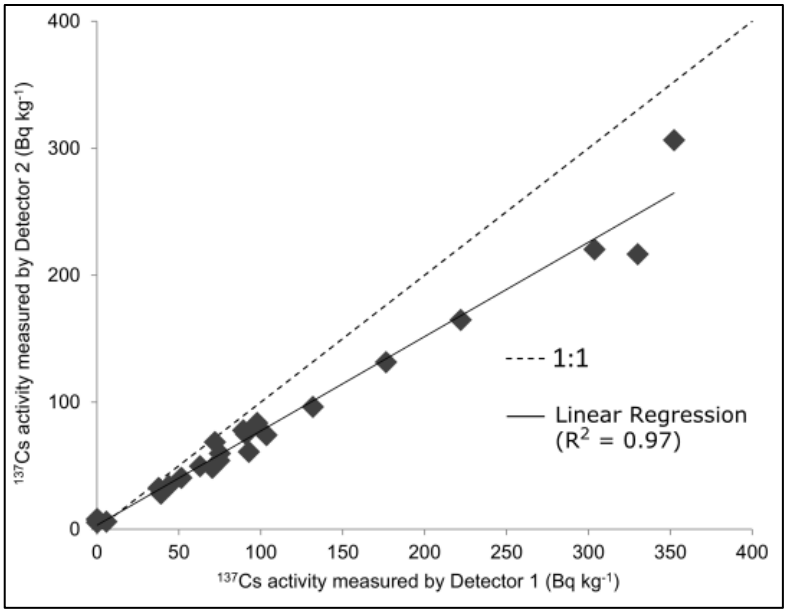

Figure 2-5: The comparison between the ^{137}Cs measurements of a subset of samples (n=16) performed with two different HpGe detectors, where detector 1: detector hosted at the Physics department of the University of Basel (CH) and detector 2: detector hosted at the State-Laboratory of Basel (CH) .

Total ^{137}Cs inventories (decay-corrected to 2015) of the six reference sites collected in the Urseren Valley in 2013 ranged from 3858 to 5057 Bq m^{-2}, with a mean value of 4515 Bq m^{-2} and a standard deviation (SD) of 468 Bq m^{-2}. Data from 2015 ranged between 3925 to 8619 Bq m^{-2}, with a mean value of 5701 Bq m^{-2} and a SD of 1730 Bq m^{-2} (Figure 6).

When following the CheSS decision tree, we investigated the variation in the ^{137}Cs total inventories at each reference site (node 1). The replicate samples were analyzed separately only during the second sampling campaign (t1), while during the first sampling campaign (t0) only composite samples were analysed. Reference sites 3, 5 and 6 presented signs of high small scale variability, as expressed by a CV of 48 % (Table 1). Such variability excluded them from any further use as reference sites

without subsequent additional sampling. For reference sites 1, 2 and 4, the CV was between 19 – 31%.

Passing to node 2 of the CheSS decision tree, the analysis focused on the variation of the shape of the ^{137}Cs depth profile (Figure 7). Here, we examined the regression between the reference depth profiles in t0 and t1. For the three sites with acceptable spatial variability (i.e. reference site 1, 2 and 4) the site REF4 showed sign of deposition with a regression coefficient between t0 and t1 = 1.34. The deposition was confirmed by field observation of construction works that were conducted between the two sampling campaigns. Thus, after this disturbance, the site is not a suitable reference site anymore. Among the sites with high spatial variability REF6 showed signs of erosion with a regression coefficient between t0 and t1 = 0.79.

In node 3, the temporal differences in total inventories between t0 and t1 were assessed. Here, only REF4 showed a significant difference of the total ^{137}Cs inventories between t0 and t1. This confirmed the unsuitability of the site to provide a reference value after the construction works.

To further investigate the causes for the spatial variation, $^{239+240}$Pu inventories measured at the three replicates of each site were analysed for t0 = 2010 and t1 = 2015 (Figure 8). Clearly, deposition for REF4 and erosion processes for REF6 were confirmed with an increase of 46% and a decrease of 27% in the total $^{239+240}$Pu inventory between t0 and t1, respectively.

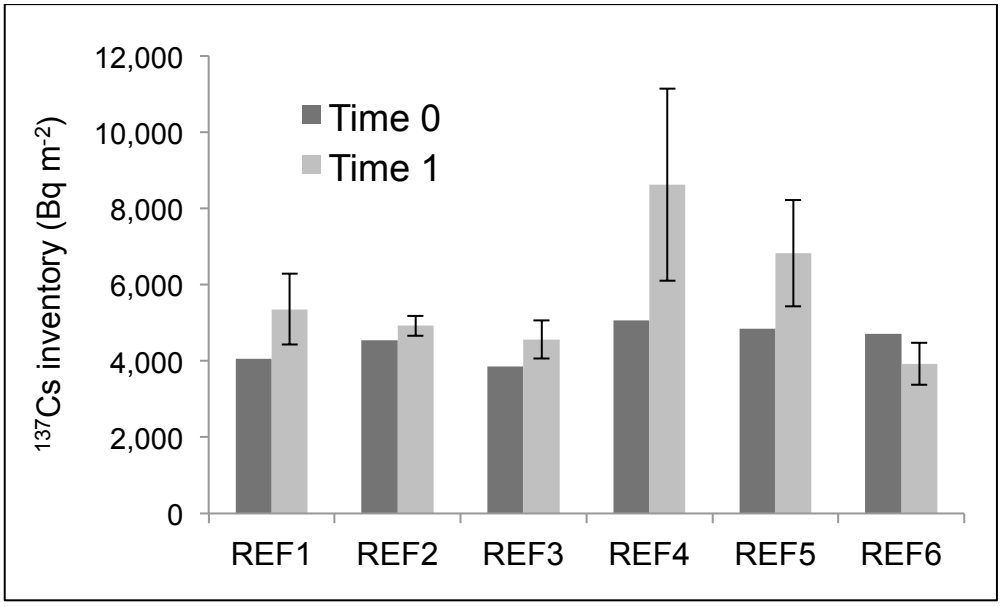

Figure 2-6: Temporal variation between the total ^{137}Cs inventories measured at the reference sites in the Urseren Valley, where Time 0 = 2013 and Time 1 = 2015. The errors bars indicate the standard deviations of the inventories among the replicates collected at each reference in 2015.

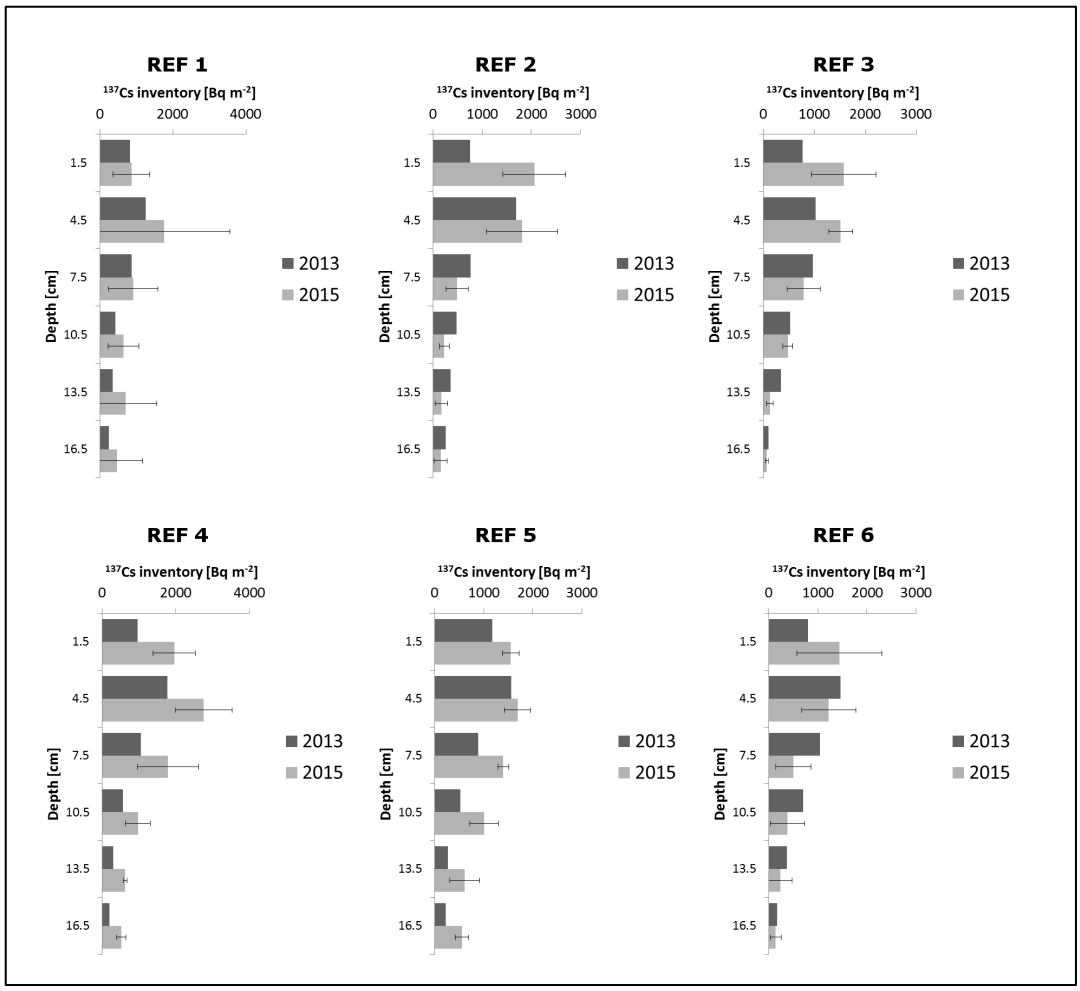

Figure 2-7: The ^{137}Cs depth profiles of the nine investigated reference sites in the Urseren Valley for the two different sampling campaigns. The errors bars indicate the standard deviations of the inventories among the replicates collected at each reference site 2015.

Further, the depth profiles of the three replicates at reference site 1 presented also significant differences. We then looked at the differences in the skeleton content of the three replicates (Figure 2, B). An ANOVA test showed a significant difference (p-value of 0.025), which indicates that a difference in the presence of stones in the three soil cores might have affected the FRN depth distribution. In particular, a Tukey's HSD (Honest Significant Difference) Post-hoc pairwise comparison identified the replicate number 3 at REF1 as a potential outlier. To validate the suitability of REF1 as a reference site, more replicates should be collected and measured, in order to compare their ^{137}Cs depth profiles to those results obtained during the first sampling campaign. In summary, REF2, REF4 (before the construction works) appeared to be most suitable for ^{137}Cs-based studies. As for sites REF3 and REF5, a visual inspection of their soil profiles excluded that any soil disturbance affected the sites (Figure 2, C). Consequently, at those sites, the variation in their depth profiles is due to a heterogeneous fallout with high spatial variability (Figure 2, D).. These sites may be suitable for studies based on other FRNs or even on ^{137}Cs if more samples are collected to constrain the spatial heterogeneity that was introduced by the ^{137}Cs Chernobyl fallout.

2.5 Conclusion

With the decision tree CheSS, the authors developed a support tool to verify the suitability of reference sites for a ^{137}Cs based soil erosion assessment. Great attention has to be given to the analysis of the small scale variability of ^{137}Cs distribution in the reference areas, especially in those regions affected by Chernobyl fallout. To cope with small scale variability, sampling numbers might be increased or the temporal variation of another artificial radionuclide, such as $^{239+240}$Pu might be analyzed. The CheSS test in the Urseren Valley indicated that the heterogeneity of ^{137}Cs distribution prejudiced the suitability of most reference sites. At reference site 1 the presence of stones affected the shapes of the depth profile in at least one replicate sample. Therefore, the application of the traditional ^{137}Cs approach, based on a spatial comparison between reference and sampling sites, is compromised. To derive soil redistribution rates, a ^{137}Cs repeated sampling approach should be preferred. This approach is based on a temporal comparison of the FRN inventories measured at the same site in different times (Kachanoski & de Jong, 1984). It doesn't require the selection of reference sites, because the inventory documented by the initial sampling campaign is used as the reference inventory for that point (Porto *et al.*, 2014).

Accurate soil erosion assessment is crucially needed to validate soil erosion modelling, which can help prevent and mitigate soil losses on a global scale. In this context, the ^{137}Cs method could play a decisive role, if we are able to overcome its potential pitfalls, especially related to the selection of suitable reference site. The decision tree CheSS is a tool for objective and comparable testing, which enables to exclude those sites which present signs of uncertainty. With this we are convinced to contribute improving the reliability of the ^{137}Cs based soil erosion assessments. With the decision tree CheSS, a support tool was proposed to verify the suitability of reference sites for a ^{137}Cs based soil erosion assessment. Great attention has to be given to the analysis of the small scale variability of ^{137}Cs distribution in the reference areas, especially in those regions affected by heterogeneous post-accidental nuclear fallout. To cope with a small scale variability, sampling numbers might be increased, or the temporal variation of ^{137}Cs or another radionuclide, such as $^{239+240}$Pu, might be analysed. The CheSS test in the Urseren Valley indicated that the heterogeneity and disturbance of ^{137}Cs distribution prejudiced the suitability of some reference sites. In addition, the presence of stones affected the shapes of the depth profile in at least one replicate sample. Including unsuitable reference sites, the application of the traditional ^{137}Cs approach, based on a spatial comparison between reference and sampling sites, is compromised. To derive soil redistribution rates, a ^{137}Cs repeated sampling approach should be preferred. This approach is based on a temporal comparison of the FRN inventories measured at the same site in different times (Kachanoski & de Jong, 1984). It doesn't require the selection of

reference sites, because the inventory documented by the initial sampling campaign is used as the reference inventory for that point (Porto *et al.*, 2014).

Accurate soil erosion assessments are crucially needed to validate soil erosion modelling, which can help prevent and mitigate soil losses on larger spatial scales. In this context, FRN could play a decisive role, if we are able to overcome its potential pitfalls, especially those related to the selection of suitable reference sites. The decision tree CheSS provides a new concept for an objective and comparable reference site testing, which enables to exclude those sites which present signs of uncertainty and should therefore not be used as reference sites With this approach we are convinced to contribute improving the reliability of the FRN-based soil erosion assessments.

Acknowledgements

The authors would like to thank Annette Ramp, Gregor Juretzko, Simon Tresch, Carmelo La Spada and Axel Birkholz for support during field work. This work was financially supported by the Swiss National Science Foundation (SNF), project no. 200021-146018, and has been finalized in the framework of the IAEA Coordinated Research Project (CRP) on "*Nuclear techniques for a better understanding of the impact of climate change on soil erosion in upland agro-ecosystems*" (D1.50.17).

CHAPTER 3: SHORT-TERM SOIL EROSION DYNAMICS AT ALPINE GRASSLANDS - RESULTS FROM A^{137}CS REPEATED SAMPLING APPROACH

This chapter contains unpublished and preliminary results obtained during the PhD, which will be used for a publication in preparation.

3.1 Introduction

The analysis of fallout radionuclides (FRN) is today the only promising approach to quantify soil erosion in mountainous grasslands areas, such as the Swiss Alps, where the characteristic topography and the climatic conditions limit the application of conventional techniques (see chapter 2; and Alewell *et al.*, 2008, Schaub and Alewell, 2009, Schaub *et al.*, 2010, Konz *et al.*, 2012, Meusburger *et al.*, 2013, Alewell *et al.*, 2014, Arata *et al.*, 2016b). The classical approach of the FRN method is based on a qualitative spatial comparison: the inventory (total radionuclide activity per unit area) at a given sampling site is compared to that of an undisturbed reference site, where no soil redistribution processes have occurred since the main deposition of the selected FRN. To derive quantitative estimates of soil erosion and deposition rates from FRN measurements specific conversion models are needed (IAEA, 2014). The results represent an integrated estimate of the total net soil redistribution rate since the time of the main fallout, including all erosion processes by water, wind and snow during summer and winter season (Meusburger *et al.*, 2014).

This traditional reference-site approach however encounters a number of limitations in the Alps, especially related to the use of ^{137}Cs, the most widely used FRN for soil erosion studies and to the selection of suitable reference sites (Alewell *et al.*, 2014). The presence of ^{137}Cs in the Alps is connected to two main episodes: the nuclear weapons tests (which mainly took place between 1950 and 1970) and the Chernobyl nuclear power plant accident (26 April 1986). Due to its relatively short half-life (30.17 years), the activity of ^{137}Cs derived from the nuclear tests is considerably low. This means that most of ^{137}Cs present today in the Alps originates from the Chernobyl power plant accident, and in particular, from a few single precipitation events occurring in late April and beginning of May 1986. At that time the Alps were partially covered with snow. The snow present at the sites acted as a sink for airborne radionuclides before their subsequent transfer to the soil (Pourcelot *et al.*, 2003). Snow melting could have led to heterogeneous accumulation of radionuclides in local depressions, and meltwater runoff could further change the patterns of their deposition (Chawla *et al.*, 2010). The subsequent rain events on snow cover have most probably contributed to randomly distribute the radioactive isotopes over the slopes. This resulted in an unusually high heterogeneity of ^{137}Cs distribution in Alpine soils (Alewell *et al.*, 2014). In addition, finding undisturbed slopes with no erosional activity during the last 30 years (time since the main ^{137}Cs fallout) may be challenging. Alpine slopes are often subjected to soil degradation processes, which, in the case of landslides or snow avalanches, involve a large amount of soils over relatively wide areas. Flat areas where those dynamics are less prone to occur are usually used for houses and farming practices (e.g hayfields, grazing). As a consequence, the choice of undisturbed reference sites is spatially restricted.

To overcome the above described limitations, the aim of this study is to replace the classical ^{137}Cs approach, where an undisturbed reference site is compared to erosional sites (spatial approach), with a repeated sampling approach (temporal approach; for an exhaustive overview of this technique, see Porto *et al.* (2014)). This approach is based on the direct comparison of ^{137}Cs inventories measured at the same sites in different times. Using temporal instead of spatial reference allows short term erosion assessment, and, more important, does not require finding undisturbed reference sites in the geomorphological and anthropogenic highly active slopes of the Alps.

We will analyze the temporal (4 years) variation of ^{137}Cs inventories at different points in a study area in the Piora Valley which is located at the southern part of the Alps (Canton Ticino, Switzerland). Previous studies conducted in the same valley showed an extremely high small scale variability of ^{137}Cs distribution at the reference sites (Alewell *et al.*, 2014). Thus, the application of the repeated sampling approach is the only option in the valley to derive quantitative estimates of soil redistribution processes through FRN.

To convert the ^{137}Cs inventories into soil redistribution rates within the repeated sampling campaign different conversion models have been proposed (e.g. Kachanoski, 1987; Jong and Kachanoski, 1988; Kachanoski, 1993; Fornes *et al.*, 2005; Tiessen *et al.*, 2009, Li *et al.*, 2011). In all of the available models the inventory documented by the initial sampling campaign is employed as the reference inventory for that point. Nonetheless, none of them consider the information on the depth distribution of ^{137}Cs. At unploughed sites (such as the alpine sites investigated in this study) the ^{137}Cs inventory is concentrated near the surface, and the concentration of ^{137}Cs declines exponentially with depth (Walling and Quine, 1993). This means that a loss of a given percentage of the reference inventory does not correspond to the same magnitude of loss of soil (Walling *et al.*, 2002). We recognize the importance of taking the behavior of ^{137}Cs in the soil into account, when converting inventories into soil redistribution rates. However, as no available models available consider it, for this study our choice fell on the power model for the calculation of erosion rates (Kachanosky, 1987) and on the linear model for the calculation of deposition rates (Kachanoski, 1993), where soil redistribution rates are derived from the inventory change between the two sampling campaigns. The results will offer a preliminary overview of sheet erosion dynamics in the study area, and represent a first attempt to estimate short term soil redistribution rates in the Alps.

3.2 Materials and Methods

3.2.1 Study area, sampling design and ^{137}Cs measurements

The study area is situated in the Piora Valley (22.6 km^2) (Canton Ticino, South Central Alps, Switzerland). The elevation ranges from 1850 to 2773 meters a.s.l. The "Piora-

Mulde", which became famous in the context of the Gotthard-Tunnel, constitutes the valley floor. The bedrock is dominated by mica schist and gneiss with smaller sediment layers and areas of granites (Gotthard-Massiv in the north, Lukmanier-Massiv in the south). The average annual precipitation is between 1500 and 1750 mm. Soils of the catchment are mainly Podsols and dystric Cambisols or cumulic Anthrosols. Streets and paths mostly located at the bottom of the south-exposed slopes are often prone to avalanches (Knoll-Heitz, 1991). Pasture is the dominant land use in the valley. Land use management has been relatively constant over centuries due to management rules established in a contract from the year 1227 regulating the alp zoning and stocking (Knoll-Heitz, 1991).

3.2.2 Soil sampling design

The first sampling campaign was held in 2010, when four transects of approximately 40 m have been sampled on different slopes. Along each transect three points have been sampled, on the basis of their location along the slope: Upper slope (U), Mean (M) and Lower slope (L). The altitude range of the points is 1850 – 2050, and on average, the difference in altitude between the Lower and the Upper points of each transect is 80 m. Each sampling point has been sampled with a 1 m soil corer, with three replicates each, which have been later combined together. Each resulting core has been cut into 15 cm depth increment, and then in 5 cm increments, before further analysis. The second sampling campaign was held in summer 2014, all transects have been resampled. Along each transect the same three points were resampled, with five replicates each. The replicates were cut into 15 cm depth increment, and then in 5 cm increments. Each resulting sample was then analyzed separately, to investigate the small scale variability of ^{137}Cs distribution. In three points (T1-M, T2-L and T3-U) three of the five replicates have been cut in 3 cm increments, and then bulked together, to investigate the ^{137}Cs distribution along the depth profile.

3.2.3 Measurement of ^{137}Cs activities and inventories

All cores have been air-dried (40°C for 72h), and sieved (<2 mm) before being measured with high resolution HPGe detectors. The ^{137}Cs measurements of all samples have been held at the State laboratory Basel-City using standard coaxial high resolution germanium detectors with 25% to 50% relative efficiencies (at 1.33 MeV, ^{60}Co). Counting times were set to provide a precision of less than ±10% for ^{137}Cs at the 95% level of confidence. For lower Caesium activities counting time was set to 24 hours.

All soil samples were counted in closed discs (65 mm diameter, 12 mm height, 32 cm^3 volume). All measurements were corrected for sample density and background. All detectors were calibrated with a reference solution of the same geometry. The reference contained ^{152}Eu and ^{241}Am (2.6 kBq rsp. 7.7 kBq) to calibrate the detectors

from 60 to 1765 keV, which was obtained from Czech Metrology Institute, Prague. This solution was bound in silicon resin of a density of 1.0. The efficiency functions were corrected for coincidence summing of the ^{152}Eu lines using a Monte Carlo simulation program (Gespecor). The ^{137}Cs was counted at 662 keV with an emission probability of 0.85 and a resolution of 1.3 to 1.6 keV (FWHM). All measurements and calculations were performed with gamma software Interwinner 7. All ^{137}Cs activity measurements were decay corrected to the year 2014. In this study we consider the ^{137}Cs activity of the soil samples up to a depth of 15 cm. Previous studies showed that in the study area the ^{137}Cs activity below 15 cm is to be considered not significant.

The activities of ^{137}Cs (*act*, Bq kg^{-1}) were converted into inventories (Bq m^{-2}) according to the following equation:

$$Inv = act \times M \qquad (1)$$

where *M* is the measured mass depth of fine soil material (<2 mm fraction) (kg m^{-2}) of the respective soil sample. We define as repeated-sampling inventory change (Inv_{change}):

$$Inv_{change} = \frac{Inv_{t0} - Inv_{t1}}{Inv_{t0}} \times 100 \qquad (2)$$

where *t0* and *t1* are the dates of the first and the second sampling campaigns respectively, Inv_{t1} is the FRN inventory (Bq m^{-2}) at *t1*, and Inv_{t0} is the FRN inventory at *t0*. Positive values of Inv_{change} indicate erosion, whereas negative values indicate deposition.

3.2.4 Analysis of the spatial variability of ^{137}Cs inventory

To investigate the small scale spatial variability of ^{137}Cs at the sites, the authors analyzed the coefficient of variation (CV) between the ^{137}Cs inventories of the samples collected at each sampling point during the second sampling campaign (2014). At each sampling point five replicates were collected. At sites T1-M, T2-L and T3-U three replicates were cut in 3 cm depth increments, and the resulting samples were combined together, in order to have sufficient soil for the gamma detection of the ^{137}Cs activity. The sum of the ^{137}Cs inventories measured at each depth increments up to a depth 15 cm was then considered as a single sample and compared to the ^{137}Cs inventories of the remaining 2 samples which were not cut. As a result, at these sites the spatial variability was investigated only on 3 samples. At sites T4-L and T4-M the five replicates were accidentally bulked together, and therefore no information on the spatial variability could be produced. A statistical test (i.e. Shapiro-Wilk test, □=0.05) was also run on the ^{137}Cs inventories of the replicates collected at each sampling site in 2014, to check the normality of the distribution. No statistical analysis was run on the replicates collected during the first sampling campaign as at that time they were bulked together.

3.2.5 Estimation of short term erosion and deposition rates

The power model proposed by Kachanoski (1993) was used to derive quantitative estimates of soil erosion and deposition rates from the temporal variation of ^{137}Cs inventory at each sampling point. The power model derives erosion rates (*E*, t ha^{-1} yr^{-1}), with the following equation:

$$E = M(1 - (Inv_{t1}/Inv_{t0})^{1/(t1-t0)}) \quad (3)$$

Where *M* is the measured mass depth of fine soil material (<2 mm fraction) (kg m^{-2}) of the soil sample, and Inv_{t1} and Inv_{to} are the ^{137}Cs inventories measured at *to* and *t1*, respectively.

The power model is not appropriate for estimating soil accumulation (de Jong *et al.*, 1983; Lobb and Kachanoski, 1999, Tiessen *et al.*, 2009). Thus, at deposition sites (where Invt1 > Invt0), we used the linear model (Kachanoski *et al.*, 1987, Tiessen *et al.*, 2009). The linear model estimates deposition rates (*D*, t ha^{-1} yr^{-1}) as:

$$D = \frac{M(Inv_{t0} - Inv_{t1})}{(t1-t0)Inv_{t0}} \quad (4)$$

3.4 Results and discussion

3.4.1 Temporal variation of ^{137}Cs inventory at the sites

The values of ^{137}Cs inventory obtained for the 12 cores collected in 2010, decay corrected to the year 2014, ranged from 2867 to 13130 Bq m^{-2}, with a mean of 6744 Bq m^{-2} and a standard deviation of 3054 Bq m^{-2}. The equivalent values for the 12 cores collected during the second campaign in 2014 ranged from 2500 to 10277 Bq m^{-2}, with a mean of 6165 Bq m^{-2} and a standard deviation of 2160 Bq m^{-2}. The results of the repeated sampling approach highlighted high dynamics of soil redistribution processes along the transects within the investigated time window (Figure 3-1). All transects except for transect 4 present signs of both erosion and deposition processes. Inventory changes range between -73 to 145% (Table 3-1). Surprisingly, at transects 1 and 3 the upper points along the slopes present signs of deposition, indicating soil movement patterns at higher altitudes.

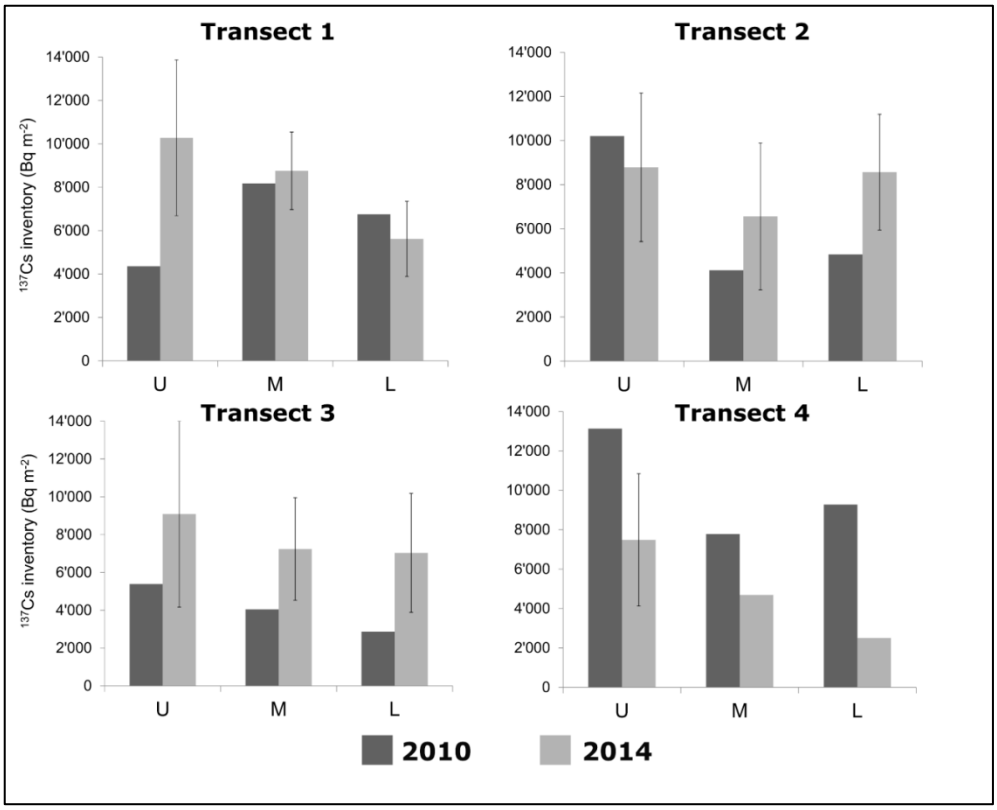

Figure 3-1: Temporal variation of ^{137}Cs inventories at the four transects, where three points have been sampled. L: lower slope, M: medium slope and U: Upper slope. The errors bars indicate the standard deviations of the inventories among the replicates collected at each reference in 2014.

Table 3-1: ^{137}Cs Inventory at t0 and t1 and Inventory changes (Inv_{change}) at each sampling site along the four transects. Analysis of the spatial variability of the replicate cores collected at each sampling site during the second sampling campaign (t1:2014), with *CV*: Coefficient of Variation, Stdev: Standard deviation, and the resulting *p-value* of the Shapiro-Wilk test (□=0.05). Erosion (E) and Deposition (D) Rates estimated at each sampling site, where PM: Power Model (eroded sites) and LM: Linear Model (deposited sites).

Transect	Position	Inv_{t0}	Inv_{t1}	Inv_{change}	*CV at t1*	*Stdev at t1*	*p-value*	*E (PM)*	*D (LM)*
		Bq m^{-2}	Bq m^{-2}	%	%	Bq m^{-2}		t ha^{-1} yr^{-1}	t ha^{-1} yr^{-1}
T1	Upper	4358	10277	-136	3589	36	0.25		30.4
	Middle	8171	4158	49	1785	22	0.9	-18.2	
	Lower	6756	5618	17	1735	31	0.08	-4.4	
T2	Upper	10203	8785	14	3366	38	0.93	-3.5	
	Middle	4119	6560	-59	3328	51	0.87		15.7
	Lower	4837	5102	-5	2624	30	0.17		1.2
T3	Upper	5387	4532	16	4921	53	0.55	-3.1	
	Middle	4049	7239	-79	2713	40	0.79		19.7
	Lower	2867	7033	-145	3145	44	0.58		36.4
T4	Upper	13130	7485	43	3361	50	0.41	-12	
	Middle	7778	4686	40	ND	ND	ND	-12.1	
	Lower	9275	2500	73	ND	ND	ND	-30.2	

3.4.2 Spatial variability of ^{137}Cs inventory at sampling sites collected in 2014 and analysis of the depth profiles

When applying the repeated sampling approach, the spatial variability present at the sites should be carefully considered. The analysis of the replicates collected at each sampling site during the second sampling campaign showed the presence of a small scale variability of the ^{137}Cs distribution in the soils (Table 3-1). The Coefficients of Variation (*CV)* of the replicate samples range from 22 to 53%. The latter reflect the heterogeneity of unploughed grasslands soils, which is typically characterized by a coefficient of variation between 19 and 47% as reported by Sutherland (1996). The statistical test didn't indicate any significant difference between the replicates (table 3-1). There is no information on the small scale variability of ^{137}Cs distribution at the time of the first sampling campaign. However a similar range of variability can be assumed.

In 2014 we also analyzed the ^{137}Cs depth profiles measured at three points along transects 1, 2 and 3. The results show how at all three points the shapes of the profiles reflect an exponential distribution, with a low ^{137}Cs content in the upper most layer, and a peak in the following layer (figure 3-2) .

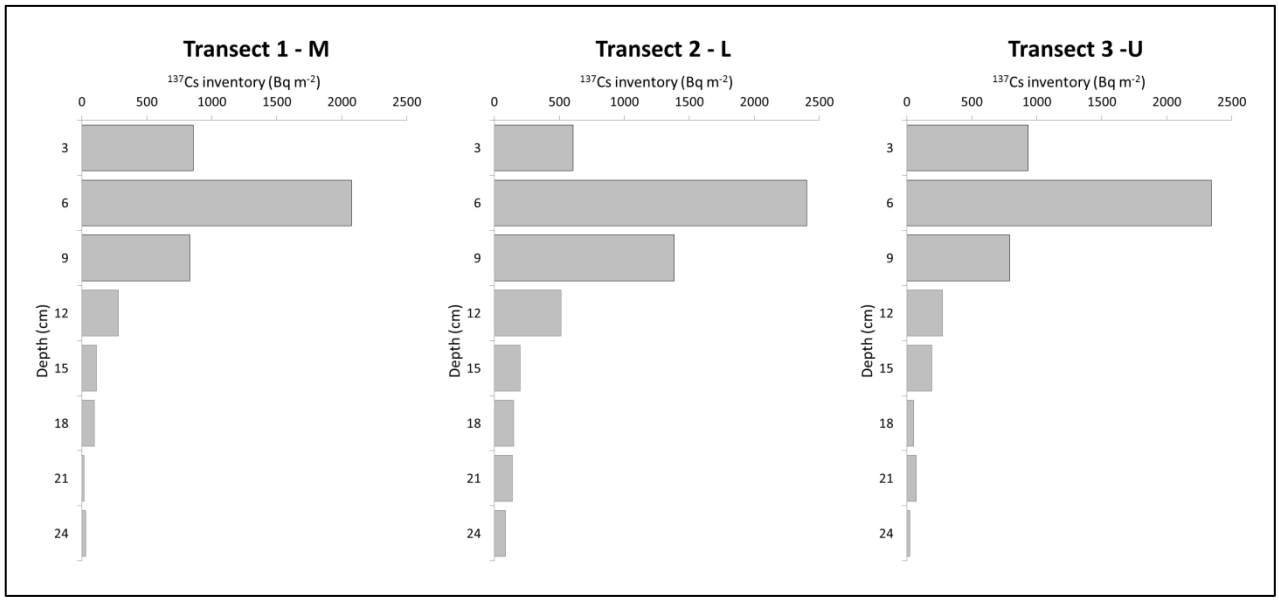

Figure 3-2: The ^{137}Cs depth profiles of sites Transect 1 – Middle slope (M), Transect 2 – Lower slope (L) and Transect 3 –Upper slope (U) measured in 2014.

3.4.3 Quantitative estimates of soil redistribution rates

Soil erosion rates were estimated with the Power Model (PM), whereas deposition rates were calculated with the Linear Model (LM) (Table 3-1). The same order of magnitude was found between erosion and deposition rates. In particular, erosion rates calculated with the Power Model range between -3.1 and -30.2 t ha^{-1} yr^{-1}, whereas deposition rates estimated with the Linear Model range between 1.2 and 36.4 t ha^{-1} yr^{-1}. As expected, a highly significant correspondence (i.e. correlation

factor of 0.99) between the results of PM and LM and the repeated sampling inventory changes was found (Figure 3-3). It is important to consider that the results might be connected to high risk of errors, as they do not take the specific depth distribution of ^{137}Cs along the soil profile at the site into account. As the analysis of the depth profiles in 2014 showed (figure 3-2), most of the ^{137}Cs is present in the upper layers of the profile, and particularly in the second layer from the surface. This means that the removal of a small amount of soil would return a high inventory change, and consequently relatively high erosion rates.

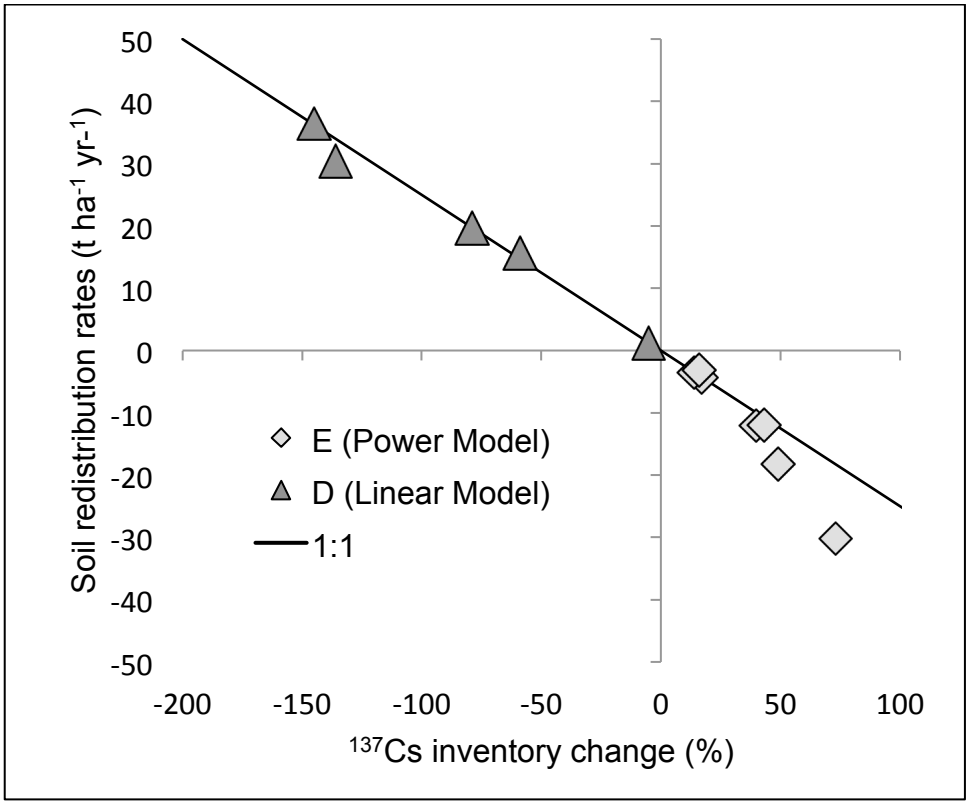

Figure 3-3: The relationship between the erosion rates (E) and the deposition rates (D) and the repeated-sampling inventory change measured at the sites.

3.5 Summary

The application of a ^{137}Cs repeated sampling approach in the Piora Valley indicated high temporal variations in ^{137}Cs inventories along the four transects, where the mean inventory change is 36% at eroded sites and -85% at deposition sites. Quantitative estimates of soil redistribution rates, calculated with the Power Model and the Linear Model, indicate mean erosion rates of 12 t ha^{-1} yr^{-1} and mean deposition rates of 21 t ha^{-1} yr^{-1}. High spatial variability of ^{137}Cs activities at all sites has been observed, reflecting the heterogeneous distribution of ^{137}Cs fallout after the Chernobyl power plant accident in 1986. The ^{137}Cs repeated sampling approach allowed gaining information on short term redistribution dynamics. However a special focus should be addressed in better considering the spatial variability of ^{137}Cs inventories at the same site, by analyzing the ^{137}Cs inventories of a larger number of replicates (Kirchner,

2013, proposed a range of 10-20 replicated samples per site). The ^{137}Cs depth distribution in the soil should also be effectively taken into account, when converting ^{137}Cs inventories into soil redistribution rates, within the repeated sampling approach. For this purpose, the depth profiles of ^{137}Cs measured during both two sampling campaigns should be analyzed, compared and included in the conversion model.

CHAPTER 4: MODELLING DEPOSITION AND EROSION RATES WITH RADIONUCLIDES (MODERN) - PART 1: A NEW CONVERSION MODEL TO DERIVE SOIL REDISTRIBUTION RATES FROM INVENTORIES OF FALLOUT RADIONUCLIDES

This chapter is published in the *Journal of Environmental Radioactivity* as: Arata, L[1].*, Meusburger, K. [1]*, Frenkel, E. [2], A'Campo-Neuen, A. [3], Iuran, A.R. [4,5], Ketterer, M.E. [6], Mabit, L. [7], Alewell, C. [1], 2016. *Modelling Deposition and Erosion rates with RadioNuclides (MODERN) - Part 1: a new conversion model to derive soil redistribution rates from inventories of fallout radionuclides.* Journal of Environmental Radioactivity, 162, 45-55.

(1) Environmental Geosciences, Department of Environmental Sciences, University of Basel, Switzerland,

(2) Institute de Recherche Mathématique Avancée (IRMA), University of Strasbourg, France,

(3) Department of Mathematics and Computer Science, University of Basel, Switzerland,

(4) Faculty of Environmental Science and Engineering, Babes-Bolyai University, Cluj-Napoca, Romania,

(5) Consolidated Radioisotope Facility, Plymouth University, Plymouth, UK,

(6) Chemistry Department, Metropolitan State University of Denver, Colorado, USA,

(7) Soil and Water Management & Crop Nutrition Laboratory, FAO/IAEA Agriculture & Biotechnology Laboratory, Seibersdorf, Austria.

* Shared first authorship.

4.1 Abstract

The measurement of fallout radionuclides (FRN) has become one of the most commonly used tools to quantify sediment erosion or depositional processes. The conversion of FRN inventories into soil erosion and deposition rates is done with a variety of models, which suitability is dependent on the selected FRN, soil cultivation (ploughed or unploughed) and movement (erosion or deposition). The authors propose a new conversion model, which can be easily and comprehensively used for different FRN, land uses and soil redistribution processes. The new model MODERN (Modelling Deposition and Erosion rates with RadioNuclides) considers the precise depth distribution of any FRN at the reference site, and allows adapting it for any specific site conditions. MODERN adaptability and performance in converting different FRN inventories is discussed for a theoretical case as well as for two already published case studies i.e. a ^{137}Cs study in an alpine and unploughed area in the Aosta valley (Italy) and a 210Pbex study on a ploughed area located in the Transylvanian Plain (Romania). The tests highlight a highly significant correspondence (i.e. correlation factor of 0.91) between the results of MODERN and the published results of other models currently used by the FRN scientific community (i.e. the Profile Distribution Model and the Mass Balance Model). The development and the cost free accessibility of MODERN (see modern.umweltgeo.unibas.ch) will ensure the promotion of wider application of FRNs for tracing soil erosion and sedimentation.

4.2 Introduction

Soil erosion is one of the major threats to soil stability and productivity but its monitoring remains a challenge. In the last 50 years, fallout radionuclides (FRN), e.g artificial ^{137}Cs and $^{239+240}$Pu, natural ^{210}Pb fallout and cosmogenic ^{7}Be, have been widely used as soil tracers to provide estimates of water induced soil erosion rates under different environmental conditions (e.g. Ritchie and McHenry, 1990; Walling, 1997; Ritchie and Ritchie, 2001; Zapata, 2002; Mabit *et al.*, 2008). Once deposited on the ground, FRN strongly bind to fine particles at the surface soil and move across the landscape primarily through physical processes (IAEA, 2014). As such these conservative radiotracers provide an effective track of soil and sediment redistribution.

FRN methods perform efficiently to investigate temporal soil redistribution processes for arable lands, where soil degradation due to agriculture practices affects soil properties and landscape processes (IAEA, 2014). It is also highly effective in assessing erosion and deposition patterns in mountain grasslands where the extreme topographic and climatic conditions hinder the application of more conventional techniques such as sediment traps, erosion pins or irrigation experiments (Konz *et al.*, 2012, Alewell *et al.*, 2014). The FRN method provides information of erosion processes affecting a specific study area since the time of deposition of the selected FRN and

can be performed during a single sampling campaign, thus avoiding time-consuming and costly procedures commonly required to monitor sites over extended time periods (Mabit *et al.*, 2008, 2013). The method is based on a targeted FRN qualitative comparison: the inventory (total activity per unit area) at a given sampling site versus the inventory measured in an adjacent and undisturbed reference site, where no soil erosion and deposition have occurred.

One of the major challenges regarding the application of FRN as soil tracers is the conversion of FRN inventories to quantitative estimates of soil redistribution. Different conversion models have been proposed by the scientific community and differ mainly in their underlying assumptions of soil stratification and descriptions of FRN transport processes (IAEA, 2014). Current available models range from relatively simple (e.g the Profile Distribution Model, Walling and Quine, 1990 or the Inventory Method by Lal *et al.*, 2013) to more complex (e.g. Mass Balance Model and the Diffusion and Migration Model, cf. Walling *et al.*, 2002). As depth distribution of FRN is strongly dependent on cultivating measures such as ploughing, different models have been developed for ploughed or unploughed soils (please note that previous studies used the terms ploughed, cultivated and disturbed versus unploughed, uncultivated and undisturbed synonymously. The authors think that the pair ploughed and unploughed are the most precise term, as unploughed grasslands are indeed cultivated and might be seriously disturbed).

The Profile Distribution Model (PDM) (Walling *et al.*, 2002, 2011, 2014) is a very convenient model to estimate erosion rates of unploughed soils. However, as highlighted by Walling *et al.* (2014), it involves a number of simplifying assumptions on the depth distribution of FRN in the soil (e.g., the exponential depth distribution of FRN in the soil). The Mass Balance Model (MBM) and the Diffusion and Migration Model (DMM) (Walling *et al.*, 2002, 2011, 2014) consider different vertical distribution of the FNR in the soil depending on the land use (ploughed or unploughed) and on the migration processes since the main FRN deposition. In ploughed soils, the Mass Balance Model assumes FRN to be mixed uniformly within the plough layer. In unploughed soils, the Diffusion and Migration model considers the downward diffusion and migration of FRN in the soil profile, and that most of the FRN is located near the surface, usually in the upper 15 cm (Walling *et al.*, 2002).

The MBM and the DMM algorithms include parameters which should accurately describe the physical processes affecting FRN distribution in the soil since the main fallout. The values of these parameters, if not carefully selected, can significantly bias the results of soil erosion calculations (Por□ba and Bluszcz, 2008, Iurian *et al.*¸2014). Moreover, their algorithms change when measuring erosion or deposition rates, as different sediment dynamics are considered.

The International Atomic Energy Agency (IAEA) has supported the development of an Excel™ based software which allows the conversion of FRN inventories into soil redistribution rates, through the application of different models (among them the

PDM, the DMM and the MBM). The software was initially developed for ^{137}Cs and later extended for the application of ^{7}Be and $^{210}Pb_{ex}$ (Walling *et al.*, 2014). The software is public and freely downloadable, but its code is not editable and thus cannot be adapted to specific environmental conditions (e.g. a particular depth profile of the FRN distribution) or be used for other FRN such as $^{239+240}Pu$.

The aim of this study is to present a new conversion model, called MODERN (Modelling Deposition and Erosion rates with RadioNuclides). The MODERN model is based on a unique algorithm to convert FRN inventories into both erosion and deposition rates. It can be applied under every agro-environmental condition and land use, and accurately describes the soil profile shape of any selected FRN. The free and public release of MODERN, developed in the Matlab™ environment, make its code transparent and easily adaptable. The development of MODERN aims to promote the use of FRN as soil erosion tracers for scientific and applied purposes.

4.3 MODERN: Modelling Deposition and Erosion rates with RadioNuclides

4.3.1 Model concept and assumptions

MODERN (Modelling Deposition and Erosion rates with RadioNuclides) is a new model able to convert inventories of FRN into soil redistribution rates. One key advantage of MODERN is its ability to describe accurately specific depth distribution of any FRN in the soil, independent of its depth function's shape. Moreover, MODERN can be applied under various land use conditions (i.e. ploughed and unploughed soils).

The underlying idea behind the model is the comparison of the depth profile of the reference site with the total inventory of a sampling site. MODERN returns soil erosion and deposition rates in terms of thickness of the soil layer affected by soil redistribution processes. To estimate the thickness of soil losses/gains, MODERN aligns the total inventory of the sampling site to the depth profile of the reference site. The point of intersection along the soil profile represents the solution of the model (Figure 4-1). As with all conversion models, a key assumption of MODERN is that the evolution of the depth distribution of the selected FRN is the same at the reference and the sampling sites. If the soil properties of reference and sampling sites are comparable, the mechanisms influencing the downward diffusion and migration of the radionuclide in the soil should also be similar. MODERN also take into account other assumptions usually undertaken for the application of FRN as soil erosion tracers (e.g. uniform spatially distribution of the local fallout; Rapid, strong and non-exchangeable adsorption of FRN to fine soil particles; Soil associated redistribution of FRN through physical processes). Compared to other models (i.e. the Diffusion Migration Model and the Mass Balance Model) the application of MODERN does not require a transect sampling approach, where the sampling points need to be

located along a transect, but performs efficiently also when the sampling points are spatially distributed.

4.3.1.1 Adaptation of sampling depth

Difference in sampling depths between reference and sampling site can be also accounted for by MODERN. Measuring the depth profile of FRN distribution at the reference site usually results in an abrupt step to zero concentrations in the lower layers of the profile (Figure 4-2, upper left). Indeed, deep horizons contain very low FRN activities. As these horizons are bulked within a fixed depth, the low activities may result in values below the energy range of a standard detector. If this is the case, MODERN can adapt the depth distribution of the reference site, and simulate an arbitrary number of layers below the measured depth profile. In those simulated layers MODERN smooths the FRN inventories exponentially to zero (Figure 4-2, Adaptation 1). Notice that such adaptation of the depth profile is optional. However, without it, MODERN would not be able to find a solution in case the sampling site has a FRN inventory lower than the inventory of the last measured layer of the reference depth profile.

4.3.1.2 Considering ploughed versus unploughed land management

The determination of soil erosion at ploughed sampling sites very often confronts with the problem of finding an undisturbed reference site. Often these reference sites may be unploughed grasslands with very different FRN depth distribution compared to the ploughed sampling site. When comparing an undisturbed reference site to a ploughed site, MODERN allows an adaptation of the depth profile of the reference site to consider the processes that affect soil redistribution. Regular ploughing affects FRN vertical distribution in the soil, as all soil layers up to the ploughing depth are mixed more or less homogeneously. Therefore, to simulate similar mechanical mixing processes, MODERN adjusts the reference depth profile, where it assumes an average inventory value at the layers above the ploughing depth (Figure 4-2, Adaptation 2).

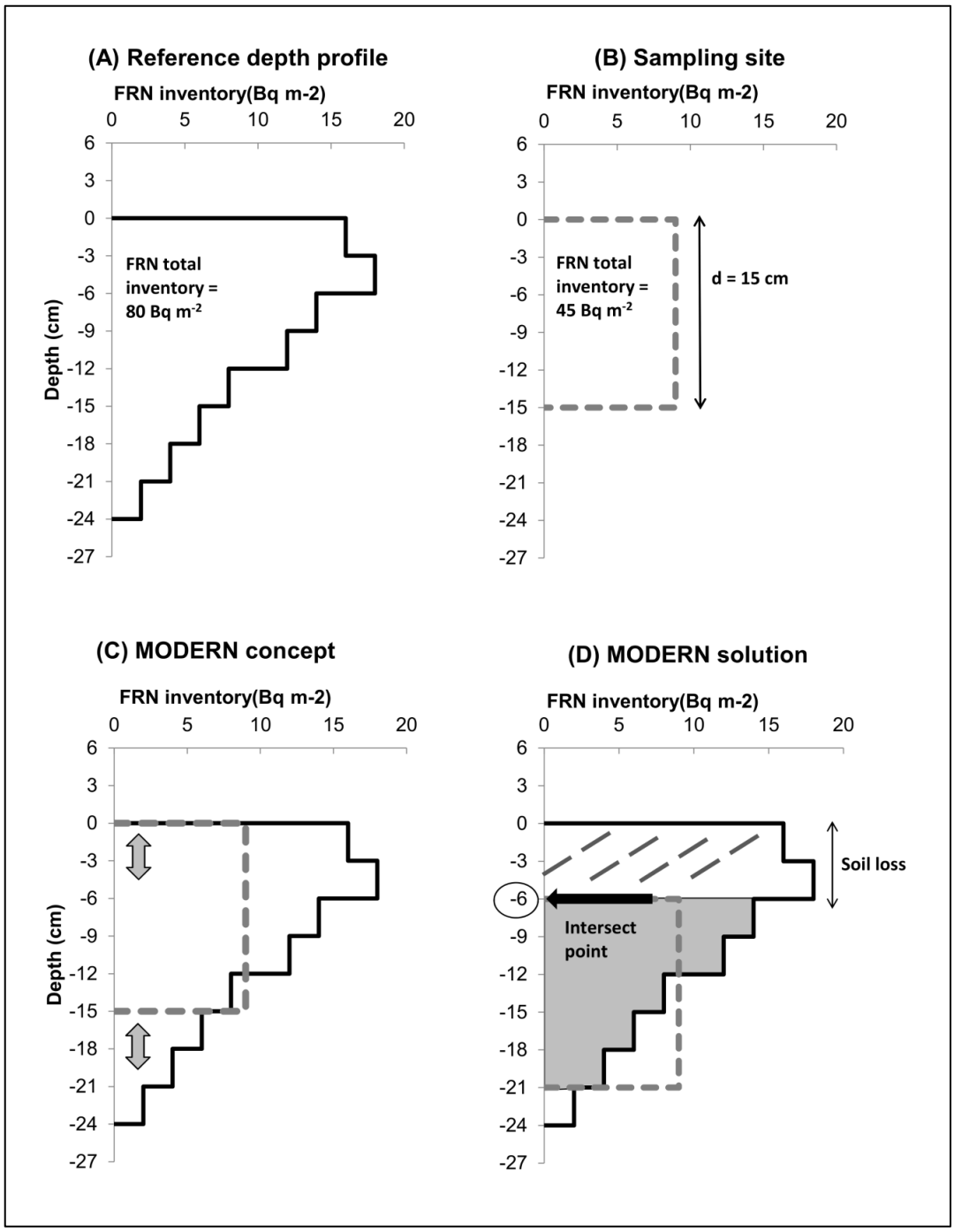

Figure 4-1: Concept of MODERN.MODERN compares the area covered by the depth profile of the reference site (A) with the area of the total inventory of a sampling site (B). MODERN overlaps the two area (C) until it finds the intersect point where they match (D).

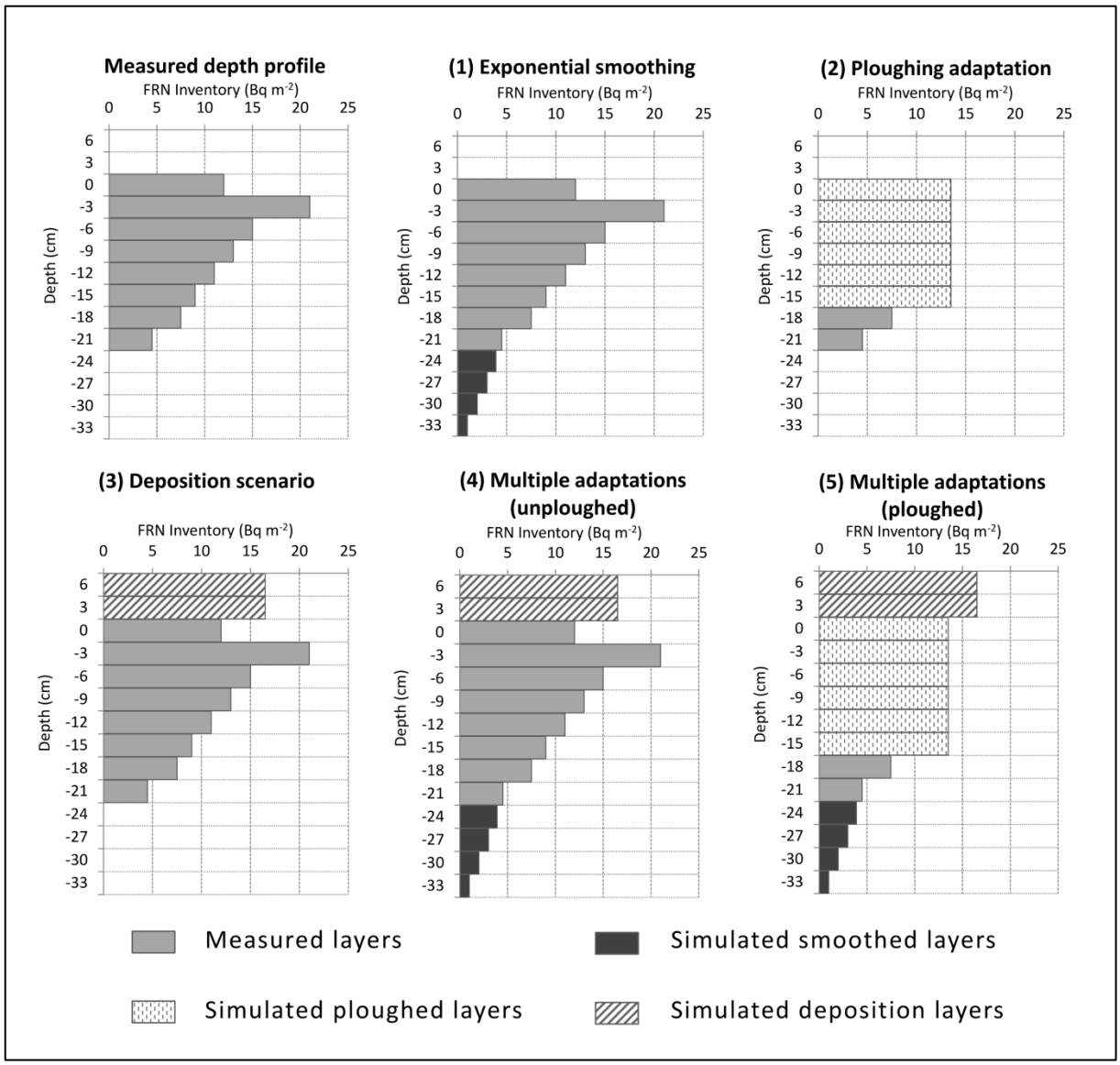

Figure 4-2: Possible adaptations of a FRN depth profile performed by MODERN. Upper left: a hypothetical depth profile, measured in depth increments of 3 cm, from 0 to 21 cm; (1): MODERN's adaptive simulation of 4 additional layers below the last measured layer of the depth profile, with an exponential smoothing of the FRN inventories. (2): MODERN's adaptive simulation of mixing processes of FRN distribution due to ploughing activities, with ploughing depth = 15 cm; (3): MODERN simulation of 2 additional layers above the measured depth profile, with sediments originated from an horizon of 6 cm depth, which was homogenously mixed during detachment and transport; (4): MODERN simulation of a depth profile as a result of a combination of multiple adaptations in a unploughed site; (5): MODERN simulation of a depth profile as a result of a combination of multiple adaptations in a ploughed site.

4.3.1.3 Modelling deposition of eroded material

In case of higher FRN inventory at the sampling site compared to the reference site, net deposition of material is assumed. The assessment of deposition rates with FRN always requires assumptions on the origin of soil layers involved and the thickness of deposited sediment layers. Variability of sources with different FRN concentration can be considered in MODERN. An arbitrary number of layers can be simulated above the measured FRN depth profile, and different deposition scenarios might be assumed (Figure 4-2, Adaptation 3). The selected scenarios arise from the likelihood that deposition dynamics involve mostly top soil and rarely deeper soil layers.

4.3.1.4 Considering particle size selectivity

The particle size factor is particularly important as water erosion triggers a selective and preferential loss of small grain size fractions. Moreover, the distribution of FRN in soil also demonstrates a significant preferential adsorption of these radionuclides by finer soil particles (He and Walling, 1996). Usually eroded sites are depleted in small fractions while reference sites display the original grain size composition. As fine soil particles are preferentially eroded this will result in an overestimation of FRN based erosion rates if the erosion selectivity is not taken into consideration. However, the authors acknowledge that measuring the particle size factor for a specific site can be very challenging. If a particle size factor is determined, it is possible to consider it in MODERN, by simply dividing the results by it.

MODERN permits to perform multiple adaptations simultaneously and to adjust the reference depth profile to the specific conditions encountered at each sampling site (Figure 4-2, Adaptation 5). Then, it is possible to produce a range of potential solutions, which need to be evaluated by expert knowledge and can be considered as uncertainty assessment.

4.3.2 Model solving method

Using MODERN, the FRN depth profile of the reference site is modelled as a step function *g(x)*, which at each increment *inc* returns a value Inv_{inc}. Please, note that MODERN does not make any assumption or generalization on the shape of the reference site depth profile, but it reproduces accurately the specific measured depth distribution of the FRN. Finally, *Inv* is the FRN total inventory of a sampling site, measured for the whole depth profile *d* (cm).

The model targets the level x**(cm)* from x* to x*+ *d* (cm), where the sum of all Inv_{inc} of the reference site is equal to the total FRN inventory of the sampling site, *Inv*. Therefore x* should fulfil the following equation:

$$\int_{x^*}^{x^*+d} g(x)dx = Inv \quad (1)$$

In order to find all possible solutions, a number of simulated layers, are added below and above the reference profile (see 2.1. above and Figure 4-1), to assess potential soil losses or gains. The new simulated depth profile is described by the integral function *S*, where:

$$S(x) = \int_{x}^{x+d} g(x')dx' \quad (2)$$

The function *S* can be solved through the primitive function *G* of the distribution function *g(x)* as follows:

$$S(x) = G(x+d) - G(x) \quad (3)$$

MODERN returns the results in cm of soil losses or gains. The conversion to yearly soil losses or gains *Y* in t ha^{-1} yr^{-1} can be calculated using the following equation:

$$Y = 10 \times \frac{x^* \cdot xm}{d \cdot (t_1 - t_0)} \quad (4)$$

where *xm* is the mass depth (kg m^{-2}) of the sampling site, *d* is the total depth increment considered at the sampling site as above, t_1 is the sampling year (yr), and t_0 (yr) is the reference year. In case the selected FRN are artificial the latter can be either the year of the main fallout or the year when a particular environmental condition occurred (e.g. a major change in the land use). When using natural radionuclides, as $^{210}Pb_{ex}$ and ^{7}Be, the investigated time window can be adjusted accordingly. In particular, the application of $^{210}Pb_{ex}$ provides a retrospective assessment of long-term soil redistribution rates over a period of up to 100 years (Mabit *et al.*, 2008). Conventionally, the parameter t_0 (yr) is set to 100 years prior to the sampling year t_1. The very short half-life of ^{7}Be (53 days) permits to trace short-term erosion processes, on a time window of maximum 6 months (IAEA, 2014).

Table 4-1: Parameters included in MODERN.

Parameter	Description
Inv_{inc}	FRN inventory at the reference site at each increment *inc* (Bq m^{-2})
inc	Depth increment of the reference site (cm)
Inv	FRN inventory at the sampling site (Bq m^{2})
d	Depth increment of the sampling site (cm)
P	Particle size (unitless)
pd	Ploughing depth (cm)
g(x)	Function describing the FRN depth profile of the reference site (Bq m^{-2})
S(x)	Simulated total inventory of reference sites (Bq m^{-2})
*x**	Erosion or deposition rates (cm)
xm	Mass depth of the sampling site (kg m^{-2})
t_1	Sampling year (yr)
t_0	Reference year (yr)
Y	Erosion or deposition rates (t ha^{-1} yr^{-1})

4.4 Application of MODERN

4.4.1 A theoretical example

As an example, a hypothetical situation is presented where the inventories of two sampling sites are compared to a fictive reference site (i.e. site R), whose total FRN inventory is assumed to be 100 Bq m^{-2}. The shape of the depth profile is characterized by a FRN peak in the subsurface horizon with an exponential decline below (Figure 4-3). The first of the two sampling sites (i.e. site A) presents a lower FRN inventory than the reference site (*Inv*= 78 Bq m^{-2}), which indicates erosion, while the second (i.e. site B) has a higher FRN inventory than the reference site (*Inv*= 115 Bq m^{-2}), highlighting deposition process. At both reference and sampling sites the FRN inventory is

measured until a depth (*d*) of 30 cm. At the reference site the depth increments (*inc*) are 3 cm each.

As a first step, two layers below the measured depth profile are simulated to reach a zero content layers with an asymptotic function (as described above)(Figure 4-3). In order to simulate deposition processes at Site B, two layers above the measured reference depth profile were modelled following two possible scenarios. For Scenario 1, the authors hypothesize that sediments derive from an upslope top soil horizon (e.g. the first 3 cm). The FRN inventories of the additional layers were set to be equal to the inventory of the first 3 cm of the reference profile. For Scenario 2 the authors hypothesize that the deposited materials originate from an eroded horizon of about 6 cm depth, which was homogenously mixed during detachment and transport processes. Therefore, FRN inventories of the additional layers are equal to the average inventory of the first 6 cm of the reference profile (Figure 4-3, Scenario 1 and Scenario 2).

In case of erosion (site A), MODERN estimates a soil loss of 4.1 cm, independently of the scenario assumed. If the site is affected by deposition (site B), there are different solutions for the scenarios considered. In our example, MODERN returns a deposition of 3.3 cm for Scenario 1 and a deposition of 4.7 cm for Scenario 2.

To obtain the mass of the eroded soil *Y*, a mass depth of 100 kg m^{-2} has been assumed for the sites A and B. To calculate yearly erosion or deposition rates, the authors assumed the peak fallout (t_0) of the FRN to be 1963 and the sampling year (t_1) to be the year 2000. The resulting solution is an erosion rate of 3.9 t ha^{-1} yr^{-1} at site A and a deposition magnitude of 3.4 to 4.8 t ha^{-1} yr^{-1} depending on the scenario chosen for site B.

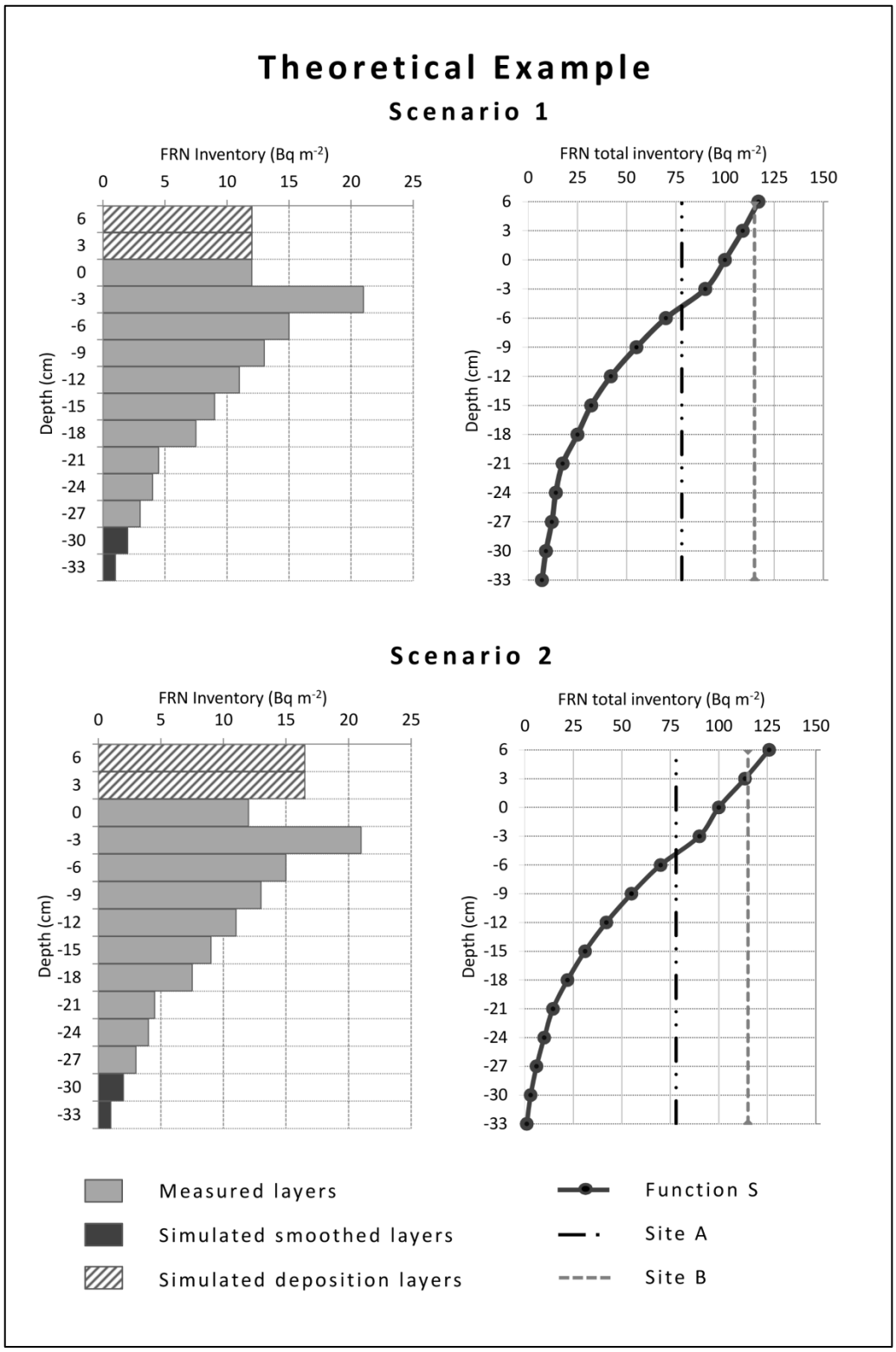

Figure 4-3: Example of two hypothetical MODERN scenarios. The Reference FRN depth profile with measured layers is presented with filled light grey bars. The simulated layers for two deposition scenarios are presented with striped bars, while the smoothed layers added below the measured depth profile are presented in dark grey (left). Resulting function S, describing the cumulated FRN inventory of the simulated reference profile, considered for each increment of length *d* = 30. The intersection with total inventories of site A and site B values are also shown (right).

4.4.2 MODERN application to a case study in the Aosta valley tracking ^{137}Cs in unploughed soils (Test 1)

The artificial radionuclide ^{137}Cs (half-life = 30.2 years) is the most frequently employed FRN to study soil redistribution under different agri-environmental conditions (Mabit *et al.*, 2013; Zapata, 2002). In undisturbed conditions, ^{137}Cs depth distribution in the soil follows an exponential function, with the highest ^{137}Cs concentrations located in the uppermost soil layers (Walling *et al.*, 2002; Mabit *et al.,* 2008).

To test MODERN for soil erosion assessment based on ^{137}Cs inventories at unploughed sites, the authors selected a subset of data from a previous study conducted in an alpine catchment in the province of Aosta (Italy), heavily affected by snow avalanches (Ceaglio *et al.*, 2013; for all data used see Table 4-2). The detailed description of the investigated site, the specific sampling design and the results obtained in the frame of this study have been reported by Ceaglio *et al.* (2013).

Soil samples were collected along a main avalanche path in 2010. In the track area, two transects (TA1 and TA2) were sampled, with 5 cores collected within a distance of 15 m to each other. As for the reference sites, 3 reference samples, located in a nearby flat area, were collected, cut in 3 cm depth increments, and used to determine average profile distribution and maximum depth of ^{137}Cs. All samples were oven-dried at 40°C, lightly ground and sieved and ^{137}Cs activity was measured with a Lithium-drifted Germanium Detector. A least squares exponential fit of the ^{137}Cs depth profile at the reference sites is characterized by R^2 of 0.58.

^{137}Cs inventories of the sampling sites, considered for a depth increment of 9 cm, were converted to soil erosion rates with the Profile Distribution Model (PDM, Walling *et al.*, 2000). The PDM assumes an exponential decline of ^{137}Cs activity in the depth profile, which can be described by the following function:

$$Inv(xm_r) = Inv_{ref}(1 - e^{-xm_r/h_0}) \quad (5)$$

Where xm_r (kg m^{-2}) is the mass depth from the soil surface of reference sites and h_0 (kg m^{-2}) is a coefficient describing the profile shape. The greater the value of h_0, the deeper is the penetration of the radionuclide into the soil (Walling *et al.*, 2002).

At an eroding point (where the total inventory *Inv* is less than the reference inventory Inv_{ref}), the erosion rate *Y* (t ha^{-1} yr^{-1}) can be estimated using the following equation (Walling and Quine, 1990):

$$Y = -\frac{10}{(t^1 - t^0)}\left[\ln\left(1 - \frac{Inv_{change}}{100}\right)\right] h_0 \quad (6)$$

where Inv_{change} is the % reduction of ^{137}Cs total inventory with respect to the local ^{137}Cs reference value (defined as: (Inv_{ref}□Inv)/Inv_{ref} ×100). The parameters t^1 and t^0 (yr) are the sampling and the main deposition years, respectively. Because more than 80% of ^{137}Cs input is connected to the Chernobyl power plant accident (1986) (Facchinelli *et al.*, 2002), the erosion rates were calculated for the time window 1986-

2010. The application of PDM resulted in average erosion rates from all sites at the two transect of 8.8 t ha^{-1} yr^{-1} (Ceaglio *et al.*, 2013).

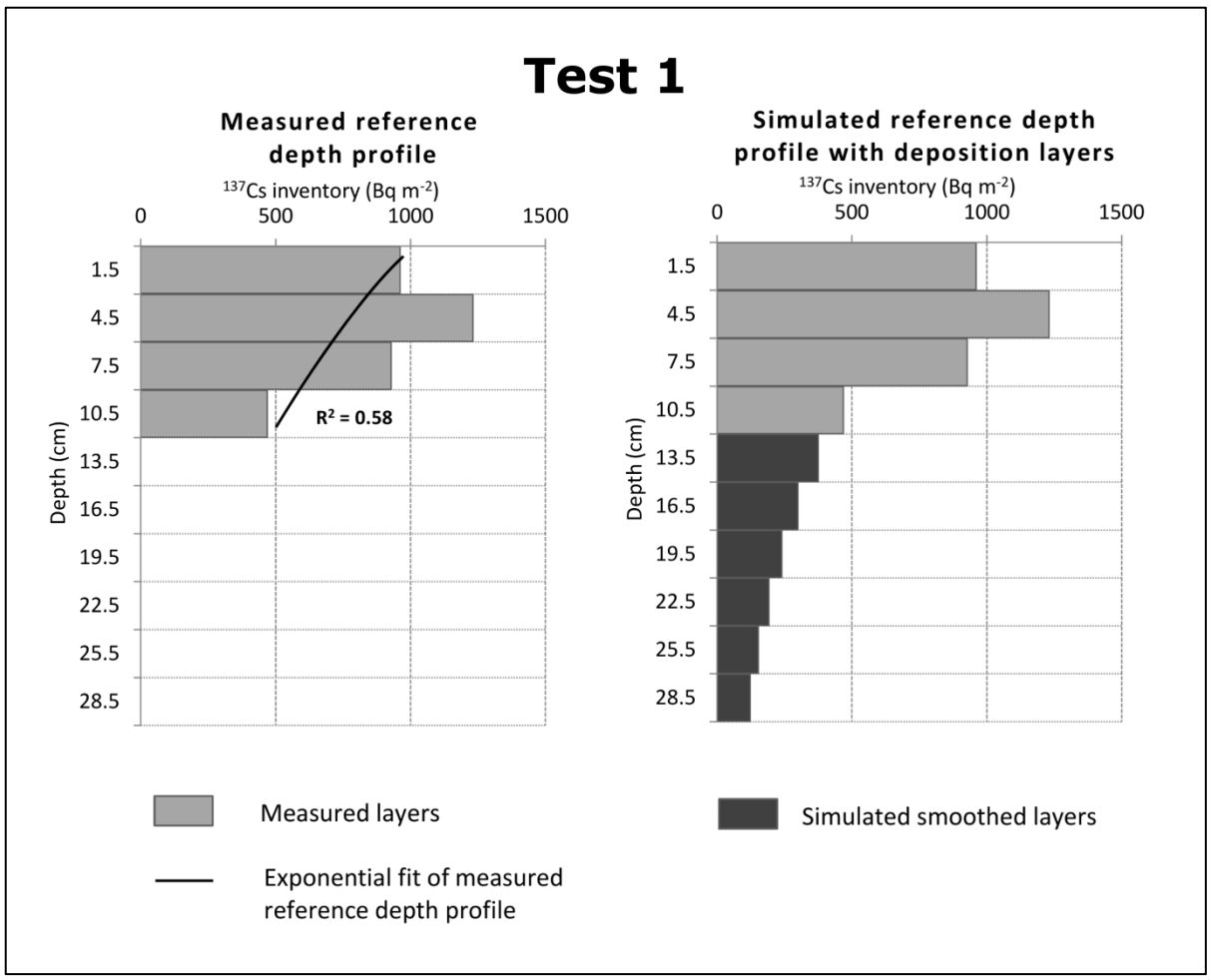

Figure 4-4: ^{137}Cs depth profile of the reference site of Test (1), with ^{137}Cs data on an unploughed study area in Aosta valley (Italy) from Ceaglio *et al.*, 2013, with exponential fit (left); Simulated depth profile with deposition layers (right).

To apply MODERN, the authors represented the reference depth profile according to the ^{137}Cs inventories of the three reference samples which have been sliced per 3 cm increments (Figure 4-4). Six additional layers - below the last measured horizon - were simulated with ^{137}Cs inventories declining exponentially. The ^{137}Cs inventories of the sampling sites are smaller than the reference inventory (i.e. 3588 Bq m^{-2}), pointing out net erosion processes affecting all investigated sites. Thus, no deposition layers have been modelled.

The average erosion rate estimated with MODERN is 8.5 t ha^{-1} yr^{-1}, which is consistent with the erosion rates of 8.8 t ha^{-1} yr^{-1} achieved using the Profile Distribution Model (Table 4-3). In particular, at sites with low inventory change, there is a high correspondence between the results obtained with MODERN and the PDM. For sites with larger deviations from the reference inventory (sites T11 and T25), the results show a significant discrepancy. The latter can be due to the fact that the PDM assumes an exponential decline of ^{137}Cs in the measured depth profile, even if the fit

of the depth profile to an exponential function returns a low R^2 of 0.58. MODERN instead follows the real ^{137}Cs depth distribution.

Table 4-2: Parameters used for MODERN tests on unploughed soil with ^{137}Cs data from Ceaglio *et al.*, 2013 (1) and on ploughed soil with $^{210}Pb_{ex}$ data from Iurian *et al.*, 2013 (2).

Parameter		Test 1 (^{137}Cs)	Test 2 ($^{210}Pb_{ex}$)
Inv_{inc}	Bq m^{-2}	469-1231	66-2579
inc	Bq m^{-2}	3	2.5
Inv	Bq m^{-2}	126-3192	3660-10970
d	cm	9	35-60
P	unitless	Not determined	0.74 – 2.39
P'	unitless	Not determined	0.47 – 0.83
*x**	cm	Target variable	Target variable
xm	kg m^{-2}	20-50	432-1054
t_1	yr	2010	2011
t_0	yr	1986	1911
Y	t ha^{-1} yr^{-1}	Target variable	Target variable

Table 4-3: Results of the MODERN test (1) compared to published results of the Profile Distribution Model (PDM, Ceaglio *et al.*, 2013).

Test 1: Uncultivated soil (^{137}Cs)		
Site	PDM	MODERN
	t ha^{-1} yr^{-1}	t ha^{-1} yr^{-1}
Transect 1		
T11	-10.1	-16.1
T12	-2.4	-2.5
T13	-6.6	-7.0
T14	-7.4	-5.3
T15	-3.1	-3.8
Transect 2		
T21	-10.7	-7.1
T22	-9.1	-10.5
T23	-5.6	-5.2
T24	-1.1	-1.6
T25	-32.1	-26.3

4.4.3 MODERN application to a case study in a Romanian valley tracking $^{210}Pb_{ex}$ in ploughed soils (Test 2)

With a half-life of 22.3 years, geogenic ^{210}Pb is a natural radioactive form of lead which originates as a decay product of ^{238}U. During this decay process, ^{222}Rn partially escapes from the soil surface into the atmosphere, producing ^{210}Pb fallout. The part

of ^{210}Pb which remains in the soil is usually termed supported lead and the fallout fraction, reaching the ground via precipitation, is called unsupported lead or lead in excess ($^{210}Pb_{ex}$). $^{210}Pb_{ex}$ is being used as a soil erosion and sediment tracer since many years (Mabit *et al.*, 2008, 2014; Matisoff, 2014).

To perform our next test, the authors used the $^{210}Pb_{ex}$ determination and the resulting soil redistribution rates obtained in the frame of a recent study which was conducted in a cultivated area located in the central part of the Transylvanian Plain, in Romania (Iurian *et al.,* 2013). In this study, where a $^{210}Pb_{ex}$ reference inventory of 9640 Bq m^{-2} was established, two parallel transects having different ploughing practices (up and down the slope and across the slope) were investigated and a total of 14 soil cores (12 bulk and 2 incremental) were collected and the $^{210}Pb_{ex}$ inventories were calculated (Table 4-2). The conversion of $^{210}Pb_{ex}$ inventories into soil redistribution rates for these ploughed soils (t ha^{-1} yr^{-1}) was done using the Mass Balance Model (MBM, Walling *et al.* 2002), where the total $^{210}Pb_{ex}$ inventory (*Inv*, Bq m^{-2}) at year *t* (yr) can be expressed as:

$$Inv = Inv_{ref}\left(1 - P\frac{\Delta L}{D}\right)^{(t^1 - t^0)} \quad (7)$$

where ΔL = annual soil loss (m), *D* = cultivation depth (m) and *P* is the particle size factor (unit less) for erosional sites, a parameter which takes the grain size selectivity of erosion and deposition processes into account. Iurian *et al.* (2013) considered *P* at eroding sites to range between 1.25 and 2.1 in Transect 1, and 0.74 and 2.39 in Transect 2. In deposition sites, *P* was estimated to range between 0.37-0.85 (Transect 1) and 0.47-0.83 (Transect 2), which highlights preferential transport of finer particles. The parameters t^1 and t^0 (yr) are the sampling and the reference years, respectively. When using $^{210}Pb_{ex}$ as soil erosion tracer, it is commonly assumed that it provides information about erosion magnitude on a time scale of approximately 100 years.

ΔL is calculated as:

$$\Delta L = D\left[1 - \left(1 - \frac{Inv_{change}}{Inv_{ref}}\right)^{\frac{1}{(t^1 - t^0)}}\right] \quad (8)$$

The soil erosion rate Y (t ha^{-1} yr^{-1}) is finally calculated as:

$$Y = \frac{10B\Delta L}{P} \quad (9)$$

where *B* (kg m^{-3}) is the bulk density measured at the site. The model assumes that the original exponential depth distribution is distributed uniformly within the plough layer and that a downward migration beyond the cultivation depth is negligible.

The MBM results in average erosion rates of 20.1 t ha^{-1} yr^{-1} (Transect 1) and 17.3 t ha^{-1} yr^{-1} (Transect 2) (Iurian *et al.*, 2013). In sites P13 (Transect 1), P6 and P14 (Transect 2) the $^{210}Pb_{ex}$ inventories are higher than the reference inventory (10970, 9770 and 10600 Bq m^{-2}, respectively), highlighting deposition processes. Deposition rates

calculated with MBM were 12.2, 0.7 and 5.5 t ha^{-1} yr^{-1} for the sites P13, P6 and P14, respectively.

The authors took into account the influence of agricultural practices on the distribution of $^{210}Pb_{ex}$ in the sampling sites for the MODERN application. Thus, the depth profile was first reproduced as it was measured, and then it was adapted as if $^{210}Pb_{ex}$ has been mixed within the ploughed layers. As the ploughing depth of the sites is 20 cm, the simulated horizons of the reference profile from 0 to 20 cm depth were set to have an averaged $^{210}Pb_{ex}$ inventory (Figure 4-5).

To investigate deposition processes with MODERN, the authors simulated two deposition layers above the measured depth profile. The $^{210}Pb_{ex}$ inventory of those simulated layers was set as the average value of the $^{210}Pb_{ex}$ inventory measured in the top horizon of the reference site (Figure 4-5, Deposition scenario). To convert MODERN results from cm to t ha^{-1} yr^{-1}, selecting a reference year (t^0) as starting point of the investigated time window is required. To be consistent with MBM assumptions, the authors defined a time window of 100 years (with t^0= 1911). The particle size factor provided for each site by Iurian *et al.*, 2013, was also considered.

Table 4-4: Results of the MODERN test (2) compared to published results of the Mass Balance Model (MBM) (Iurian *et al.*, 2013).

Test 2: Cultivated soil ($^{210}Pb_{ex}$)		
Site	MBM t ha^{-1} yr^{-1}	MODERN t ha^{-1} yr^{-1}
Transect 1		
P1	-19.6	-10.8
P3	-18.9	-10.1
P5	-6.7	-5.0
P7	-26.3	-13.8
P9	-23.1	-10.1
P11	-26.2	-15.0
P13	12.2	10.2
Transect 2		
P2	-12.5	-7.1
P4	-16	-9.4
P6	0.7	0.8
P8	-12.2	-7.4
P10	-26.4	-14.5
P12	-19.5	-10.2
P14	5.5	4.3

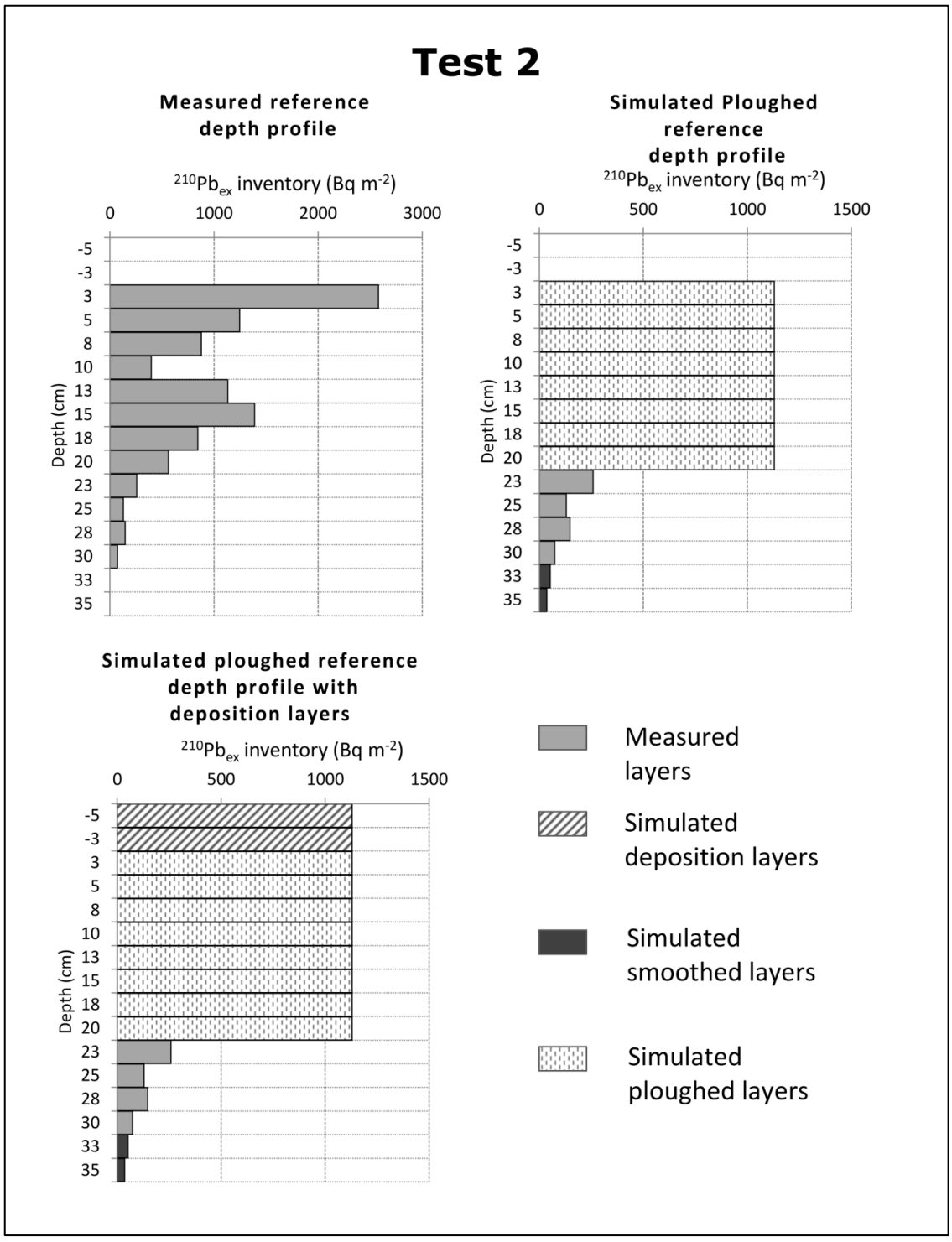

Figure 4-5: $^{210}Pb_{ex}$ of the reference site of Test (2), with $^{210}Pb_{ex}$ data on a ploughed study area in Transylvanian Plain (Romania) from Iurian *et al.*, 2013 (upper left); Simulated ploughed depth profile with the inventories of the top 20 cm of the reference profile to have an averaged $^{210}Pb_{ex}$ inventory as a result of soil mixing processes due to tillage (upper right); Simulated ploughed depth profile with additional ploughed layers (bottom left).

Average erosion rates estimated with MODERN are lower than the obtained MBM results, with average erosion rates of 10.8 t ha^{-1} yr^{-1} (Transect 1) and 9.7 t ha^{-1} yr^{-1} (Transect 2) (Table 4-4). However, deposition rates calculated with the two models are similar, with a mean standard deviation of 0.8 t ha^{-1} yr^{-1}. The correlation coefficient between MODERN and MBM results reaches 0.99.

The application of MODERN to the two selected studies highlighted its potential to convert FRN inventories into soil redistribution rates for two different FRN and with different land use of the sites. The results of MODERN correlate closely with the previously published results (R = 0.91) (Figure 4-6).

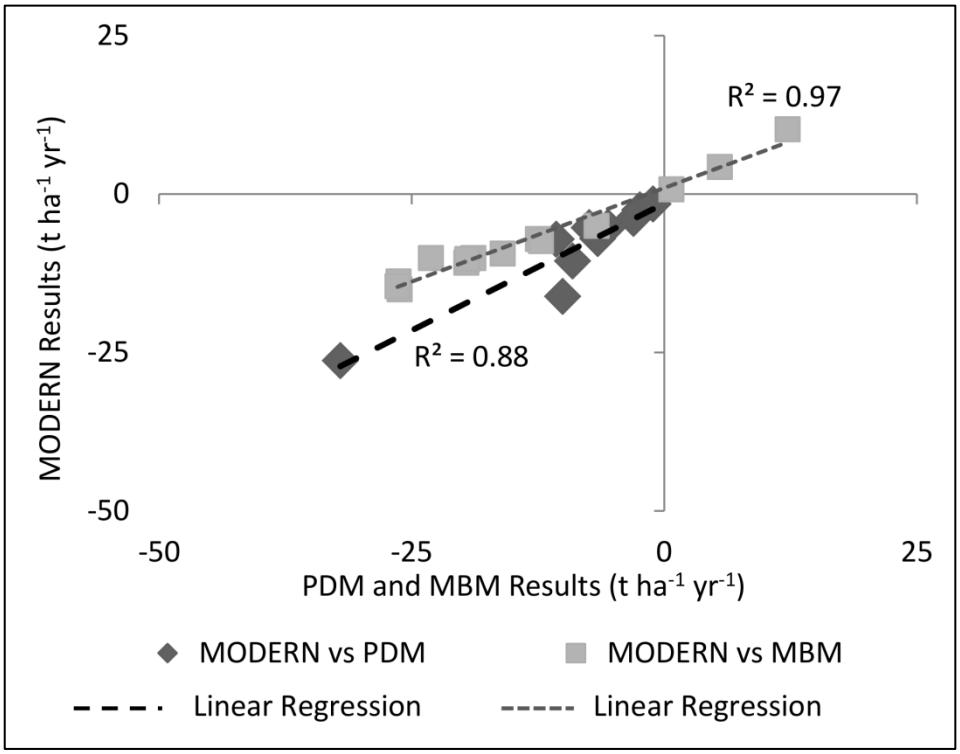

Figure 4-6: Relationship between the soil redistribution rates of MODERN and the Profile Distribution Model (PDM) (Test 1) and of Mass Balance Model (MBM)(Test 2).

4.5 Conclusions

A new FRN conversion model to assess soil redistribution has been proposed, described and tested for different FRN and land use conditions. This model, MODERN, is based on a unique algorithm and a clear and transparent concept. The ability of MODERN to reproduce precisely any FRN depth profile permits a high adaptability to different environmental conditions. The FRN depth profile in the reference site plays a fundamental role in the conversion of FRN inventories into soil redistribution rates, as it is often implemented to describe the shape of FRN depth distribution in the investigated sites before disturbance. The FRN distribution reflects the influence of (i) the behaviour of the selected FRN in the soil and (ii) the characteristic of a study area, in respect to land use, weather conditions, and soil properties. As each study on soil erosion processes presents its own site specific characteristics, any general assumption on the depth distribution of FRN in the soil may prejudice the correct estimation of soil redistribution rates. MODERN allows also to reflect the variability of environmental and agriculture processes responsible for soil redistribution through the establishment of different deposition scenarios. Given the high uncertainty related to deposition dynamics, the authors believe that a presentation of a range of possible solutions and deposition scenarios is the best option in soil erosion studies.

The main limitations of MODERN are the following. So far time-variant fallout input and time-variant migration processes of FRN into soil are not accounted for by MODERN. In both ploughed and unploughed soils some of the fresh fallout that accumulates close to the soil surface is likely to be removed by erosion prior to moving further down into the soil by diffusion or migration or being incorporated into the plough layer by tillage. If this is the case, MODERN might overestimate results. MODERN also does not consider the decay of the selected FRN. Prior the application, the FRN measurements need to be decay corrected to the same year.

Major advantages of the MODERN model can be summarised as follows (i) it is applicable for both erosion and deposition scenarios; (ii) it considers the precise depth distribution of the reference site, independently of its shape; (iii) the parameters required for its application are simple and can be determined with certainty; and (iv) it can easily be adapted to different land use scenarios (e.g. ploughed and unploughed sites). A free and public release of the MODERN model will be associated with this publication. The model codes can be downloaded at modern.umweltgeo.unibas.ch and can be modified for any scientific purpose. This transparent and easily modifiable model will promote a wider application of FRN to assess soil erosion/sedimentation under various agro-climatic and land use conditions.

Acknowledgements

This work was funded by the Swiss National Science Foundation (SNF), project no. 200021-146018. The authors also acknowledge the International Atomic Energy Agency (IAEA) for support provided through the technical project 20435 and the Coordinated Research Project (CRP) D1.50.17 on "*Nuclear techniques for a better understanding of the impact of climate change on soil erosion in upland agro-ecosystems*".

CHAPTER 5: MODELLING DEPOSITION AND EROSION RATES WITH RADIONUCLIDES (MODERN) - PART 2: A COMPARISON OF DIFFERENT MODELS TO CONVERT $^{239+240}$PU INVENTORIES INTO SOIL REDISTRIBUTION RATES AT UNPLOUGHED SITES

This chapter is published in the *Journal of Environmental Radioactivity* as: Arata, L.[1], Alewell, C. [1], Frenkel, E. [2], A'Campo-Neuen, A. [3], Iurian, A.-R. [4,5], Ketterer, M. E. [6], Mabit, L. [7], and Meusburger, K. [1]: *Modelling Deposition and Erosion rates with RadioNuclides (MODERN) – Part 2: A comparison of different models to convert 239+240Pu inventories into soil redistribution rates at unploughed sites*, Journal of Environmental Radioactivity, 162–163, 97-106, 2016.

(1) Environmental Geosciences, Department of Environmental Sciences, University of Basel, Switzerland,

(2) Institute de Recherche Mathématique Avancée (IRMA), University of Strasbourg, France,

(3) Department of Mathematics and Computer Science, University of Basel, Switzerland,

(4) Faculty of Environmental Science and Engineering, Babes-Bolyai University, Cluj-Napoca, Romania,

(5) Consolidated Radioisotope Facility, Plymouth University, Plymouth, UK,

(6) Chemistry Department, Metropolitan State University of Denver, Colorado, USA,

(7) Soil and Water Management & Crop Nutrition Laboratory, FAO/IAEA Agriculture & Biotechnology Laboratory, Seibersdorf, Austria.

5.1 Abstract

Sheet erosion is one of the major threats to alpine soils. To quantify its role and impact in the degradation processes of Alpine grasslands, the application of Fallout Radionuclides (FRN) showed very promising results. The specific characteristics of Plutonium 239+240 ($^{239+240}$Pu), such as the homogeneous fallout distribution, the long half-life and the cost and time effective measurements make this tracer application for investigating soil degradation in Alpine grasslands more suitable than any other FRN (e.g. ^{137}Cs). However, the conversion of $^{239+240}$Pu inventories into soil erosion rates remains a challenge. Currently available conversion models have been developed mainly for ^{137}Cs with later adaptation to other FRN (e.g. Excess ^{210}Pb, and ^{7}Be), each model being defined for specific land use (ploughed and/or unploughed) and processes (erosion or deposition). As such, they may fail in describing correctly the distribution of Pu isotopes in the soil. A new conversion model, MODERN, with an adaptable algorithm to estimate erosion and deposition rates from any FRN inventory changes was recently proposed (Arata *et al.*, 2016). In this complementary contribution, the authors compare the application of MODERN to other available conversion models. The results show a good agreement between soil redistribution rates obtained from MODERN and from the models currently used by the FRN scientific community (i.e. the Inventory Method). MODERN outputs are the least sensitive to the reference inventory variability.

5.2 Introduction

The application of fallout radionuclides (FRN) as soil tracers is currently one of the most promising and effective approaches to assess soil erosion and deposition rates in mountainous grasslands (e.g Schaub *et al.,* 2010, Konz *et al.*, 2012). Conventional methods (e.g. sediment cups, erosion pins or irrigation experiments) are laborious and constrained by the extreme topographic and climatic conditions of the Alps. They may also fail to track the influence of snow processes and animal activity (sheep and cattle trails) to soil redistribution processes in the Alps (Meusburger *et al.*, 2014).

The artificial fallout radionuclide ^{137}Cs (half-life = 30.2 years) is the most commonly employed FRN to study soil redistribution (Mabit *et al.*, 2008, 2013). However the application of ^{137}Cs in alpine grasslands is compromised by the high spatial heterogeneity of the fallout at the reference sites (Alewell *et al.*, 2014). The cause of such heterogeneity is most likely due to the origin of the ^{137}Cs fallout in the Alps, which is linked to single rain events just after the Chernobyl accident when most of Alpine soils were still covered with snow (Schaub *et al.*, 2010).

As a suitable alternative, the two long-life Plutonium isotopes (i.e. ^{239}Pu [half-life = 24110 years] and ^{240}Pu [half-life = 6561 years]) have been suggested and tested as soil erosion tracers in the Alps (Schimmack *et al.*, 2002, Alewell *et al.*, 2014). In

contrast to ^{137}Cs, $^{239+240}$Pu is part of the non-volatile fraction of reactor releases in case of nuclear power plant accidents. As such, there was no long range transport of Chernobyl Pu influencing Alpine areas (Eikenberg *et al.*, 2001). The origin of Plutonium fallout is rather linked to the nuclear bomb tests, which took place mostly from 1954 to the mid-1960s (Ketterer *et al.,* 2004). Therefore, the $^{239+240}$Pu deposition is not connected to few specific rain events, and as a result, its distribution in the Swiss alpine soils is more homogeneous than ^{137}Cs deposit (Schimmack *et al.*, 2002, Alewell *et al.*, 2014). The longer half-life of $^{239+240}$Pu ensures also its longer term environmental availability, with respect to ^{137}Cs. In addition, isotopic measurements of Pu can be performed by ICP-MS, a more cost and time effective technique compared to classical spectrometry determination (Ketterer *et al.,* 2004)

To convert $^{239+240}$Pu inventories into quantitative estimates of soil redistribution rates, a specific conversion model is needed. Such models compare the total radionuclide activity per unit area (inventory) in a given sampling site to an undisturbed reference site, where no soil redistribution processes have occurred since the main deposition. To estimate soil erosion rates in alpine grasslands, the conversion model needs to take into account the specific depth distribution of FRN in unploughed soils, where soil stratification reflects near-natural conditions. In unploughed soils, the Profile Distribution Model (PDM) and the Diffusion and Migration Model (DMM) (Walling and Quine, 1990, Walling and He 1997, Walling *et al.*, 2002, 2011, 2014) are the most widely employed and established models to convert FRN inventories to soil erosion rates. These models were originally developed to convert ^{137}Cs inventories into soil redistribution rates. Their application to $^{239+240}$Pu inventories may produce significant bias, because ^{137}Cs and $^{239+240}$Pu can have differing depth distribution patterns in soils (attributed to differing time since main fallout in Chernobyl affected areas and differing sorption behaviour in soils). Upon authors knowledge, only scarce applications of Pu isotopes in soil erosion have been performed so far (Schimmack *et al.*, 2002, Everett *et al.*, 2008, Tims *et al.*, 2010, Hoo *et al.*, 2011, Lal *et al.*, 2013, Xu *et al.*, 2013, Alewell *et al.*, 2014, Zollinger *et al.*, 2014, Xu *et al.*, 2015) and only recently, Hoo *et al.* (2011) and Lal *et al.*, (2013) proposed algorithms to derive erosion rates from Pu inventories. Efforts by the authors to apply the model suggested by Hoo *et al.* (2011) were not successful, as the calibration of a parameter (i.e. □) included in the algorithm returned calculation errors. Thus, the Inventory Method (IM) of Lal *et al.* (2013) remains the only model which was suggested specifically for the conversion of $^{239+240}$Pu inventories into erosion rates for unploughed soils.

The Inventory Method assumes that the FRN depth distribution in the soil is characterized by an exponential function. In the Swiss Alps, the exponential distribution could be applied for ^{137}Cs, which is especially located in the upper most horizons, as its main fallout was in 1986 and it is known to have a slow migration rate in soils (Bossew and Kirchner, 2004). But, as $^{239+240}$Pu fallout begun in the early '50s, with a maximum around 1963, its depth distribution in soil has a different

characteristics. Previous results show that the $^{239+240}$Pu depth profile in Swiss alpine soils follows a polynomial profile with the peak content between 3 and 6 cm soil depth (Chawla *et al.*, 2010, Alewell *et al.*, 2014). Plutonium is preferentially adsorbed by organic matter, and especially by humic acids, and therefore retained near the surface (Chawla *et al.*, 2010, Alewell *et al.*, 2014). The lower concentrations in the very top soil may be due to plant uptake after fallout deposition (Chawla *et al.* 2010). The accurate description of $^{239+240}$Pu concentration in the top soil is fundamental, as a wrong assumption on the $^{239+240}$Pu depth profile may bias the assessment of soil erosion rates considerably.

The accurate description of $^{239+240}$Pu concentration in the top soil is fundamental, as a wrong assumption on the $^{239+240}$Pu depth profile may bias the assessment of soil erosion rates considerably. Recently, the new conversion model MODERN (Modelling Deposition and Erosion rates with RadioNuclides, Arata *et al.*, submitted) has been proposed. Due to its characteristics, MODERN enables to represent the precise depth distribution of any FRN at a given reference site.

The aim of this study is to evaluate the applicability of MODERN to convert $^{239+240}$Pu inventories in soil redistribution rates in Alpine grasslands. Thus in this manuscript, the authors compare the performance of MODERN to the application of three established models to assess soil erosion rates from FRN inventories in unploughed soils: (i) the Inventory Method (IM) (Lal *et al.*, 2013), (ii) the Profile distribution model (PDM) (Walling *et al.*, 2002, 2011, 2014) and (iii) the Diffusion and Migration Model (DMM) (Walling *et al.*, 2002, 2011, 2014). The parameters included in the models (e.g. the migration velocity v and the diffusion coefficient D) were specifically adapted for the application to $^{239+240}$Pu inventories. MODERN allows describing not only erosion but also sediment deposition processes. In the depositional areas of the study areas, the stratification of the sedimentation layers resembles the situation of ploughed and thus homogenized layers. For this reason, MODERN deposition outputs were compared to the application of the Proportional Model (PM) (Walling *et al.*, 2002, 2011, 2014) which was originally developed to assess soil redistribution rates in ploughed soils.

5.3 Materials and methods

5.3.1 Study area and $^{239+240}$Pu measurements

The authors used the dataset established by Alewell *et al.* (2014). The targeted study area is the Urseren Valley (Canton Uri), in Central Switzerland Alps, where 6 reference sites and 9 sampling points were sampled in 2007. The 9 sampling points were collected on three different land use types with three replicates each: hayfield (HF1, HF2, HF3), pasture with dwarf shrubs (PAW1, PAW2, PAW3) and pasture without dwarf shrubs (PAWO1, PAWO2, PAWO3). For a more detailed description of the study site, see Meusburger and Alewell (2008).

The reference soil cores were sectioned into 3 cm increments down to a depth of 30 cm, to obtain detailed information on the $^{239+240}$Pu depth distribution. The cores of the sampling sites were sectioned in 10 cm increments down to a depth of 40 cm. All cores were oven-dried at 40°C for 48 h, sieved to the 2 mm fraction and dry-ashed. The measurement of Plutonium isotope ($^{239+240}$Pu) activities was performed at the Northern Arizona University using a Thermo X Series II quadrupole ICP-MS instrument which includes a high-efficiency desolvating sample introduction system (APEX HF, ESI Scientific, Omaha, NE, USA). A detection limit of 0.1 Bq kg^{-1} for $^{239+240}$Pu was obtained for samples of nominal 1 g of dry-ashed material; for $^{239+240}$Pu activities > 1 Bq kg^{-1}, the measurement error was 1–3%. Prior to mass spectrometry analysis, the samples were dry-ashed and spiked with ~ 0.005 Bq of a ^{242}Pu yield tracer (obtained as a licensed solution from NIST). Pu was leached with 16 M nitric acid overnight at 80°C, and was subsequently separated from the leach solution using a Pu-selective TEVA resin (Ketterer *et al.*, 2004). The masses of ^{239}Pu and ^{240}Pu present in the sample, determined by isotope dilution calculations, were converted into the summed $^{239+240}$Pu activity.

5.3.2 Conversion models to estimate erosion and deposition rates from $^{239+240}$Pu inventories

The $^{239+240}$Pu activities (*Pu act*, Bq kg^{-1}) were converted into inventories (Bq m^{-2}) according to the following equation:

$$Inv = Pu\ act \times xm \quad (1)$$

where *xm* is the measured mass depth (*xm*) of fine soil material (<2 mm fraction) (kg m^{-2}) of the respective soil sample.

The Inventory change (Inv_{change}) at each sampling site, with respect to the reference site, was calculated as:

$$\mathrm{Inv_{change}} = \frac{\mathrm{Inv_{ref}} - \mathrm{Inv}}{\mathrm{Inv_{ref}}} \times 100 \quad (2)$$

where Inv_{ref} is the local reference total inventory as mean of all reference sites (Bq m^{-2}) and *Inv* is the measured total inventory at a specific sampling point (Bq m^{-2}). Positive values of Inv_{change} indicate erosion, whereas negative values indicate deposition.

The **Inventory Method (IM)** (Lal *et al.*, 2013) has been developed specifically for the application of $^{239+240}$Pu. It considers that the inventory *Inv* (mBq cm^{-2}) of fallout plutonium in a soil column is:

$$Inv = \int_0^{z_{max}} N(z)dz \quad (3)$$

where z_{max} is the depth to the bottom of the soil column, and N(z) (mBq cm^{-3}) is the concentration of Pu at depth z (cm).

The loss of Pu inventory at the site i, Inv_{loss} (Bq m^{-2}), is the difference between the average Pu inventory from the reference sites Inv_{ref} and the measured Pu inventory at the investigated site. It can be expressed as:

$$Inv_{loss} = Inv_{ref} - Inv \quad (4)$$

The model assumes that the shape of Pu depth profile approximates an exponential function (Lal *et al.*, 2013), described by the exponent □. The loss of soil, *L* (cm), is obtained by solving the equation:

$$Inv_{loss} = \int_0^L N(z)dz = \int_0^L N(0)e^{-\alpha z}dz \quad (5)$$

And, with $Inv_{ref} = N(0)/$□, it results in:

$$L = -\frac{1}{\alpha}\ln(1 - \frac{Inv_{loss}}{Inv_{ref}}) \quad (6)$$

To consider the grain size selectivity of soil redistribution processes, an additional parameter is also included in equation (6), which results in:

$$L = -\frac{1}{\alpha P}\ln(1 - \frac{Inv_{loss}}{Inv_{ref}}) \quad (7)$$

where *P* (unit less) is the particle size factor which takes the grain size selectivity of erosion and deposition processes into account. To convert IM results (*L)* from cm to erosion rates *ER* (t ha^{-1} yr^{-1}), the following formula is used:

$$ER = 10 \times \frac{L \cdot xm}{d \cdot (t_1 - t_0)} \quad (8)$$

where *xm* is the mass depth (kg m^{-2}) of the sampling site, *d* is the depth increment considered at the sampling site, t_1 is the sampling year (here 2007). t_0 (yr) is the starting year of the Pu fallout (1954).

The **Profile Distribution Model** is a conversion model developed for unploughed soils, widely used especially for ^{137}Cs (e.g. Porto *et al.*, 2001). It assumes an exponential decline of the depth distribution of the radionuclide in the soil (as the Inventory Method), which can be described by the following function:

$$Inv(xm_r) = Inv_{ref}(1 - e^{-xm_r/h_0}) \quad (9)$$

Where xm_r (kg m^{-2}) is the mass depth of the reference site (obtained as a mean value of the mass depths of the reference sites) and h_0 (kg m^{-2}) is a coefficient describing the profile shape. The greater the value of h_0, the deeper is the penetration of the radionuclide into the soil (Walling *et al.*, 2002).

At an eroding point (where the total inventory *Inv* is less than the reference inventory Inv_{ref}), the erosion rate *ER* (t ha^{-1} yr^{-1}) can be estimated using the following relationship (Walling and Quine, 1990):

$$ER = -\frac{10}{P \times (t' - t)}\left[\ln(1 - \frac{Inv_{change}}{100})\right]h_0 \quad (10)$$

Where *t'* and *t* (yr) are the sampling year and the starting year of Pu fallout, respectively.

The **Diffusion and Migration Model (DMM)** is a one-dimensional transport model (Walling *et al.*, 2002, 2011, 2014). It considers a diffusion coefficient *D* (kg^{-2} m^{-4} yr^{-1}) and a migration rate *v* (kg m^{-2} yr^{-1}) for the FRN in the soil profile. The diffusion coefficient (*D*) and the migration rate (*v*) characterize the evolution of the shape of the FRN profile with time. High values of *D* and *v* imply a deeper penetration of the FRN into the soil profile. The model also takes into account the potential temporal variation of the radionuclide distribution with soil depth.

The DMM is based on the equation describing the variation of the FRN concentration *C* (Bq kg^{-1}) in a soil at time *t* (yr):

$$C(t) \approx \frac{I(t)}{H} + \int_{t}^{t-1} \frac{I(t')e^{-R/H}}{\sqrt{D\pi(t-t')}} e^{-v^2(t-t')/(4D)-\lambda(t-t')}\, dt' \quad (11)$$

H (kg m^{-2}) is the relaxation mass depth of the initial distribution of the FRN in the soil profile, and is defined as the mass depth at which the FRN concentration reduces to 1/*e* of the surface concentration, assuming an exponential depth distribution. This value can be determined experimentally by observing the behaviour of the applied radionuclide on a soil surface using a rainfall simulator. Walling *et al.* (2002, 2011, 2014) suggested a value of ~5 kg m^{-2} for ^{137}Cs. As Cs and Pu showed to have comparable migration rates (Kirchner *et al.*, 2009), and in the existing literature no values are available for Pu, the same value of the relaxation mass depth was used for Pu as indicated for ^{137}Cs. The parameter is the $^{239+240}$Pu effective decay constant, calculated using the weighted mean of ^{239}Pu and ^{240}Pu half-lives and their relative isotopic concentrations. *I(t)* is the annual atmospheric FRN deposition flux at time t. Values of *I(t)* are reported for ^{137}Cs, from 1954 to the present, and based on the record of ^{137}Cs deposition in the northern hemisphere as a result of the nuclear weapon tests (Bq m^{-2} yr^{-1}). So far, no measurements of $^{239+240}$Pu annual deposition in the Swiss Alps have been published in the literature. To determine *I(t)*, the authors used the ratio between $^{239+240}$Pu and ^{137}Cs inventories in the study area, as calculated by Alewell *et al.* (2014), which has a mean value of 0.0029. Multiplying this specific ratio by the annual atmospheric ^{137}Cs deposition in the Norther Hemisphere, for each year since 1954, the values for *I(t)* of $^{239+240}$Pu were defined.

The $^{239+240}$Pu migration velocity *v* and the diffusion coefficient *D* values were determined using the least squares method to fit the function *C(t)* to the vertical distribution data of Pu from the reference site, using the following equation (Bossew and Kirchner, 2004):

$$C(x,t,I_0,D,v) = I_0 e^{-\lambda t}\left\{\frac{1}{\sqrt{\pi D t}} e^{-(x-vt)^2/(4Dt)} - \frac{v}{2D} e^{vx/D} erfc\left(\frac{v}{2}\sqrt{\frac{t}{D}} + \frac{x}{2\sqrt{Dt}}\right)\right\} \quad (12)$$

where *C(x,t,J$_0$,D,v)* is the $^{239+240}$Pu content in soil originating from nuclear tests and *I$_0$* (Bq cm^{-2} yr^{-1}) the initial nuclear tests deposition considered for the time of the

maximum release. The values of the diffusion constant, *D* (cm^2 yr^{-1}), and velocity, *v* (cm yr^{-1}) were distinctly derived for each of the six reference profiles by applying the least square fitting procedure. Furthermore, using the mean bulk density *B* (g cm^{-3}) of each incremental reference soil core, averaged *D* (kg^2 m^{-4} yr^{-1}) and *v* (kg m^{-2} yr^{-1}) values were included in the DMM model (see Table 5-1). For an eroding point, the erosion rate *ER* (t ha^{-1} yr^{-1}) may be estimated from the reduction in the inventory Inv_{loss} (Bq m^{-2}) using the relationship:

$$\int_0^t P \cdot ER \cdot C_u(t')e^{-\lambda(t-t')}dt' = Inv_{loss} \quad (13)$$

The **Proportional Model (PM)** is the most simple and commonly used empirical model for estimating soil sedimentation rates from FRNs. It was established for the assessment of soil redistribution rates in ploughed soils and has been used worldwide by many authors (see Ritchie and McHenry, 1990). This model is based on the assumption that all deposited FRN are mixed within the plough layer and that the proportion of eroded soil is directly proportional to the reduction of FRN inventory in the soil profile. One major advantage of the PM is that it can be also used to estimate deposition rates (see Walling *et al.*, 2002), with just a small change in the formula, where *P* (i.e. a particle size correction factor for eroded sites) is substituted with *P'*, a specific particle size correction factor adapted to deposition sites. The PM was used only to estimate deposition rates at deposition sites, where the deposited layers are assumed to be almost completely mixed, similar to ploughed layers.

The deposition rate *DR* (t ha^{-1} yr^{-1}) can be expressed as:

$$DR = 10\,\frac{B \times d \times Inv_{change}}{P' \times (t'-t) \times 100} \quad (14)$$

where *B* (kg m^{-3}) is the bulk density of the soil and *d* (m) is the depth of the plough layer. As for this study the authors considered as *d* the total depth of the layer (0.15 m).

The new conversion model **MODERN** (MOdelling Deposition and Erosion rates using RadioNuclides) allows to reproduce the measured depth distribution of the $^{239+240}$Pu isotopes at the reference site, avoiding any assumption or generalisation of its shape (Arata *et al.*, submitted). By overlapping the total inventory of the sampling site to the depth profile of the reference site, MODERN permits to find the intersect point along the soil profile where their values match. For a detailed description of the MODERN algorithm see Part 1 of the present study (Arata *et al.*, submitted).

The $^{239+240}$Pu depth profile at the reference sites is modelled as a step function *g(x)*, which for each increment *inc* returns the value *Inv(inc)* (Bq m^{-2}). The plutonium total inventory of a sampling site is given by *Inv* (Bq m^{-2}), measured for the whole increment of depth *d* (cm). The model targets the level *x*(cm)* from *x** to *x*+ d* (cm), where the cumulated value of the plutonium inventory at the reference site is equal to *Inv*. Therefore *x** should fulfil the following equation:

$$\int_{x^*}^{x^*+d} g(x)dx = Inv \quad (15)$$

A speciality of MODERN is its ability to adapt the depth profile of the reference site, through the addition of simulated layers on top or below the measured depth profile. These adaptations aim to return a solution for extremely high or low FRN inventories at the sampling sites. Note that MODERN does not make any assumption or generalisation of the shape of the measured reference site depth profile. Five layers below the measured depth profile were simulated in this study, and an exponential smoothing of the inventories is modelled (Figure 5-1).

The adaptation of the depth profile with additional layers above the measured layers permits the estimation of deposition rates. In this study the authors simulate three layers above the measured depth profile and assume that on average the deposition material origins from the top 6 cm of eroded soil that is homogenously mixed during transport. Consequently the $^{239+240}$Pu inventory contained in each deposited layer is assumed to be equal to the mean inventory of the first two surface reference layers i.e. layers 1 and 2 (Figure 5-1).

The cumulated total $^{239+240}$Pu inventory of the reference site, including the new simulated layers, is described by the integral function *S* (Figure 5-1), where:

$$S(x) = \int_{x}^{x+d} g(x')dx' \quad (16)$$

The function *S* can be solved through the primitive function *G* of the distribution function *g(x)* as follows:

$$S(x) = G(x+d) - G(x) \quad (17)$$

MODERN returns the results (*L*) in cm. To convert them to yearly soil losses/gains *ER*/*DR* in t ha^{-1} yr^{-1}, the equation (8) is used. If the particle size factor is available, it is possible to consider this parameter with MODERN in simply dividing the results by it.

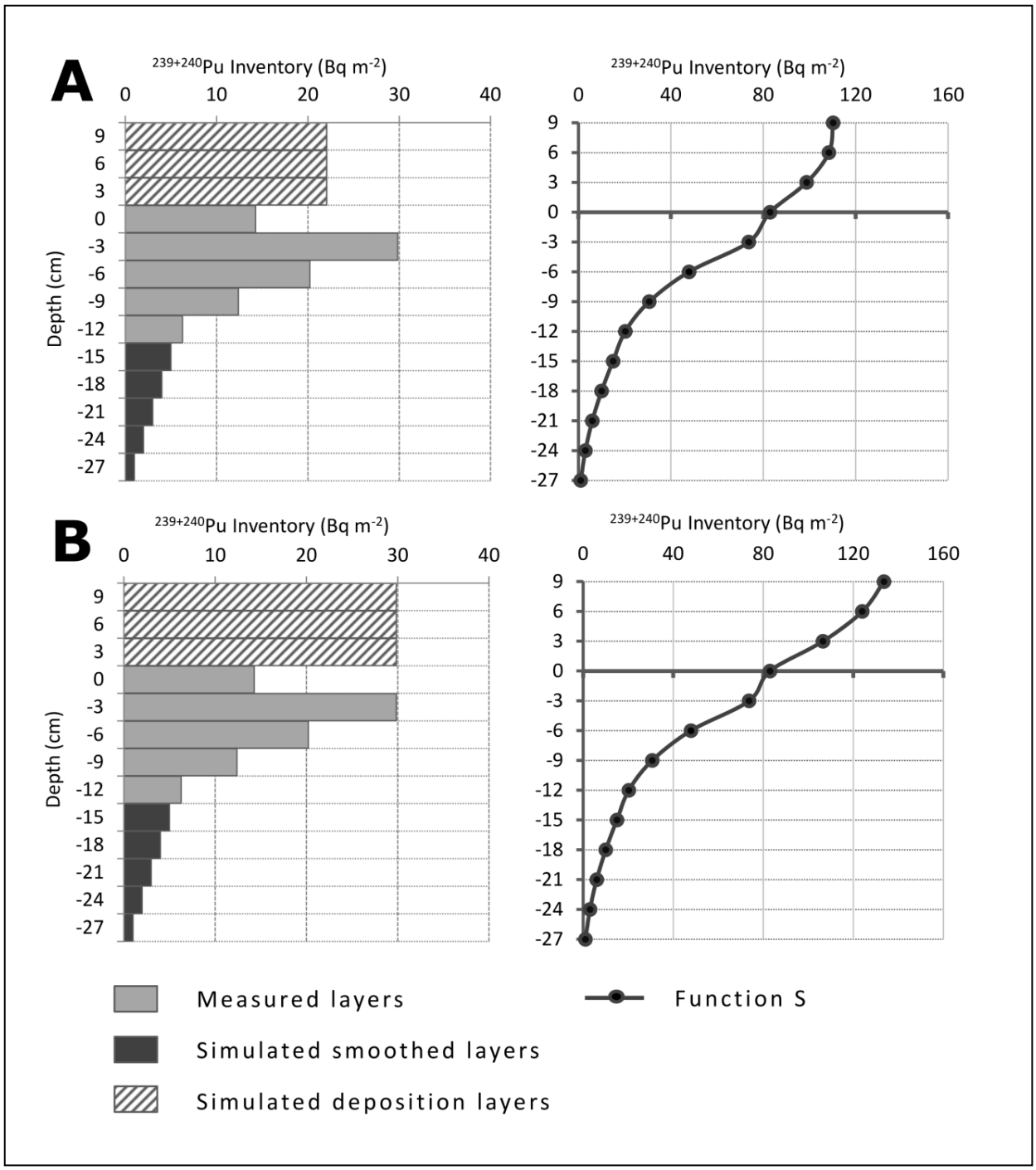

Figure 5-1: (A): Adaptation of the reference depth profile with MODERN. Five layers have been simulated below the measured depth profile, where an exponential smoothing of the inventories is modelled. Three layers have been simulated above the measured depth profile, where we assume that the deposition material origins from the top 6 cm of soil, and that is mixed during the transport (left). Resulting functions S, which describes the cumulated 239+240Pu inventory of the simulated reference depth profile, considered for each increment of length d= 15 cm (right). (B): Adaptation of the reference depth profile with MODERN for sites HF 3 and PAW 2, where the deposition material origins from the most enriched layer of the measured depth profile (left). Resulting functions S (right).

Table 5-1: List of parameters included in the conversion models to estimate soil erosion rates from 239+240Pu inventories. The mean measured values (with standard deviation) for the study area and the set values (indicated by the symbol *) used for the application of the models are indicated, where IM: Inventory Method, PDM: Profile Distribution Model, DMM: Diffusion and Migration Model, PM: Proportional Model, and M: MODERN. x indicates that the parameter is included in the model, whereas x' indicates that the parameter is needed to convert the result from cm to t ha-1 yr-1.

			Models				
Parameters	Description	Mean value	IM	PDM	DMM	PM	M
Inv_{ref}	Pu Reference total inventory (Bq m^{-2})	83 ± 11	x	x	x	x	
Inv_{inc}	Pu reference Inventory at each increment *inc* (Bq m^{-2})	6-30					x
inc	Depth increment of the reference site (cm)	3					x
Inv	Pu total Inventory at sampling site (Bq m^{-2})	84 ± 30	x	x	x	x	x
g(x)	Step function describing Pu inventory at reference site	-					x
S(x)	Simulated total inventory of reference sites (Bq m^{-2})	-					x
Inv_{change}	Inventory change (%)	14 ± 31		x		x	
Inv_{loss}	Inventory loss (Bq m^{-2})	12 ± 26	x		x		
t	Sampling year (yr)	2007*	x'	x		x	x'
t'	Starting fallout year (yr)	1954*	x'	x		x	x'
B	Bulk density of the sampling site (kg m^{-3})	1.17				x	
d	Depth of the plough/sampled layer (m)	0.15*				x	x
P	Particle size correction factor for Erosion (unitless)	1*	x	x			x
P'	Particle size correction factor for Deposition (unitless)	1*				x	x
xm	Mass depth of the sampling site (kg m^{-2})	110	x'				x'
xm_r	Mass depth of the reference site (kg m^{-2})	117		x			
h_0	Profile shape factor (kg m^{-2})	47		x			
□	Exponential factor (cm^{-1})	-0.09	x				
C	Pu concentration in top layer at reference site (Bq kg^{-1})	1.14			x		
D	Diffusion coefficient (kg^2 m^{-4} yr^{-1})	16			x		
v	Migration rate (kg m^{-2} yr^{-1})	0.96			x		
H	Relaxation depth (kg m^{-2})	5*			x		
□	$^{239+240}$Pu effective decay constant (yr^{-1})	0.00004*			x		
R	Erosion rate (t ha^{-1} yr^{-1})	Target Variable		x	x		
L	Erosion rate (cm)	Target Variable	x				x
DR	Deposition rate (t ha^{-1} yr^{-1})	Target Variable				x	x

5.3.3 Particle-size selectivity of erosion and deposition processes

Small grain size fractions in soil samples tend to be enriched in FRN concentrations and might be preferentially transported during sheet erosion processes (IAEA, 2014).

To take into account the preferential transport of smaller grain size particles with higher specific surface area – and thus higher FRN content – a particle size correction factor (*P* or *P' in case of deposition)* is usually proposed by most conversion models.

Since information on the FRN concentration in soil mobilised by erosion and deposited with the sediments may be very difficult to obtain, estimates of these parameters can be deduced from the information obtained on the grain size composition of the surface soil, eroded sediment and deposited sediment. As proposed by He & Walling (1996), the value of *P* can be expressed as:

$$P = (\frac{S_{ms}}{S_{sl}})^{v} \quad (18)$$

Where S_{ms} is the specific surface area of mobilized sediment (m^2 g^{-1}); S_{sl} is the specific surface area of the source soil (m^2 g^{-1}) and *v* is a constant with a value of ~0.65 (He & Walling, 1996). For deposition sites, the value of *P'* can be determined using the below equation:

$$P' = (\frac{S_{ds}}{S_{ms}})^{v} \quad (19)$$

Where S_{ds} is the specific surface area of deposited sediment (m^2 g^{-1}) and the value of *v* is the same as for equation (18). However, even the estimation and the definition of the specific surface area of the preferentially transported sediments are very demanding. Thus, even though particle size factors might influence model results considerably, published results on implementation of *P*/*P'* into models are scarce (e.g. Van Pelt *et al.*, 2007, Por□ba and Bluszcz, 2008).

In our study area, two rainfall simulation tests have been conducted to investigate the transport of different grain sizes due to soil erosion processes (Tresch, 2014). A stable isotope analysis was performed on the eroded samples obtained by the rainfall simulations (n = 22), to investigate any significant difference in Soil Organic Carbon (SOC) content between eroded and reference samples. Indeed, higher SOC content would indicate higher clay content and therefore smaller grain sizes. The preliminary results indicate very small differences in $\delta^{13}C$ values between eroded and reference samples (0.5-0.8%), and therefore no preferential transport of specific grain sizes. Thus, a particle size correction factor of 1 for all models selected in this study was assumed. Nevertheless, the authors recognize that a further analysis on this parameter is definitively needed in order to investigate its influence on the modelling procedures and the outputs produced.

5.4 Results and discussion

5.4.1 $^{239+240}$Pu inventories of the study area

At the reference sites, the $^{239+240}$Pu activity was measured down to a depth of 15 cm. The radionuclide maximum activity was found between 3 and 6 cm depth, with

values ranging from 0.8 to 2.6 Bq kg^{-1}. The depth profile of Pu inventories, as a mean value of 6 reference sites, follows a polynomial function, where a third-degree polynomial fit returns an R^2 reaching 0.97. In contrast, a least squares exponential fit of the Pu depth profile at reference sites is characterized by a lower R^2 of 0.49 (Figure 5-2, A). The mean total inventory, referring to a depth of 15 cm, is 83 Bq m^{-2} with a standard deviation of 11 Bq m^{-2}. The coefficient of variation (CV) of 13% among the reference sites inventories indicates a relatively homogeneous initial distribution of plutonium over the study area, and confirms its suitability as a potential tracer for soil redistribution investigation.

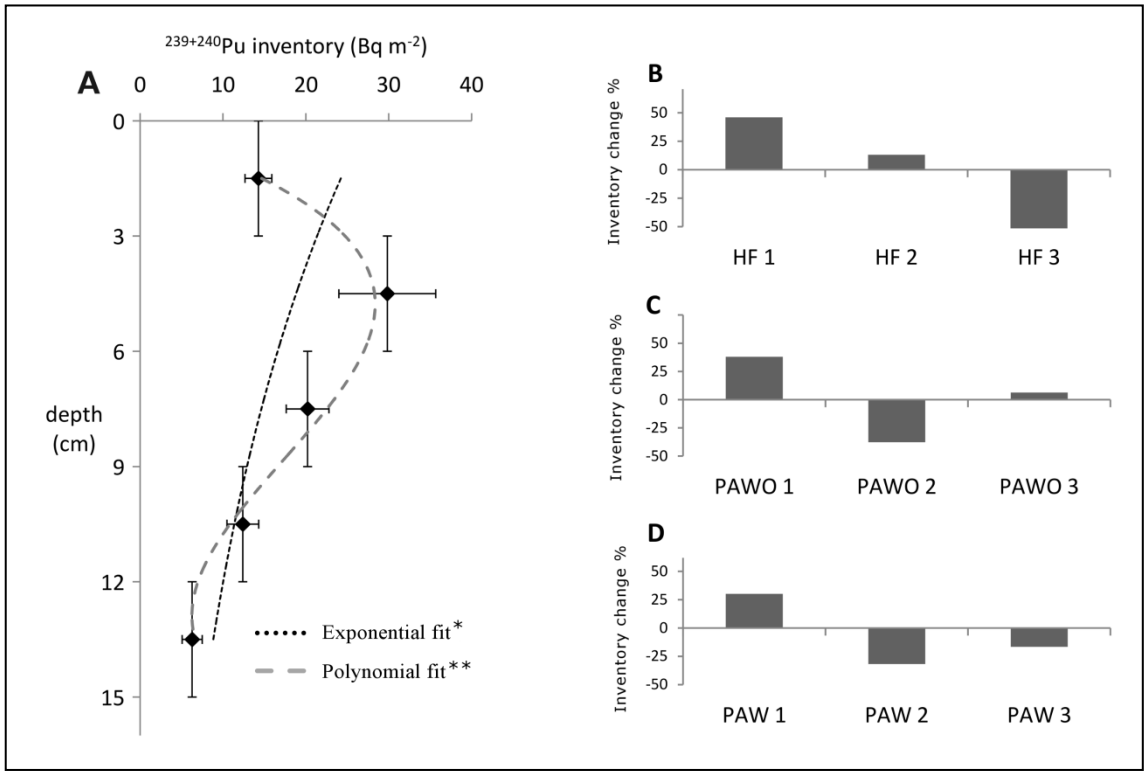

Figure 5-2: $^{239+240}$Pu depth profile in the reference sites (mean values of 6 references sites)(A). The x-axis error bars reflect standard deviations, whereas the y-axis error bars represent the depth interval of the sample. *R^2=0.49 (p-value=0.79, □=0.05). **R^2=0.97 (*p* =0.98, □=0.05). Inventory changes in hayfields (B), pastures without dwarf shrubs (C) and pastures with dwarf shrubs (D), where positive values indicate erosion and negative values indicate deposition

Total inventories at the sampling sites range from 45 to 130 Bq m^{-2} with a standard deviation of 30 Bq m^{-2}. Data from previous projects were used, where Pu activity at erosional sites was measured to a depth of 10 cm (Alewell *et al.*, 2014). To allow a comparison of the total inventories at reference and sampling sites, the activity measurements of the upper 10 cm of the soil cores are extrapolated, according to the shape of the average reference depth profile. In this way it was possible to derive the sample inventory to a depth of 15 cm. Inventory changes between the total reference inventory and the inventories of the sampling sites vary from -45% to +57%, with five of the investigated sites having positive inventory changes highlighting erosion processes. The negative inventory changes of the other four sites

indicate that deposition processes took place since the beginning of the fallout (Figure 5-2, B, C and D).

5.4.2 Conversion of $^{239+240}$Pu inventories: the comparison of the models

Soil erosion rates were estimated with the Inventory Method (IM), the Profile Distribution Model (PDM), the Diffusion and Migration Model (DMM) and MODERN (M), whereas deposition rates have been calculated using the Proportional Model (PM) and MODERN (M) (Figure 5-3).

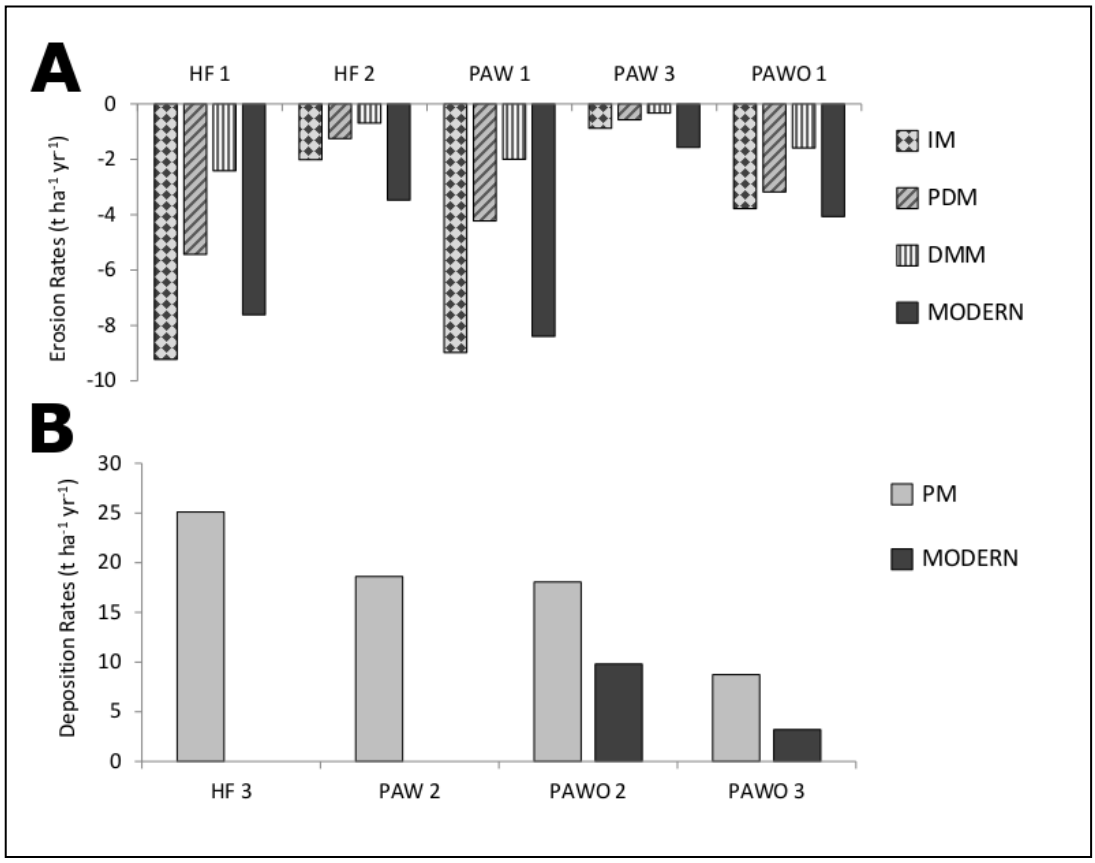

Figure 5-3: Erosion rates estimated with four conversion models (A). Inventory Method = IM, Profile Distribution Model = PDM, Diffusion and Migration Model = DMM, Proportional Model = PM, and MODERN. Deposition rates estimated with two conversion models (B). Proportional Model = PM. HF = Hayfields, PAW = Pastures with dwarf shrubs, PAWO = Pastures without dwarf shrubs.

PDM and IM perform similarly at sites with low inventory change (HF 2 and PAW 3). For higher inventory changes, the two exponential models deviate more, with IM values increasing considerably (Figure 5-4, A). The fitting of the measured Pu depth profile to an exponential function is performed differently by the two models, as expressed by equations (3) and (8) (Figure 5-4, C). When comparing the erosion estimates (*ER*, t ha^{-1} yr^{-1}) of the PDM with the soil loss (*L*, cm) obtained with IM, it is possible to notice a small deviation of the two curves (Figure 5-4, B). In order to convert the soil loss into soil erosion rates (*ER*, t ha^{-1} yr^{-1}), the Inventory Method subsequently considers the sampling depth *d* and the mass depth of each sampling

site (*xm*, equation (8)). At sites HF 1 and PAW 1, which have high values of mass depths (106 and 133 kg m^{-2} respectively), the conversion of soil loss (cm) to soil erosion rates further enhance the deviation between the IM and PDM outputs (Figure 5-4, B).

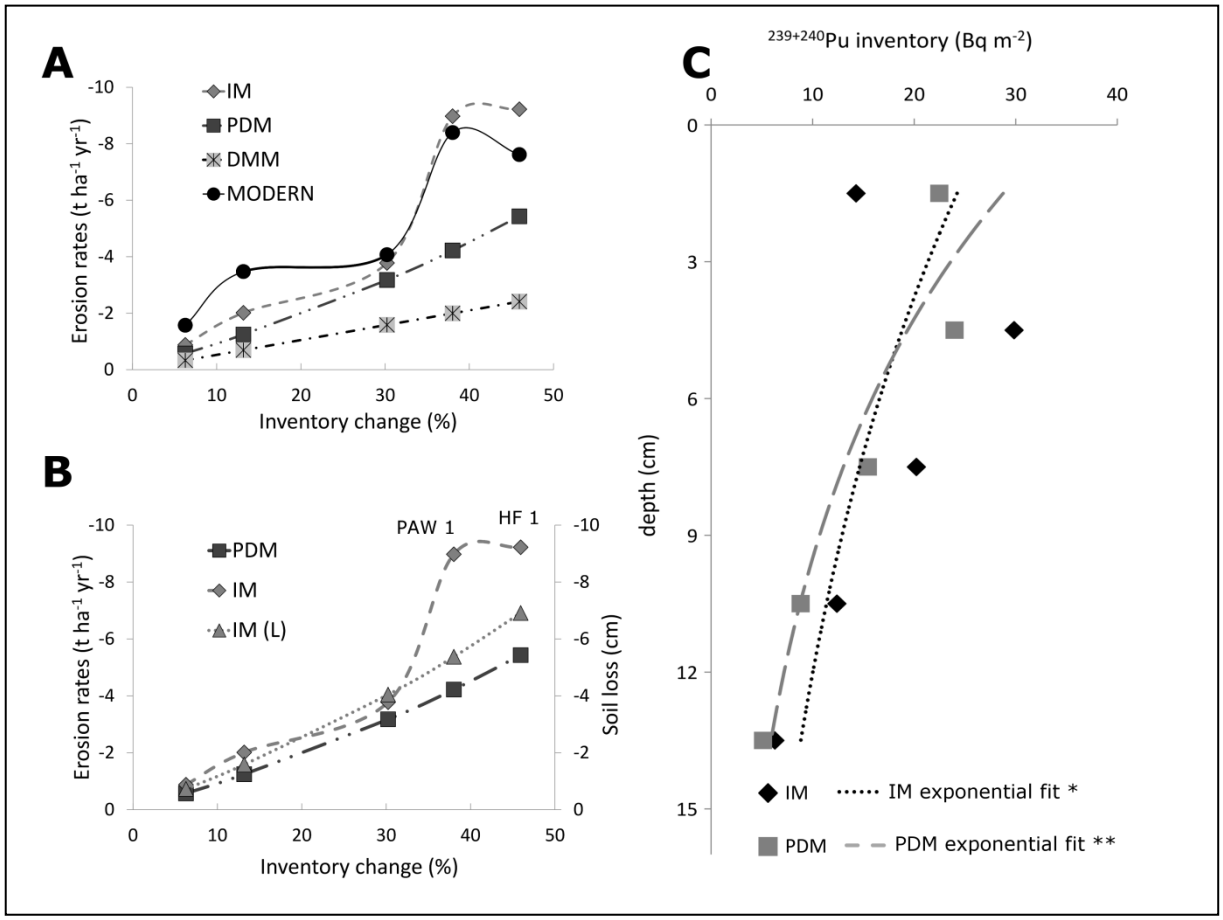

Figure 5-4: Relation between inventory change and soil erosion rates estimated with MODERN, Inventory Method (IM), Profile Distribution Model (PDM), Diffusion and Migration Model (DMM) (A). Relation between inventory change and erosion rates estimated by PDM and IM and soil loss (L, cm) estimated by IM (B). Exponential fits of the $^{239+240}$Pu distribution at the reference site by IM and PDM (C). * R^2 = 0.49 (p= 0.79, □= 0.05). ** R^2 = 0.91 (p=0.99, □=0.05).

DMM returns the lowest soil loss rates ranging from -2.4 t ha^{-1} yr^{-1} (PAW 3) to -0.3 t ha^{-1} yr^{-1} (HF 1) (Figure 5-3), because it considers a function which describes the time-variant depth migration of Pu isotopes into the soil. At the beginning of the fallout most of the Pu isotopes were located in the top soil, prior to migrate in the deeper layers. At that time a modest erosion process affecting the site would result in a significantly high inventory change between the site and the reference site. To avoid the risk of overestimation of erosion rates, the DMM weights the yearly erosion rates to reflect the migration of the radionuclides in the soil since the beginning of the fallout. However, to the latter might also be considered an additional obstacle in applying the DMM, since the two crucial factors in the function (the diffusion coefficient (*D*) and the migration rate (*v*)) have to be estimated and introduce a high modelling uncertainty.

MODERN follows the same trend as IM, with erosion rates ranging from -8.4 to -1.6 t ha^{-1} yr^{-1}. A paired samples *t* test failed to reveal a statistically significant difference between these models outputs ($t(4) = 0.112$, $p = 0.916$, $\alpha = 0.05$). However, MODERN returns slightly higher rates at low inventory changes, and lower rates in case of high inventory changes (Figure 5-4, A). The deviations are caused by the different depth functions of the two models. MODERN follows the measured FRN depth distribution, which resembles a polynomial function, and has lower inventories in the upper most layers as compared to IM. Thus, small changes in the inventory will be translated into relatively higher erosion rates as compared to the IM (Figure 5-4, A). When comparing to the DMM the authors cannot exclude that the results of MODERN may overestimate the soil redistribution processes, as it does not consider any time-variant migration of radionuclides in the soil. However, judging from expert knowledge (e.g. comparing micro-morphological changes before and after the winter season) at hot spots of erosional slopes, the DMM might underestimates erosion processes considerably at least compared to recent rates (last 5 years).

At depositional sites PAWO 2 and PAWO 3, the PM indicates high deposition rates of 25.1 and 18.6 t ha^{-1} yr^{-1} whereas MODERN returns rates of 9.8 and 3.2 t ha^{-1} yr^{-1}, respectively (Figure 5-3, B). At sites PAW 2 and HF 3, the defined MODERN deposition scenario didn't enable a solution of equation (17) due to high $^{239+240}Pu$ inventories (114 and 130 Bq m^{-2}, respectively). In order to find a solution at these sites, an additional deposition scenario was defined, where it was assumed that the deposition material origins from the most enriched layers of the measured depth profile (Figure 5-1, B). In particular, three layers above the top soil were added, having the same $^{239+240}Pu$ inventory as the second layer of the reference profile, where Pu activity peaked. The resulting deposition rates are 7.9 cm (HF 3) and 4.3 cm (PAW 2), corresponding to 13.7 t ha^{-1} yr^{-1} and 7.7 t ha^{-1} yr^{-1}, respectively. This scenario is not very likely (e.g. the second horizon only is deposited) except deposition processes occurred rapidly after the fallout when most of the $^{239+240}Pu$ was still concentrated in the top horizon.

The assessment of sedimentation rates in Alpine grasslands is connected to high uncertainty, as in addition to the unknown temporal dynamic, neither source location nor source area size of eroded sediments is known. As such, MODERN is a unique tool to simulate different deposition scenarios which can then be evaluated using expert knowledge.

5.4.3 Model sensitivity associated to reference inventory uncertainty

For all FRN based estimations of soil redistribution rates, the selection, the homogeneity and the representability of the reference site are crucial (e.g Walling *et al.*, 2002; Mabit *et al.,* 2013). Recently, Iurian *et al.* (2014) reported that the DMM appears to be very sensitive to uncertainties of the reference inventory value.

Indeed, a variation of only 15% of the reference inventory value (considered as a good measurement uncertainty/coefficient of variation), with no change in any other parameters of the model, resulted in an increase of the derived net erosion rates by about 100% at the investigated site (Iurian *et al.*, 2014).

Table 5-2: Sensitiveness of the models to changes of the Reference Inventory (Invref).

	Relative Change in the model output (%)	
	Inv_{ref}< 13%	Inv_{ref} > 13%
IM	15	-26
PDM	47	-71
DMM	58	-82
MODERN	31	-6

To test the sensitivity of the models to variation of (or uncertainty in) the reference inventory, a 13% error of Inv_{ref} was considered (Table 5-2). This value corresponds to the coefficient of variation (CV) among the six reference sites sampled in the study area (see Alewell *et al.*, 2014). No modifications to any other model parameters were performed. The test was conducted only at erosional sites and only for models used to derive erosion rates (namely the Inventory Method, the Profile Distribution Model, the Diffusion and Migration Model and MODERN).

Our data confirmed Iurian *et al.*, (2014) that the DMM is very sensitive to uncertainties around the reference inventory value. An increase or decrease of the reference inventory by 13% results in a deviation of erosion rates by 58 and -82%, respectively. Similarly, the PDM responds are sensitive to variations in the reference inventory (Table 5-2). In contrast, the IM is less responsive to variations of the reference inventory (deviation of erosion rates by 15 and -26%) and MODERN is least susceptible to modifications with a deviation of the erosion rates by -6 and 31% for an increase or decrease of the reference inventory, respectively (Table 5-2). The algorithm of MODERN does not include any specific assumptions on the reference inventory, but only uses information on the FRN inventory of each layer of the reference profile. Therefore, it is less sensitive to such deviation of the reference inventory. At pasture sites, a high variability of the reference inventories (CV between 5 and 41%) could be expected (Sutherland, 1996). Thus, the lower sensitivity of MODERN to the reference inventory changes seems advantageous and might result in lower bias.

5.5 Conclusions

Four widely recognized models to convert FRN inventories into soil redistribution rates have been described and applied to a $^{239+240}Pu$ dataset collected in Swiss Alpine grasslands. In presenting the first application of the new model MODERN to assess soil erosion or deposition rates from $^{239+240}Pu$ inventories, the authors compare this

innovative model to commonly used and established ones. Regarding erosion rates, MODERN and the IM (which was specifically designed for Pu) compare best. Both models consider the specific mass depth of the sampling site to derive erosion rates. The deviation between the models may be explained by the fact that IM assumes an exponential distribution of the Pu distribution at reference sites, whereas MODERN reproduces precisely the depth profile following the accuracy of the incremental measurements. As for deposition rates, MODERN results in lower erosion rates than the PM. The authors would like to point out, that uncertainty in assessing deposition rates is high, since size and location of sediment source areas in Alpine grasslands are unknown. MODERN enables to simulate and assess different deposition scenarios which can then be evaluated using expert judgment. Sensitivity of model outputs to reference inventory uncertainty is highest for the DMM and smallest for MODERN and IM.

The application of MODERN confirmed its potential to convert $^{239+240}$Pu inventories into soil erosion rates and its adaptability to any specific site conditions (e.g., ploughed or unploughed or even artificial soil layers). The algorithm of MODERN is also suitable for the estimation of deposition rates. Nevertheless, as no time-variant migration of Pu in the soil is considered, the authors acknowledge the risk of overestimating erosion rates. Reliable and quantitative estimates of soil degradation processes are crucial for optimizing land management of Alpine grasslands. Such an estimate of soil loss rates is important to ensure the effectiveness of land management practices for ensuring the productivity and sustainability of alpine upland agro-ecosystems.

Acknowledgements

This work was financially supported by the Swiss National Science Foundation (SNF), project no. 200021-146018. The authors also acknowledge the International Atomic Energy Agency (IAEA) for support provided through the technical project 20435 and the Coordinated Research Project (CRP) D1.50.17 on "*Nuclear techniques for a better understanding of the impact of climate change on soil erosion in upland agro-ecosystems*".

CHAPTER 6: MODERN: AN R PACKAGE TO CONVERT FRN (FALLOUT RADIONUCLIDES) INVENTORIES INTO SOIL EROSION/DEPOSITION RATES

This chapter was submitted to *Computer and Geoscience* as: Chiaradia E.[1], Arata L.[2] and Meusburger, K.[2]: *modeRn: an R package to convert FRN (Fallout RadioNuclides) inventories into soil erosion/deposition rates*.

(1) Department of Agricultural and Environmental Sciences, University of Milan, Italy,

(2) Environmental Geosciences, Department of Environmental Sciences, University of Basel, Switzerland.

6.1 Abstract

modeRn is a new R package to convert inventories of fallout radionuclides (FRN) into both soil erosion and deposition rates. FRN analysis is, in fact, one of the most useful techniques developed in the last 50 years in order to study soil erosion processes. The package *modeRn* contains a series of functions specifically developed to analyze FRN soil profiles and it implements the state-of-art method to compare a reference inventory (a soil profile with more than one layer which has at least one FRN value) against a sampling inventory (a soil profile with a unique layer) in order to evaluate the loss or the gain of soil. This comparison permits to obtain erosion or deposition rates from FRN inventories. The package is freely available to the scientific community. Further, a test run is described to guide the user through the application of its functions.

6.2 Software availability

Title: Modelling Deposition and Erosion rates with RadioNuclides (modeRn)

Main idea and concept: Christine Alewell and Katrin Meusburger (Environmental Geosciences, Department of Environmental Sciences, University of Basel, Switzerland)

Programming and conceptualizing: Enrico Antonio Chiaradia (Department of Agricultural and Environmental Sciences, University of Milan, Italy)

Implementation and revising: Laura Arata (Environmental Geosciences, Department of Environmental Sciences, University of Basel, Switzerland)

Contact corresponding author: enrico.chiaradia@yahoo.it

First available: 2016

Software required: R

Format: .R files

Program language: R

Size: 200 KB

Availability: MODERN is free and public and can be downloaded at modern.umweltgeo.unibas.ch

License: GPL-2

6.3 Introduction

Soil erosion is the most important land degradation problem worldwide (Eswaran *et al.*, 2001) and it has effects on environment with high economic costs (e.g. agricultural production reduction, infrastructures damages and water quality decreasing, Vrieling, 2006). The scientific community is invited to produce methods,

standards, data collection and research networks for assessment and monitoring of soil and land degradation (Eswaran *et al.*, 2001).

There are several methods to measure soil erosion/deposition rates (e.g. plot studies, overflight with field survey data, sediment accumulation and transportation in watercourses, Brazier, 2004), but monitoring the fallout radionuclides activity (FRN method) was recognized as powerful tool for studying the complete erosion and sedimentation cycle across the landscape (Ritchie and McHenry, 1990).

Recently, (Arata *et al.*, 2016a, 2016b)) proposed a new model to derive a quantitative estimate of soil redistribution rates from fallout radionuclide inventories called MODERN (MOdelling Deposition and Erosion rates with RadioNuclides). The proposed model permits to compare highly detailed inventory depth profiles of fallout radionuclides (FRN, radioactivity per unit area, i.e. Bq/m^2) used as reference sites with depth-average- inventories obtained from sample sites. The model can be applied under every agro-environmental condition and land use, and it can accurately describe the measured soil profile of any selected FRN profile.

The MODERN code was originally released as a free and open source code developed in the Matlab environment. To increase the accessibility to the scientific community the aim of the current study is the implementation of the original Matlab code in the R environment. R is a free and open-source system under the GNU General Public Licence (GPL) principle, with constant upgrades and improvements from the statistic community (Robert and Casella, 2010). R is also an increasingly popular programming environment similar in scope and purpose to other scientific programming framework (Vermeesch *et al.*, 2016a) and recently, different packages were developed in environmental science as, for example, vegetation phenology monitoring (Filippa *et al.*, 2016), evapotranspiration (Guo *et al.*, 2016), sedimentary provenance data (Vermeesch *et al.*, 2016b) and models to analyze biotracer data (Inger *et al.*, 2010; Palmer *et al.*, 2010; Stock and Semmens, 2013).

The new implementation of the MODERN model was advanced with new functionalities which improve the usability and potential of the original code. In this paper we briefly introduce the FRN method (section 2), and describe the concept and the algorithm at the base of the MODERN model (section 3). Section 4 describes the modeRn package and the new functions implemented in the R package. In section 5, a case study is presented in order to introduce the reader to the use of the software. Further instructions about the package download and its installation are provided.

6.4 The application of FRN to estimate soil erosion and deposition rates

Soil erosion is one of the major threats to soil stability and productivity but its monitoring remains a challenge. In the last 50 years, fallout radionuclides (FRN), e.g.

artificial ^{137}Cs and $^{239+240}Pu$, natural unsupported ^{210}Pb fallout and cosmogenic ^{7}Be, have been widely used as soil tracers to provide estimates of soil erosion rates under different environmental conditions (e.g. (Mabit *et al.*, 2008, 2013, 2014; Ritchie and McHenry, 1990; 2003). Once deposited on the ground, FRN strongly bind to fine particles at the surface soil and move across the landscape primarily through physical processes (IAEA, 2014). As such these radiotracers provide an effective track of soil and sediment redistribution. The concept of the FRN method is based on the comparison between the inventory (total radionuclide activity per unit area) at a given sampling site and that of a so called reference site, located in a flat and undisturbed area. If the FRN inventory at the sampling site is lower than the reference site, the method indicates that the site experienced soil erosion processes since the main fallout. While, if the site presents a greater FRN inventory than the reference site, the site experienced deposition processes (Figure 6-1). From the latter comparison it is possible to derive quantitative estimates of soil erosion and deposition rates through the use of specific conversion models (IAEA, 2014).

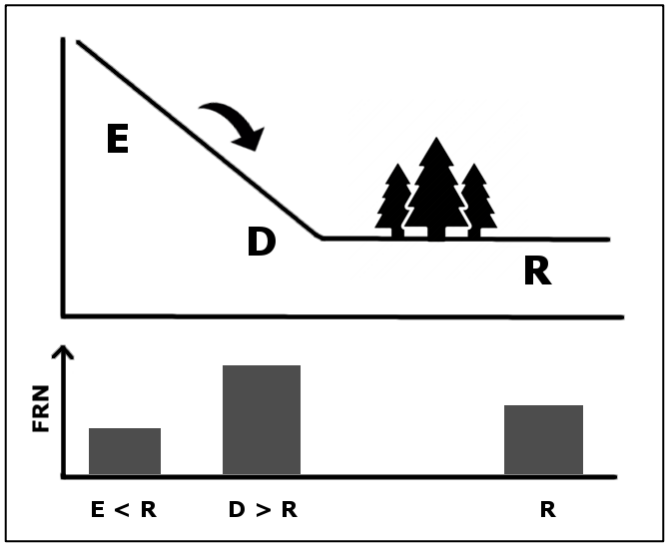

Figure 6-1: Concept of the fallout radionuclide (FRN) traditional method, in which the FRN content of a reference site located in a flat and undisturbed area (R) is compared to the FRN content of disturbed sites (E and D). If the FRN at the site under investigation is lower than at the reference site, the site has experienced erosion processes (E), while if the FRN content is greater than at the reference site, the site has experienced deposition processes (D).

6.5 The MODERN conversion model

MODERN is a conversion model used to convert measures FRN inventories to soil redistribution rates. Based on the comparison between the soils FRN depth profile at the reference site and the total FRN inventory at the sampling site, MODERN returns soil erosion and deposition rates in terms of thickness of the soil layer affected by soil redistribution processes. To estimate the thickness of soil losses/gains, MODERN aligns the total inventory of the sampling site to the depth profile of the reference site. The point of intersection along the soil profile represents the solution of the model (Arata *et al.*, 2016a, 2016b).

The novelty of MODERN, which distinguishes it from other common used conversion models, can be summarised in the following statements. MODERN does not make any assumption on the shape of the FRN depth profile, but accurately describes the measured shape of the FRN soil profile at reference sites. In addition, MODERN is capable to convert the FRN inventories of both erosion and deposition processes to soil redistribution rates, whereas other conversion models for uncultivated soils (e.g. the Profile Distribution Model, the Diffusion and Migration Model (Walling and He, 1997; Walling and Quine, 1990; Walling and Zhang, 2014; Walling *et al.*, 2003, 2009) are specifically developed to quantify rates of only one redistribution process (i.e. erosion or deposition). To enhance the estimate of soil redistribution rates, it allows adapting the depth profile, to simulate the behaviour of the selected FRN under different agro-environmental conditions (e.g. ploughing activities, erosion and sedimentation processes).

6.5.1 MODERN adaptations of the reference FRN depth profile

Three possible adaptations of the FRN depth profile at the reference site can be performed by MODERN. Firstly, MODERN can simulate an arbitrary number of layers below the measured depth profile of the reference site. In those simulated layers, MODERN smooths the FRN inventories exponentially to zero. Very often the deeper layers of the measured FRN depth profile have a FRN activity, below the detection limit of the detector. When this happens, the resulting depth profile presents an abrupt step to zero concentrations in the lower layers of the profile. Therefore, MODERN allows simulating the missing FRN layers to construct a deeper depth profile. Secondly, MODERN allows an adaptation of the depth profile of the reference site to consider ploughing processes. Regular ploughing affects the FRN vertical distribution in the soil, as all soil layers down to the ploughing depth are mixed more or less homogeneously. Therefore, to simulate similar mechanical mixing processes, MODERN adjusts the reference depth profile, where it assumes an average inventory value at the layers above the ploughing depth. Finally, to estimate deposition rates, MODERN allows defining different deposition scenarios, where the variability of sources with different FRN concentration can be considered. To this end, MODERN allows (i) simulating an arbitrary number of layers above the measured FRN depth profile, and (ii) defining the FRN inventory of each simulated deposited layer, on the basis of the assumptions on the origin of soil layers involved and the thickness of deposited sediment layers. MODERN permits to perform multiple adaptations simultaneously and to adjust the reference depth profile to the specific shape encountered at sampling specific site. The intention is to produce a range of potential solutions, which could be evaluated by expert knowledge (for more details, see Arata *et al.*, 2016b) .

6.5.2 Model solving method

Using MODERN, the FRN depth profile of the reference site, eventually modified in order to reproduce different scenarios (e.g. erosion or deposition, vertical mixing due to ploughing) is modelled as a step function *g(x)*, which at each increment *inc* returns a value Inv_{inc}. If *Inv* is the FRN total inventory of a sampling site, measured for the whole depth profile *d* (cm), the model targets the level x*(cm) from x* to x*+ *d* (cm) along the soil profile, where the sum of all Inv_{inc} of the reference site is equal to *Inv*. Therefore x* should fulfil the following equation:

$$\int_{x^*}^{x^*+d} g(x)dx = Inv \quad (1)$$

Hence, the simulated depth profile, considering the possible adaptations of the profile, is described by the integral function *S*, where:

$$S(x) = \int_{x}^{x+d} g(x)dx \quad (2)$$

The function *S* can be solved through the primitive function *G* of the distribution function *g(x)* as follows:

$$S(x) = G(x+d) - G(x) \quad (3)$$

MODERN returns the results in soil losses or gains (x), in length unit. The conversion to yearly soil losses or gains *Y* in t ha^{-1} yr^{-1} can be calculated using the following equation:

$$Y = 10 \times \frac{x^* \cdot xm}{d \cdot (t_1 - t_0)} \quad (4)$$

where *xm* is the mass depth (kg m^{-2}) of the sampling site, *d* is the total depth increment considered at the sampling site (cm), t_1 is the sampling year (yr), and t_0 (yr) is the year of the main fallout.

6.6 The modeRn package

6.6.1 Structure of the package

The internal structure of the *modeRn* package consists of two objects, the "*Inventory*" class and the "*MODERN*" class, and of a library of ancillary functions. Both "*Inventory*" and "*MODERN*" classes are of type S3, which means that they are supported from the first release of R and they are highly modifiable by the user in an interactive mode (Leisch, 2008). For an introduction to Object-Oriented Programming (OOP) in the R language, please refer to (Venables and Ripley, 2013), while for a more thorough treatment of the subject specifically for R see (Chambers, 2008) and Gentleman (2008). Both "*Inventory*" and "*MODERN*" objects implement specific other functions most of which are accessible by the user. The scheme of the internal structure of the *modeRn* package is reported in Figure 6-2.

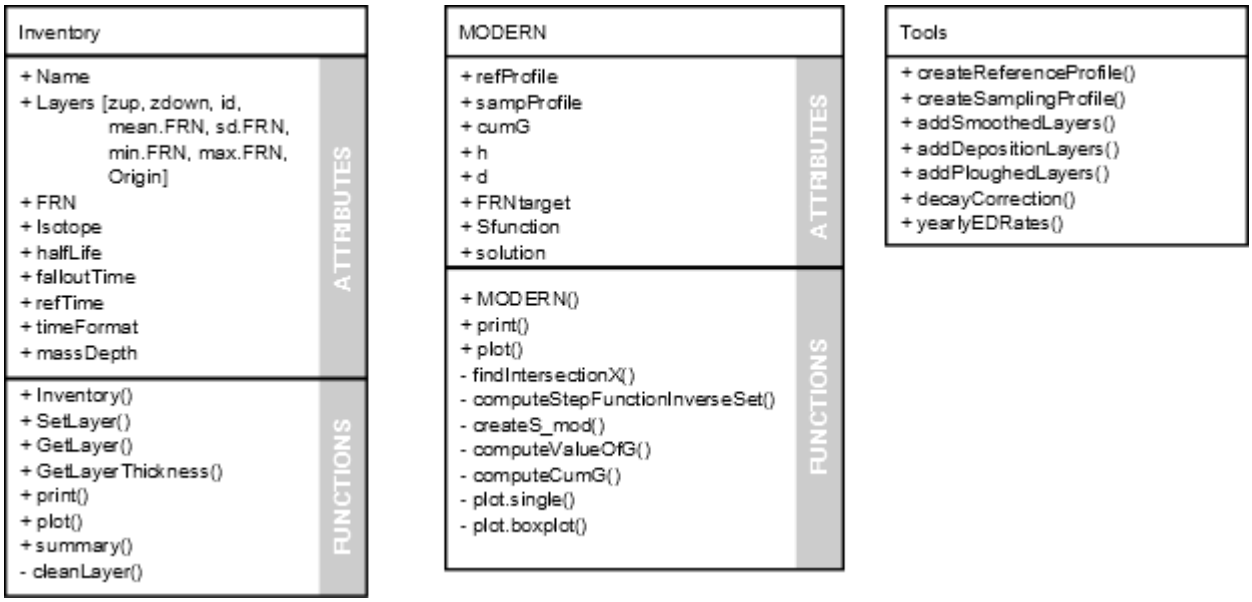

Figure 6-2: Scheme of the internal structure of the modeRn package (plus and minus signs identify the public and the private functions respectively).

The profiles of both reference and sampling sites are stored as "*Inventory*" objects. However, the profile of the sampling site includes a single layer, with one or more FRN values, whereas the object of the reference site contains information on multiple layers that describe the FRN distribution along the depth profile. A layer is represented as a record of a table with the following fields: the upper depth of each layer (*zup*); the lower depth of each layer (*zdown*); an unique identifier of the layer (*id*); the mean, the standard deviation, the minimum and the maximum FRN values of the layer (respectively *mean.FRN*, *sd.FRN*, *min.FRN* and *max.FRN*) and the source of the layer (*Origin*). The Origin field identifies the source of the layer that could derive from laboratory tests (i.e. Measured) or from specific function (i.e. ploughed, smoothed or deposited) developed in the package.

The "*Inventory*" object contains a list of 9 attributes: the name of the site (Name), a dataframe (i.e. table) containing the attribute of each layer that composes the profile (Layers), the FRN inventory for each layer with one or more repetition (FRN), the name of the isotope (Isotope), the half-life index (halflife), the fall out time (falloutTime), the date of sampling (refTime), the time format used to express dates (timeFormat) and the mass depth of the soil (massDepth). The object "*Inventory*" is also equipped with 7 public access functions which are: the constructor (*Inventory()*); two slots to set or get the attribute of a layer (respectively *SetLayer()* and *GetLayer()*); a method to calculate the average layers thickness (*GetLayerThickness()*); two methods to see the data included in the object by textual and graphical way (*print()* and *plot()*); and two methods to create and show statistics (*summary()* and *print.summary()*). Just one method is not accessible to the user, which is the one that verifies the congruency of the structure of the layers (*cleanLayer()*), every time a layer is created, added or deleted.

The object of class "*MODERN*" implements the algorithm necessary to evaluate the depth of soil lost or gained due to erosion or deposition processes. This object stores both the final and the intermediate results (e.g. the values of the function S at the different depths). The class is equipped by 3 public methods which are the constructor (MODERN()) and the two functions for plotting and printing the results (i.e. plot() and print()). All other methods necessary for the intermediate steps are not accessible by the user. The information stored in the "*MODERN*" class are related to the two profiles used for the comparison performed by MODERN, which are the depth profile at the reference profile (*refProfile*) and the profile, of just one layer, measured at the sampling site (*sampProfile*). It also contains the information on: the cumulative FRN inventory of the reference depth profile (*cumG*); the thickness of the layers for both the reference (*h*) and the sampling profile (*d*); the total FRN inventory at the sampling site (*FRNtarget*); the function S (*Sfunction*) and the solution of the model (*solution*). The latter is expressed in length unit (i.e. the same unit used to define the depth increments of the layers at the reference and sampling sites). Finally, in order to simplify the analysis procedure, different functions help the user to build the profiles and to build the hypothetical scenarios.

6.6.2 Workflow and application of the package

The first step of the workflow of the *modeRn* package consists in the creation of the FRN depth profile measured at the reference site (Figure 6-3). The user defines the FRN depth profile of the reference site, using the function named *createReferenceProfile*(). This function requires at least three arguments: a list of FRN inventories measured at each depth increment of the reference depth profile (*FRN*, Bq m^{-2}), the thickness (one value) of the layers (*thickness*) and the name of the reference site (*name*). The function returns an object of class "*Inventory*". The user can eventually adapt the measured reference profile through a series of possible simulations, on the basis of the specific conditions of the study area (e.g. deposition dynamics, ploughing activities), as described in section 3.1, and obtain a simulated FRN depth profile. A first adaptation regards the simulation of a number of layers below the measured depth profile, where the FRN inventories are smoothed exponentially to zero. This step is performed by the use of the function *addSmoothedLayers()* which accepts three arguments: (i) the depth profile to adapt (*RDF*), (ii) the thickness of soil to simulate below the measured profile (*Depth*) and the number of layers of the measured reference depth profile to derive the exponential smoothing of the FRN inventories, starting from the bottom of the profile *(NumLay*). The function requires an object of class "Inventory" as first parameter, while the second and the third one are scalars. The thickness of the simulated layers is defined by the thickness of the layers of the reference depth profile. If *Depth* is not divisible by the thickness of the layer, then the function adds as many new layers as necessary to completely cover the new thickness defined by the user. The value of the FRN inventory associated with each new layer, FRN_i, is calculated as:

$$FRN_i = FRN_{low} \times e^{-i} \quad (5)$$

where FRN_{low} is the average value of the layers of the measured depth profile defined by the parameter *NumLay* and *i* is a counter of the new layer added. The greater the value of *i*, the lower is the corresponding FRN value. A new reference profile, of class "*Inventory*", is returned.

A second adaptation allows the simulation of the mixing processes affecting the depth profile at the reference site due to ploughing activities, through the function *addPloughedLayers*(). This function requires three arguments: an object of class "*Inventory*" which represent the depth profile to adapt (*RDF*); the FRN inventory of each layer where the vertical mixing is simulated (*newvalue*, Bq m^{-2}) and *NumLay* which defines the number of layers hypothetically affected by the ploughing activities. If *newvalue* argument is left empty, the function will use as value the average FRN inventory of the layers affected by the mixing. The function returns a new reference profile, of class "*Inventory*".

Through the function *addDepositionLayers*(), the user can simulate several layers above the measured depth profile, to reproduce deposition dynamics. This function accepts three parameters: the first is the profile to adapt (*RDF*), the second is the FRN value to assign to the new layer (*newvalue*, Bq m^{-2}) and the third is the number of the new layers that will be added at the top of the soil profile (*NumLay)*. Also in this case the function returns a new "*Inventory*" object.

The profile of the sampling site is defined by an object of class "*Inventory*" created by the function *createSamplingProfile()*. The function requires at least three parameters: the total FRN inventory measured at the sampling site (*FRNinv*, Bq m^{-2}), the thickness of the layer (*thickness*) and the name of the site (*name*). Finally, the model can perform the comparison between the simulated reference depth profile and the sampling site, through the "*MODERN*" function. This function requires two parameters: the reference depth profile (*refProfile*) and the sampling site profile (*SampProfile*) and will create a new object of class "*MODERN*", which contains the solution i.e. the thickness of soil lost or gained by soil redistribution processes and the erosion or deposition rates. A single or multiple solutions are obtained, which can be plotted through the method *plot()*.

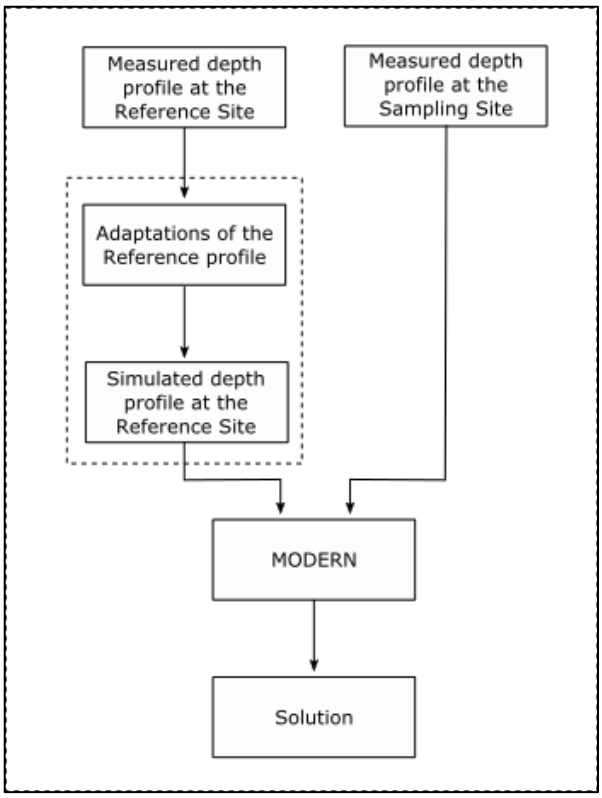

Figure 6-3: The work-flow of the processing chain in the modeRn package. The analysis starts with the definition of the measured FRN depth profile at the reference site; eventually, the user may define the optional adaptations of the profile according to specific conditions of the study area, which returns a simulated reference profile. Second, the FRN profile at the sampling site is defined. Finally the user initializes the matching algorithm between the two profiles, through the creation of the MODERN object. The results can be viewed or plotted.

6.7 Additional features of the *modeRn* package

6.7.1 The "decayCorrections" function

FRNs are subjected to radioactive decay processes, which diminish their activity over time according to the specific half-life of the FRN. Therefore, when comparing different FRN profiles measured at different times, it is necessary to properly decay correct the FRN inventories to a single and common time. The *modeRn* R package includes a new tool , which enables to decay correct any object of class "*Inventory*". The *decayCorrection()* function accepts 5 parameters: an object of class "*Inventory*", previously defined (*FRNinv)*; the half-life of the FRN used in the study, expressed in seconds (*halflife, s)*; the time at which the FRN inventory was collected and the time to which the measured values will be updated to (*oldTime* and *newTime,* respectively); the time format used to express the arguments *oldTime* and *newTime* (*timeFormat*). The function returns an object of class "*Inventory*".

6.7.2 The conversion of MODERN results to erosion/deposition rates

MODERN returns the results only in length unit, which correspond to the thickness of soil losses or gains, if the half-life of the isotope (*halfLife*), the fallout time (*falloutTime*),

the sampling time (*refTime*) and the mass depth (*massDepth*), are not specified by the user when both the reference and the sampling profile are created.. However, the function *yearlyEDrates* allows converting soil losses/gains into yearly soil erosion or deposition rates (t ha^{-1} yr^{-1}) by the application of equation (4). The function accepts 6 arguments (i) the rates of erosion/deposition expressed in unit length or a *MODERN* object (*rates*); (i) the mass depth of the sampling site (kg m^{-2})(*massDepth*); (iii) the depth of the sampling profile (which should be expressed in the same unit of *rates*) (*sampleDepth*); (iv) the time of the measurement and (v) the time of the comparison (*oldTime* and *newTime,* respectively); (vi) the time format used to express the arguments *oldTime* and *newTime* (*timeFormat*).

6.7.3 Considering the variability of FRN inventories

A novelty of the *modeRn* package, as compared to the original MODERN code, is that it allows considering the variability of the FRN inventories measured at any site. The term variability may refer, for example, to: a range of FRN inventories measured at different replicated samples collected at the same sampling site; a range of possible depth profiles, measured at different replicated samples collected at the same reference site; a range of FRN activities (and consequently inventories) measured by a detector. In this sense the "*Inventory*" object accepts as argument *FRN* also a list of values (to define the variability at the sampling site), a matrix or a dataframe (to define the variability of different depth profiles at the reference site) and even a frequency distribution of FRN inventories. Therefore, more than one solution is returned by the algorithm and statistical analysis can be performed in order to understand, for example, the effect of the variability of the FRN inventories on predicting the erosion/deposition rates. If more FRN values are defined for a single profile, the variability of the FRN inventories at each layer can be displayed through the *plot()* function. Moreover, the function *MODERN()* will return multiple solutions associated with the number of inventories or depth profiles used for the comparison. The plot of the solution will show the variability of the solution in form of a boxplot.

6.8. An explained test run of the *modeRn* package

In the following sections, a running test of the *modeRn* package is presented in details, to offer the reader an overview of the usage of the package. The data used in the test are the ones presented in in (Arata *et al.*, 2016b) where a theoretical example of the MODERN model has been run.

6.8.1 Package download and installation

The *modeRn* package can be freely downloaded at modern.umweltgeo.unibas.ch. To install the package use the command:

```
install.packages(path_to_file, repos = NULL, type="source")
```

where *path_to_file* indicates the path to the folder where the *modeRn* package has been downloaded and unzipped. After the modeRn package is correctly installed in the R environment, the first operation to do is to call the library typing the following line of code:

```
library("modeRn")
```

6.8.2 Basic features of the modeRn package: pre-processing input data, calculating and visualizing estimates

Starting from the example presented in (Arata *et al.*, 2016b), a FRN depth profile of a reference site, with a total FRN inventory of 100 Bq m^{-2}, is created through the following lines:

```
FRN = c(12, 21, 15, 13, 11, 9, 7.5, 4.5, 4, 3)

layer.thickness = 3

name = 'Reference site'

RDP = createReferenceProfile(FRN,layer.thickness, name, isotope = "137cs", halfLife = 951441000, refTime = "2000", falloutTime = "1963", timeFormat = "%Y")

plot(RDP, , main = 'A: measured depth profile RDP')
```

where *FRN* is the list of FRN inventories (Bq m^{-2}) measured at each depth increment of the profile, *name* is a new variable which stores the name of the reference site and l*ayer.thickness* is the thickness of each layer of the profile (in this case 3 cm). Using the function *createReferenceProfile* a new "*Inventory*" object called *RDP* is created. The name of the isotope used, its half-life expressed in seconds (i.e. 30.17 years = 951441000 seconds), the reference and the mean fallout years are also defined. Finally, the *plot* function creates the graphical representation of the reference site (Figure 6-4, A). Note the use of the R-style *main* parameter to set the title on the top of the plot.

Two different adaptations of the *RDP* depth profile are performed. As for the first one, 6 cm of soil (equal to 2 layers of the same thickness as those of the reference profile) are simulated below the measured profile, where an exponential smoothing of FRN inventories is simulated. For this step, the function *addSmoothedLayers* is used as follows:

```
RDP.smooth = addSmoothedLayers(RDP, Depth = 2*3, NumLay=3)

plot(RDP.smooth, main = 'B: simulated depth profile RDP.smooth')
```

A new "*Inventory* object is created (*RDP.smooth*), where the FRN inventories of the simulated layers are calculated according to equation (5) (Figure 6-4, B), considering the FRN inventories of the three bottom layers of the measured depth profile (*NumLay = 3*).

The second adaptation simulates two layers above the measured reference depth profile, to reproduce the soil deposition dynamics. In this case, (Arata *et al.*, 2016b) assumed two possible scenarios: two layers above the measured reference depth profile were modelled following two possible scenarios. For Scenario 1 (*RDP.smooth.dep1*), the authors hypothesize that sediments derive from an upslope top soil horizon (e.g. the first 3 cm).

The FRN inventories of the additional layers were set to be equal to the inventory of the first 3 cm of the reference profile. For Scenario 2 (*RDP.smooth.dep2*) the authors hypothesize that the deposited materials originate from an eroded horizon of about 6 cm depth, which was homogenously mixed during detachment and transport processes. Therefore, FRN inventories of the additional layers are equal to the average inventory of the first 6 cm of the reference profile. For this step, the function *addDepositionLayers()* is used, and the new simulated profiles are plotted (Figure 6-4, C and D).

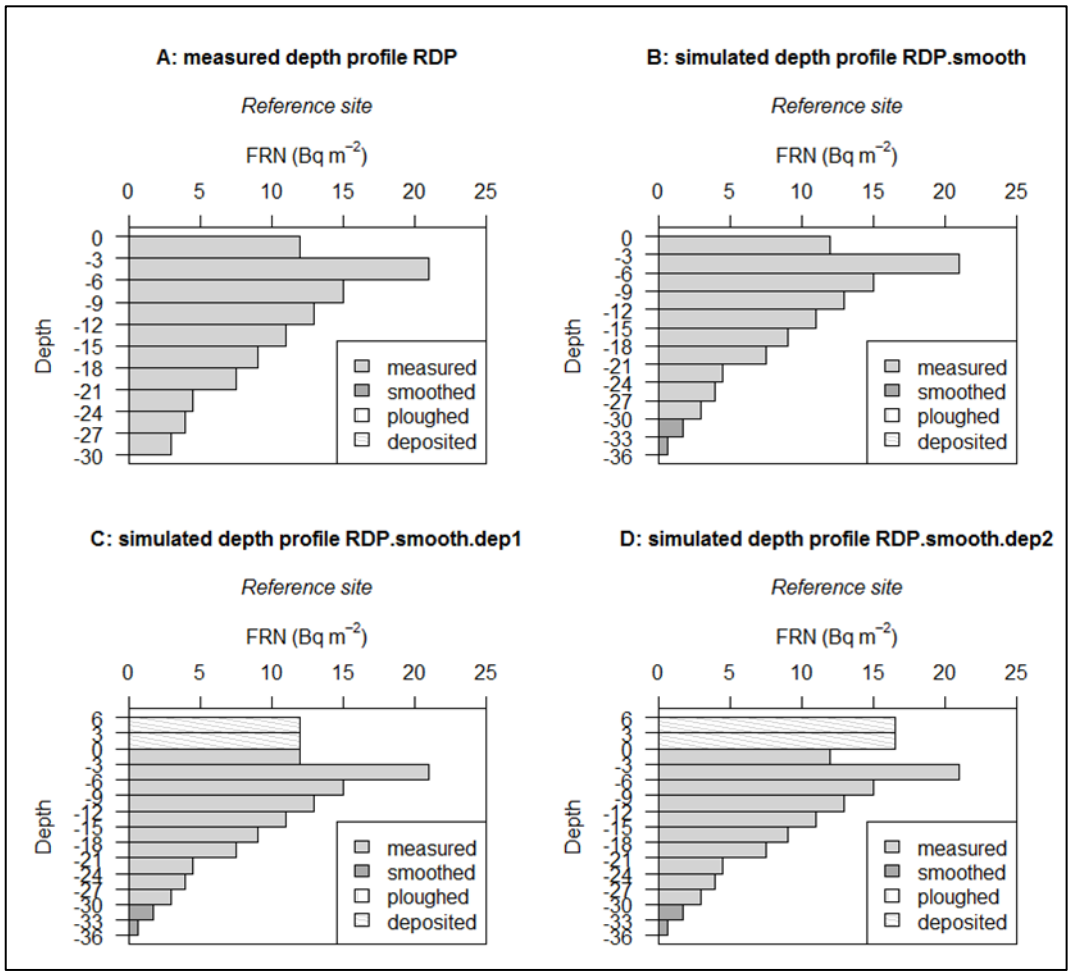

Figure 6-4: The FRN depth profiles at the reference site, where A: represents the measured one; B includes two additional simulated layers below the profile and B and C present the simulated profiles according to scenario 1 and 2 respectively.

```
RDP.smooth.dep1 = addDepositionLayers (RDP.smooth, FRN[1], 2)
RDP.smooth.dep2 = addDepositionLayers (RDP.smooth,
mean(FRN[1:2]), 2)
```

```
plot(RDP.smooth.dep1, main = 'C: simulated depth profile
RDP.smooth.dep1')
plot(RDP.smooth.dep2, main = 'D: simulated depth profile
RDP.smooth.dep2')
```

Note that each time, a new object of class "*Inventory*" is generated. The object contains, for each layer, information about the upper and lower depth limits (*zup* and *zdown*), the order of inserting (*id*) the mean, the standard deviation, the minimum and maximum value of the FRN inventory of each layer (*mean.FRN, sd.FRN, min.FRN, max.FRN*) and the origin of the layer (*Origin*, i.e. the way the values were obtained). It is possible to visualize the information stored in the object by typing the command *print()* (Figure 6-5).

At this point is possible to create an object, of class "*Inventory*", which represents a profile of a sampling site. Following the example presented in (Arata *et al.*, 2016b) two sampling sites (i.e. site A and site B) are defined, where site A presents a lower FRN inventory than the reference site (78 Bq m^{-2}), indicating erosion, while site B has a higher FRN inventory than the reference site (115 Bq m^{-2}), highlighting deposition processes. At both sites the FRN inventory is measured until a depth of 30 cm. The profiles of the sampling sites are created using the lines:

```
siteA = createSamplingProfile(78,30,'site A')
siteB = createSamplingProfile(115,30,'site B')
```

Finally, is possible to run the comparison between the simulated depth profile of the reference sites and the profiles of the sampling sites, through the algorithm of the MODERN model. For the example presented in this study three objects of class "MODERN" are created:

```
MODERN_siteA = MODERN(RDP.smooth,siteA)
MODERN_siteB_1 = MODERN(RDP.smooth.dep1,siteB)
MODERN_siteB_2 = MODERN(RDP.smooth.dep2,siteB)
```

where *MODERN_siteA_1* compares the profile of site A with the simulated depth profile *RDP.smooth*. As site A is an erosional site, it is not necessary to simulate any deposition dynamics. The objects *MODERN_siteB_1* and *MODERN_siteB_2* compare the profile of the sampling site B to the simulated reference depth profile according to scenarios 1 and 2, respectively. The model results can be visualized by the function *plot()* and *print()* (Figure 6-6 and 6-7). In particular, the function *plot()* shows two plots, where the left one presents the overlapping of the two profiles used in the comparison), while the right one presents the line of the function S as in equation (3). The solution, which represents the point of intersection along the soil profile, is visualized in red in both plots (Figure 6-6). The unit length of soil lost or gained due to soil redistribution processes, are reported by the *print()* function (Figure 6-7). MODERN solutions are expressed as table. Each record corresponds to a segment that composes the S function while, in this case, only one column of results is reported

because a reference profile with single value of FRN of each layers is compared to a sampling site with only one value for its unique layer. In this case, MODERN found only one solution that is -4.73. If all values are NAs, it means that MODERN found no solutions but the model can found more than one solution.

```
> print(RDP.smooth.dep1)
Name of the reference depth profile:
[1] "Reference site"

Layers:
   zup zdown id   mean.FRN sd.FRN    min.FRN    max.FRN    Origin
14   6     3 14 12.0000000     NA 12.0000000 12.0000000 deposited
13   3     0 13 12.0000000     NA 12.0000000 12.0000000 deposited
1    0    -3  1 12.0000000     NA 12.0000000 12.0000000  measured
2   -3    -6  2 21.0000000     NA 21.0000000 21.0000000  measured
3   -6    -9  3 15.0000000     NA 15.0000000 15.0000000  measured
4   -9   -12  4 13.0000000     NA 13.0000000 13.0000000  measured
5  -12   -15  5 11.0000000     NA 11.0000000 11.0000000  measured
6  -15   -18  6  9.0000000     NA  9.0000000  9.0000000  measured
7  -18   -21  7  7.5000000     NA  7.5000000  7.5000000  measured
8  -21   -24  8  4.5000000     NA  4.5000000  4.5000000  measured
9  -24   -27  9  4.0000000     NA  4.0000000  4.0000000  measured
10 -27   -30 10  3.0000000     NA  3.0000000  3.0000000  measured
11 -30   -33 11  1.7474273     NA  1.7474273  1.7474273  smoothed
12 -33   -36 12  0.6428426     NA  0.6428426  0.6428426  smoothed

Total FRN inventory (Bq m^-2):
    FRN1
126.3903

Mean layer thickness:
[1] 3

 === Metadata ===

Isotope:
[1] "137cs"

Half-life:
[1] "95144100000"

reference date-time:
[1] "2000-07-27 CEST"

Mass depth of the sampling site (kg m^-2):
[1] NA
>
```

Figure 6-5: The report table with the data stored in the object RDF.smooth.dep1 of class "Inventory"

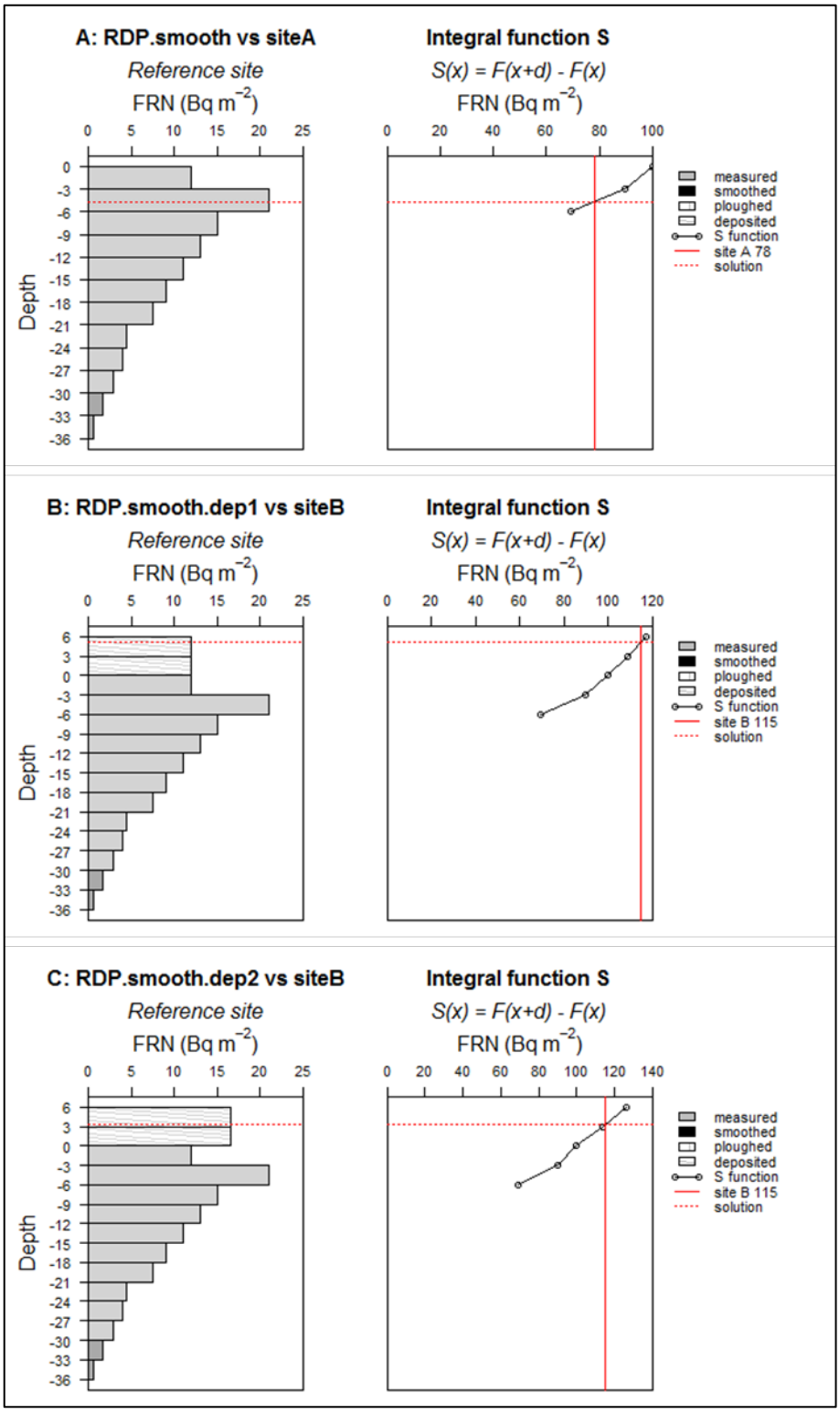

Figure 6-6: The graphical representation of the MODERN model solution for site A (A) and site B (B and C according to deposition scenarios 1 and 2 respectively)

```
> print(MODERN_siteA, digits = 3)
MODERN simulation results
   FRN1
1    NA
2 -4.73
3    NA
4    NA
5    NA

Intermediate results are accessible through these slots:
refProfile; sampProfile; cumG; h; d; FRNtarget; Sfunction; solution
Warning message:
In print.MODERN(MODERN_siteA, digits = 3) :
  Cannot calculate erosion rate(s) because one or more parameters of
sampling profile is NA
>
```

Figure 6-7: The results obtained from MODERN for the comparison between RDF.smooth and site A. As not all the attributes were properly set in the sampling profile object (e.g. mass depth, fallout time, etc.), a warning message informs the user about the impossibility to calculate the erosion/deposition rates. Note the use of digits parameters that defines how many number of digits will be printed.

6.9 Additional features of the modeRn package

The advanced features provided by the *modeRn* package and described in section 4.3 are tested here. First, it is hypothesized that the FRN measurements of the samples collected at site A and B were conducted in an antecedent period (i.e. 1 year earlier) than the ones from the reference site. For this reason is necessary to decay correct the FRN inventories of site A and B according to a hypothetical half-life of 10 years expressed in seconds (i.e. 10*365*24*3600). Therefore, the *decayCorrection* tool is used as follows:

```
siteA_dc = decayCorrection(siteA, 10*365*24*3600,'2014-10-
6','2015-10-6','%Y-%m-%d')
siteB_dc = decayCorrection(siteB, 10*365*24*3600,'2014-10-
6','2015-10-6','%Y-%m-%d')
```

The function returns an "*Inventory*" object, with the decay corrected FRN inventory. As a second feature, it is hypothesized that the FRN inventory of site A is a set of 10 replicated samples collected at the site. To consider the variability of the FRN inventories at the sampling site, a new "*Inventory*" object is created, which stores the cumulative FRN inventories measured at each replicate:

```
siteA_rep = c(72, 76, 74, 84, 85, 75, 83, 77, 81, 73)
siteA_var = createSamplingProfile(siteA_rep,30,'site1 (10
rep.)')
```

When a list of FRN values is provided to the *createSamplingProfile()* function, a warning message informs the user that the FRN values will be treated as repetitions belonging to the same layer that is unique in case of a sampling profile (Figure 6-8).

```
> siteA_var = createSamplingProfile(siteA_rep,30,'site A (10 rep.)')
Warning message:
In createSamplingProfile(siteA_rep, 30, "site A (10 rep.)") :
  List of FRN is provided, they will be used as belonging to the same
layer!
>
```

Figure 6-8: Example of the warning message which informs the user that when a list of FRN values are indicated as FRN inventories of a sampling site (through the function createSamplingProfile), they will be treated as belonging to the same sampling profile

The information about the variability of the FRN inventories at the site can also be visualized through the function *plot()* (Figure 6-9): the average FRN value is identified by the grey bar while two whiskers identify the limit defined adding or subtracting the standard deviation.

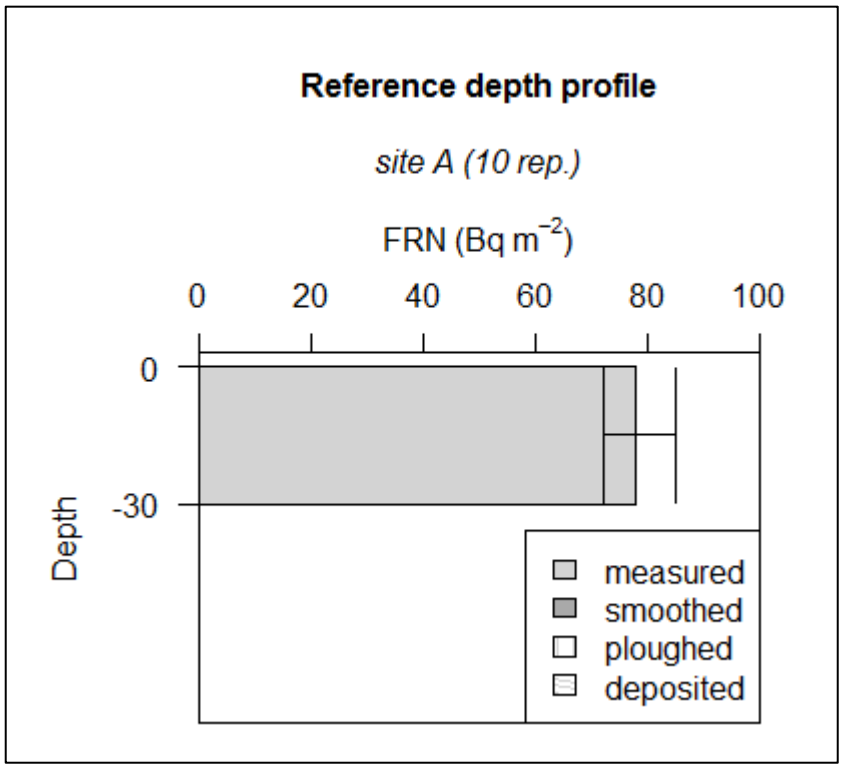

Figure 6-9: Variability of FRN inventory measured at site A (n=10).

At this point the MODERN returns multiple solutions, stored in the "*MODERN*" object, obtained by typing the command lines:

```
MODERN_siteA_mul = MODERN(RDP.smooth,siteA_var)
```

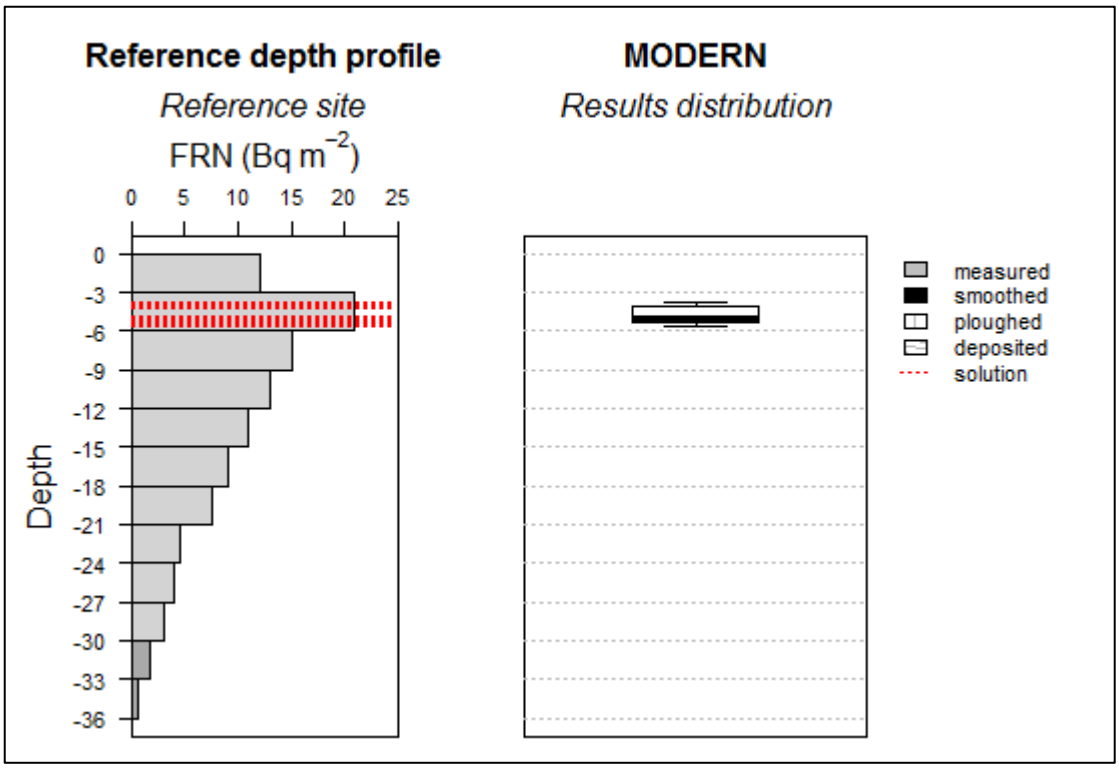

Figure 6-10: The graphical representation of the range of MODERN results obtained by comparing the reference depth profile RDF and the 10 replicated samples at site A.

```
> print(MODERN_siteA_var,digits = 3)
MODERN simulation results
   FRN1  FRN2  FRN3  FRN4 FRN5  FRN6  FRN7  FRN8  FRN9 FRN10
1    NA    NA    NA    NA   NA    NA    NA    NA    NA    NA
2 -5.62 -5.03 -5.32 -3.85 -3.7 -5.17 -3.99 -4.88 -4.29 -5.47
3    NA    NA    NA    NA   NA    NA    NA    NA    NA    NA
4    NA    NA    NA    NA   NA    NA    NA    NA    NA    NA
5    NA    NA    NA    NA   NA    NA    NA    NA    NA    NA

Intermediate results are accessible through these slots:
refProfile; sampProfile; cumG; h; d; FRNtarget; Sfunction; solution
Warning message:
In print.MODERN(MODERN_siteA_var, digits = 3) :
  Cannot calculate erosion rate(s) because one or more parameters of
sampling profile is NA
>
```

Figure 6-11: The MODERN results of the comparison between the reference depth profile RDF and the sampling site A where 10 replicated samples were collected.

Again, the solutions can be visualized by the functions *plot()* and *print()* (Figure 6-10 and 6-11). In particular the function *print()* returns all the possible solutions of the combination reference profile (one in this case) and sampling profile (with multiple FRN values). Each column corresponds to each FRN value in the *siteA_rep* variable.

At this stage, the user can still convert the results, expresses as length of soil lost or gained, into soil erosion and deposition rates (t yr^{-1} ha^{-1}) using the function *yearlyEDrates()*. Considering a mass depth of the soil samples of 100 kg m^{-2} and that

the sampling year and the main fallout year are 2000 and 1963 respectively, the erosion/deposition rates (*EDRates*) will be calculate as follows (note the use of *GetLayerThickness()* function to obtain the average sampling depth):

```
EDRates = yearlyEDRates(MODERN_siteA_var, massDepth = 100,
sampleDepth = GetLayerThickness(siteA_var), samplingTime =
'2000', falloutTime = '1963', timeFormat = '%Y')
```

The new package *modeRn* also allows considering the variability at reference sites. Let's hypothesize that at the reference site, three different soil samples have been collected and measured separately, and a variability of 20% among the inventories of three replicates was found. Then, using the standard function available from R, the resulting depth profile would be defined by a matrix of 3 columns (one for each replicate) and 11 rows (one for each depth increment), as follows:

```
FRN = c(12, 21, 15, 13, 11, 9, 7.5, 4.5, 4, 3, 2.5)
FRN = c(0.8*FRN,FRN,1.2*FRN)
FRN= matrix(FRN, nrow = 11)
```

The new matrix is passed as FRN argument in the *createReferenceProfile()* function:

```
myRDP_var = createReferenceProfile(FRN,3, name = 'Reference Site
1')
```

Then, as before, the function *plot()* would return a depth profile showing the appropriate error bars (Figure 6-12).

Running the function *MODERN()* between the reference depth profile created in the last step (*myRDP_var*) and the sampling "site A", the package would return the output of Figure 6-13. In this last case, MODERN() found a solution only for the case where the reference depth profile has the lowest FRN inventory (80% of *RDP*), while all other cases returns no solutions.

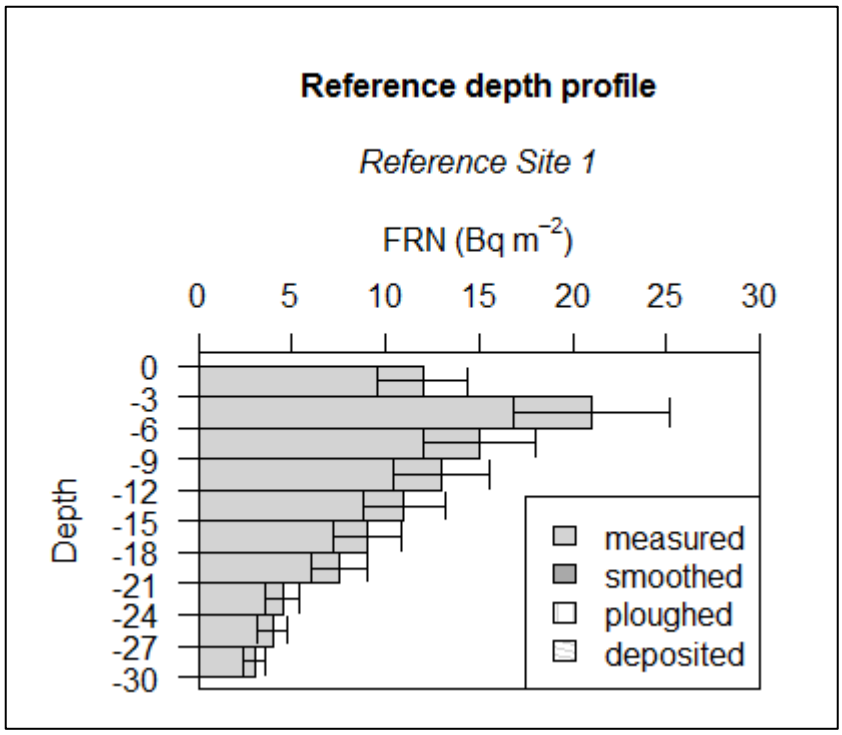

Figure 6-12: Example of FRN reference profile plot with multiple replicates provided for each layer.

```
> MODERN_myRDP_var_siteA = MODERN(myRDP_var, siteA)
Warning messages:
1: In MODERN(myRDP_var, siteA) :
  Reference time <refTime> of the reference profile is NA
2: In MODERN(myRDP_var, siteA) :
  Reference time <refTime> of the sampling profile is NA
> print(MODERN_myRDP_var_siteA, digits = 3)
MODERN simulation results in length unit:
    FRN1 FRN2 FRN3
1     NA   NA   NA
2 -0.789   NA   NA
3     NA   NA   NA

Intermediate results are accessible through these slots:
refProfile; sampProfile; cumG; h; d; FRNtarget; Sfunction; solution
Warning message:
In print.MODERN(MODERN_myRDP_var_siteA, digits = 3) :
  Cannot calculate erosion rate(s) because one or more parameters of
the sampling profile is NA
>
```

Figure 6-13: Output from the MODERN() function if a multiple reference profiles are used.

6.10 Summary and conclusions

This paper presents the R package *modeRn* for the estimation of erosion and deposition rates from t FRN inventories at reference and sampling sites. The package architecture permits to easily implement and manage FRN inventories in a flexible object class, able to consider the variability of FRN values at each site. Convenient functions are available for simulating different adaptations of the FRN depth profile.

Specific plotting and printing functions return the results in a user-friendly way. This package will increase the ability to investigate the impact of the uncertainty in the FRN inventories estimation via the use of statistics tools available in the R platform.

Acknowledgements

This work was partly funded by the Swiss National Science Foundation (SNF), project no. 200021-146018.

CHAPTER 7: FINAL REMARKS AND OUTLOOK

7.1 Conclusions

The use of artificial FRN as soil erosion tracers has a great potential in terms of providing qualitative and quantitative estimates of soil degradation processes affecting the alpine environment. Soil erosion rates based on FRN can serve as a basis for the validation of up-scaled modelling techniques and the implementation of soil protection practices. However, to ensure the validity of the outputs, great attention should be focused on the correct application of the FRN method. In this thesis, the principal critical points of the application of FRN as soil erosion tracers in the Alps have been extensively discussed. During the PhD, two main tools have been developed and tested with the aim to promote a wider application of FRN in the assessment of soil erosion/sedimentation in the Alps.

Specifically, the decision support tool CheSS (presented in Chapter 2) facilitates the understanding of the applicability of the traditional (and resampling) FRN method by proving the suitability of the reference sites, focusing especially on the analysis of the small-scale variability of the ^{137}Cs distribution. If none or not enough reliable sites can be identified at a study area, the application of a repeated sampling approach should be preferred, in which the ^{137}Cs inventories measured at sampling sites in different times are compared, as tested in Chapter 3.

The second tool developed is the new conversion model MODERN, introduced in Chapter 4. MODERN is a versatile model that enables the quantification of soil erosion under all land uses by simply comparing the depth profile of any FRN at an undisturbed site to the total inventory of a disturbed one. Due to its transparent concept, the model can easily be applied and adapted to specific conditions. Moreover, it represents the most appropriate model to convert $^{239+240}$Pu inventories into soil redistribution rates, as demonstrated in Chapter 5. The new features developed into the R package *modern* (presented in Chapter 6) further enhance the usability and capacity of the original code. The PhD was mostly driven by two main research questions which will be discussed in the next sections.

7.2 Is ^{137}Cs a suitable tracer of soil erosion processes in the Alps?

Our results highlight a significant spatial variability in the ^{137}Cs distribution at our study areas and confirm the results of previous studies conducted in the Alps, both in the

same areas and in different ones (e.g. Alewell *et al.*, 2014, Chawla *et al.*, 2010, Schaub *et al.*, 2010, Zollinger *et al.*, 2015). Such spatial variability is associated with the fact that the Alps were considerably affected by the Chernobyl fallout. Due to different snow cover and snow melting patterns, sites within the same area have received a significantly different deposition of ^{137}Cs. As a consequence, the comparison of the ^{137}Cs inventory between sites located in close proximity may be biased. Such spatial variability particularly prejudices the applicability of the traditional approach because of the difficulties associated with the selection of representative reference sites. To this end, the CheSS decision support tool allows checking the suitability of the reference sites for soil erosion assessment. By resampling the same sites after a certain time window and paying special attention to the analysis of the ^{137}Cs distribution at the sites, the validation (or invalidation) of the sites can be confirmed. The application of CheSS in the Urseren valley indicates no suitable reference sites in the valley, mostly due to the significant small-scale variability of the ^{137}Cs distribution.

The heterogeneous distribution of the ^{137}Cs fallout in the Alps might also compromise the application of the repeated sampling approach, in which the same sites are sampled in two different periods and their ^{137}Cs content is compared. Sampling sites are usually located along steep and unstable slopes, highly affected by soil degradation processes. Similarly to the reference sites, sampling sites may have experienced inhomogeneous Chernobyl fallout. It is therefore fundamental to carefully analyze the spatial variability of the ^{137}Cs distribution within the site. Indeed, a variation in the ^{137}Cs inventory between the two sampling years might be related to a different initial ^{137}Cs input and not to soil redistribution dynamics. Therefore, several replicates (between 10 and 20) should be collected at each sampling point and analyzed separately (Kirchner, 2013).

In the Piora Valley, previous findings have highlighted the difficulties in finding reliable reference sites (Alewell *et al.*, 2014). The only suitable area that has not been disturbed by grazing activities is located on a relatively small plateau. The analysis of ^{137}Cs inventories in the area show an incredibly high heterogeneity of ^{137}Cs distribution, which prohibits the application of the traditional approach in the valley. Consequently, we directly applied a ^{137}Cs repeated sampling approach (Chapter 3). The results indicate a large redistribution of soil by erosion and deposition processes, with yearly erosion and deposition rates of more than 30 t ha^{-1}. However, the results also show considerable small-scale variability at the sites, though still reflecting the typical heterogeneity measured at unploughed grasslands soils, as reported by Sutherland (1996).

The question that still remains open is: can ^{137}Cs be overall applied for soil erosion studies in the Alps? Based on our studies, we believe that the ^{137}Cs based soil studies at alpine areas are associated with a high risk of uncertainty, as demonstrated by the application of CheSS and the repeated sampling approach. Therefore, we

recommend the employment of another soil tracer, such as $^{239+240}$Pu. Different studies have already shown and confirmed the suitability of Pu isotopes as tracers and their applicability in mountain areas (Alewell *et al.*, 2014, Arata *et al.*, 2016b, Everett *et al.*, 2008, Hoo *et al.*, 2011, Lal *et al.*, 2013, Meusburger *et al.*, 2016, Schimmack *et al.*, 2002, Tims *et al.*, 2010, Zollinger *et al.*, 2014, Xu *et al.*, 2013, Xu *et al.*, 2015). The specific characteristics of $^{239+240}$Pu (i.e. the more homogeneous fallout distribution, the longer half-life, and the cost- and time-effective measurements) make the application of this tracer to the investigation of soil degradation in alpine grasslands more suitable than any other FRN (e.g. ^{137}Cs) (Alewell *et al.*, 2014). In our study areas, the small-scale variability of $^{239+240}$Pu at the reference sites is considerably lower in comparison to ^{137}Cs. Thus, the application of the traditional approach can be securely performed, and long-term erosion rates can be derived. Moreover, $^{239+240}$Pu can also be applied in the resampling and the repeated sampling approach, in order to obtain information about short-term erosion dynamics.

7.3 How can $^{239+240}$Pu inventories be properly converted into erosion and deposition rates?

If $^{239+240}$Pu is to be preferred to ^{137}Cs, great attention should be directed towards the selection of a proper conversion model. As demonstrated in Chapter 5, the behavior of plutonium in the soil is different to that of caesium. Most commonly used models do not carefully describe the depth distribution of $^{239+240}$Pu, which might lead to a misinterpretation of the results (Arata *et al.*, 2016b). Therefore, one of the principal aims of this PhD has been the development of a new conversion tool to derive soil redistribution rates from $^{239+240}$Pu inventories. The result is the MODERN model (Chapter 4), which enables the conversion of any FRN at all land use conditions. The simple concept behind the MODERN model allows its use at any specific case conditions.

MODERN does not make any assumptions about the depth profile of the FRN, but accurately describes the soil profile shape of any selected FRN at reference sites. Moreover, to better estimate soil redistribution rates, it allows the adaptation of the depth profile to simulate the behavior of the selected FRN under different agro-environmental conditions (e.g. ploughing activities, erosion, and sedimentation processes). An arbitrary number of layers can be simulated above and below the measured depth profile, and a range of possible solutions is produced.

The adaptability and performance of MODERN in converting different FRN inventories was compared to the results of two previously published case studies, namely a ^{137}Cs study in an alpine and unploughed area in the Aosta valley (Italy), and a $^{210}Pb_{ex}$ study in a ploughed area located in the Transylvanian Plain (Romania). The tests highlight a highly significant correspondence between the results of MODERN and the published results of other models currently used by the FRN

scientific community (Chapter 4). In addition, the MODERN model is based on a unique algorithm that converts FRN inventories into both erosion and deposition rates, whereas common conversion models (e.g. the Profile Distribution Model, the Diffusion and Migration Model (Walling and Quine, 1990, Walling and He 1997, Walling *et al.*, 2002, 2011, 2014) are specifically developed to quantify the rates of only one redistribution process (i.e. erosion or deposition).

Furthermore, an initial application of MODERN was performed on a $^{239+240}$Pu dataset collected in a study area in the Swiss Alps (the Urseren valley, canton Uri) (Chapter 5). Due to its characteristics, MODERN enables the representation of the precise depth profile of $^{239+240}$Pu in the soil and to consider its often observed polynomial depth distribution. Sedimentation processes typical of alpine slopes were also taken into account, and the depth profile was adapted trough the simulation of deposition layers. The results show the potential of MODERN to be the best option to convert $^{239+240}$Pu into soil redistribution rates, due to its ability to better describe the behaviour of Pu isotopes in the soil and to provide both soil erosion and deposition rates (Arata *et al.*, 2016b).

MODERN was originally developed in the Matlab™ environment, but the forthcoming release of the code in open source programming codes (i.e. R) is planned (Chapter 6). The code is transparent and easily adaptable, and is freely and publicly available on the website of our research group (see modern.umweltgeo.unibas.ch). MODERN was developed for the traditional FRN approach, in which a reference depth profile is compared to the total inventory of a sampling site. Our efforts are now directed towards adapting the previously described MODERN model code, in order to derive short-term erosion rates using the repeated sampling approach. For this aim, information about the FRN depth distribution at the sampling site should be collected and used as a reference depth profile for the comparison with the total inventories measured at the same site in different times.

7.4 Suggestions for further research

The next steps for improving soil erosion assessment at alpine grasslands through FRN include two main aspects. First, there is a need to investigate the relationship between the FRN distribution at alpine sites and different environmental factors on a larger scale (e.g. the altitude, the land cover, etc.), in order to obtain a wide-ranging overview of distribution patterns and of soil erosion estimates. So far, a big limitation of the FRN method is related to small-scale point measurements with rather time consuming and costly measurements of FRN activity in the soil. ^{137}Cs measurements are mostly conducted in a laboratory with Germanium Lithium (Ge-Li) Detectors, and the measurement time per soil sample ranges between 4 and 10 hours. $^{239+240}$Pu measurements can be performed by ICP-MS, thus drastically reducing the analysis cost and the required time (on the basis of our experience, more than 100 samples can be measured in less than a week). However, the FRN method is limited in terms

of spatial range, as it refers to single points. Upscaling its output might involve a high level of uncertainties.

A possible way to overcome this limitation is to employ airborne gamma detectors. Airborne surveys permit a rapid assessment of radiation levels of large areas. In inaccessible regions, such as alpine slopes, surveys with complete areal coverage are only possible from the air. Because of the larger ground clearance and the higher speed, the coverage per unit time of an airborne system is about 2,500 times greater than that of the equivalent ground system (Schwarz *et al.*, 1995). Although the costs for the measuring instruments and the flights are relatively high, the resulting cost per surveyed area is clearly lower than that of the comparable terrestrial survey (Schwarz *et al.*, 1995).

To this end, a new research collaboration has been initiated between our research group and the Swiss Federal Nuclear Safety Inspectorate (ENSI). On June 11th, 2015 an airborne survey was conducted over two study areas in the Central Swiss Alps: the Urseren valley (Canton Uri), and the Piora valley (Canton Ticino). A helicopter equipped with a NaI gamma detector, provided thanks to the support of ENSI, flew over the two study areas and screened the ^{137}Cs activity of the surface soil. The aims of the survey were: (i) to investigate the spatial ^{137}Cs distribution in the two study areas; (ii) to identify potential and suitable reference areas with a homogeneous distribution of ^{137}Cs activity; and (iii) to analyze the relationship between the ^{137}Cs distribution and different environmental factors. The results will then be compared with the airborne measurements performed over the same areas in 1988, just 2 years after the Chernobyl power plant accident. This will be the first attempt of this nature in sites where ^{137}Cs mostly originated from Chernobyl releases.

As a second possibility for further research, FRN-based soil redistribution rates should be used to validate the outputs of regional and large-scale soil erosion models, such as, for example, the Revised Universal Soil Loss Equation (RUSLE) by Wischmeier & Smith (1978). Different efforts have already started to adapt the model parameters to the typical topographic and climatic conditions of the alpine areas (e.g. Meusburger *et al.*, 2012, Schmidt *et al.*, 2016). In this sense, the results of this thesis will allow the verification of the outputs of the models, identifying the areas with a high soil erosion risk and addressing soil loss mitigation measures.

ACKNOWLEDGEMENTS

I would like to express my sincere gratitude to all the people who supported me during my PhD:

- I especially want to thank Prof. Dr. Chrisine Alewell for her scientific competency and her leadership skills. Her personal encouragement, her trust in me and her understanding allowed me to go through all the challenges and hard times which came up during the last years, and helped me reaching the end of my PhD.

- I greatly enjoyed the supervision of Dr. Katrin Meusburger, who patiently guided me during the whole project. I highly appreciated that she was always available to answer questions and to provide clear and helpful feedback. Her inspiring example motivated me to keep working and to combine my family and working life.

- I would like to address a particular Thank to Dr. Lionel Mabit, whose scientific support has strengthened and enabled the success of this PhD. I also appreciated his kind availability, his very welcomed and rapid feedbacks and his warm supervision.

- All co-authors are kindly acknowledged for their help in measurements, modeling of data and manuscript preparation, and especially I would like to thank Dr. Markus Zehringer and Prof. Mike Ketterer.

- I want to thank the whole Group of Environmental Geosciences which made the past three years an enjoyable and full time: PhD students, Postdocs, colleagues and HiWi students with whom I shared nice and hard times, travels and field trips, adventures, memorable and funny moments, inspiring discussions, coffee breaks and tasty lunch seminars.

- A special thank also to the UniBasel Antelopees 2016 and the Antelope organizers with whom I shared a great time in the last year of my PhD!

- I want to thank my special friend Chiara who always believed in me.

- Last, but definitely not least, this thesis is dedicated to Silvano, to Bianca, to Bruno and also to the highly awaited baby, who motivate me to be a successful woman and to never give up my professional career!

BIBLIOGRAPHY

Alewell, C., Egli, M., & Meusburger, K. 2015. An attempt to estimate tolerable soil erosion rates by matching soil formation with denudation in Alpine grasslands. Journal of Soils and Sediments, 15(6), 1383-1399.

Alewell, C., Meusburger, K., Brodbeck, M., Banninger, D. (2008). Methods to describe and predict soil erosion in mountain regions. Landscape and Urban Planning, 88(2-4), 46-53.

Alewell, C., Meusburger, K., Juretzko, G., Mabit, L., & Ketterer, M. E. (2014). Suitability of 239+ 240 Pu and 137 Cs as tracers for soil erosion assessment in mountain grasslands. Chemosphere, 103, 274-280.

Alewell, C., Schaub, M., Conen, F. 2009. A method to detect soil carbon degradation during soil erosion. Biogeosciences, 6, 2541-2547.

Arata, L., Meusburger, K., Frenkel, E., A'Campo-Neuen, A., Iuran, A.R., Ketterer, M.E., Mabit, L., Alewell, C., 2016a. Modelling Deposition and Erosion rates with RadioNuclides (MODERN) - Part 1: a new conversion model to derive soil redistribution rates from inventories of fallout radionuclides. *Journal of environmental radioactivity*, *162*, 45-55.

Arata, L., Meusburger, K., Frenkel, E., A'Campo-Neuen, A., Iuran, A.R., Ketterer, M.E., Mabit, L., Alewell, C., 2016b. Modelling Deposition and Erosion rates with RadioNuclides (MODERN) - Part 2: A comparison of different models to convert $^{239+240}$Pu inventories into soil redistribution rates at unploughed sites. *Journal of environmental radioactivity*, *162*, 97-106.

Bätzing, W., & Dickhörner, Y., 2003. Die Typisierung der Alpengemeinden nach" Entwicklungsverlaufsklassen" für den Zeitraum 1870-1990. *Mitteilungen der Fränkischen Geographischen Gesellschaft*, *48*(1), 273-305.

Beniston, M. 2003. Climatic change in mountain regions: a review of possible impacts. In *Climate variability and change in high elevation regions: Past, present & future* (pp. 5-31). Springer Netherlands.

Beniston, M. 2012. Impacts of climatic change on water and associated economic activities in the Swiss Alps. *Journal of Hydrology*, *412*, 291-296.

Bennett, G. L., Molnar, P., Eisenbeiss, H., & McArdell, B. W., 2012. Erosional power in the Swiss Alps: characterization of slope failure in the Illgraben. *Earth Surface Processes and Landforms*, *37*(15), 1627-1640.

Bossew, P., Kirchner, G., 2004. Modelling the vertical distribution of radionuclides in soil. Part 1: the convection dispersion equation revisited. *Journal of Environmental Radioactivity*, 73, 127–150.

Brazier, R., 2004. Quantifying soil erosion by water in the UK: a review of monitoring and modelling approaches. Prog. Phys. Geogr. 28, 340–365.

Bronstert, A., Niehoff, D., & Bürger, G., 2002. Effects of climate and land-use change on storm runoff generation: present knowledge and modelling capabilities. *Hydrological Processes*, *16*(2), 509-529.

Brunetti, M., Lentini, G., Maugeri, M., Nanni, T., Auer, I., Boehm, R., & Schoener, W. (2009). Climate variability and change in the Greater Alpine Region over the last two centuries based on multi-variable analysis. *International Journal of Climatology*, *29*(15), 2197-2225.

BIBLIOGRAPHY

Ceaglio, E., Meusburger, K., Freppaz, M., Zanini, E., Alewell, C., 2012. Estimation of soil redistribution rates due to snow cover related processes in a mountainous area (Valle d'Aosta, NW Italy). *Hydrology and Earth System Sciences*, *16*(2), 517-528.

Chambers, J., 2008. Software for data analysis: programming with R. Springer Science & Business Media.

Chawla, F., Steinmann, P., Pfeifer, H.R., Froidevaux, P., 2010. Atmospheric deposition and migration of artificial radionuclides in Alpine soils (Val Piora, Switzerland) compared to the distribution of selected major and trace elements. *Science of the Total Environment*, 408(16), 3292–3302.

Christensen, J. H., & Christensen, O. B., 2003. Climate modelling: severe summertime flooding in Europe. *Nature*, *421*(6925), 805-806.

Christensen, O. B., & Christensen, J. H., 2004. Intensification of extreme European summer precipitation in a warmer climate. *Global and Planetary Change*, *44*(1), 107-117.

Jong, E. D., & Kachanoski, R. G., 1988. The importance of erosion in the carbon balance of prairie soils. *Canadian Journal of Soil Science*, *68*(1), 111-119.

Descroix, L., & Mathys, N., 2003. Processes, spatio-temporal factors and measurements of current erosion in the French southern Alps: a review. *Earth Surface Processes and Landforms*, *28*(9), 993-1011.

Eikenberg, J., Bajo, S., Hitz, J., Wyer, L., 2001. Environmental radionuclide analyses around nuclear installations in Northern Switzerland. In: *Proc. 47th Annual Radiochemical Measurement Conf. Honolulu*, HI, November 4–8.

Everett, S. E., Tims, S.G., Hancock, G.J., Bartley, R., Fifield, L.K., 2008. Comparison of Pu and 137Cs as tracers of soil and sediment transport in a terrestrial environment. *Journal of Environmental Radioactivity*, 99, 383–393.

Facchinelli, A., Magnoni, M., Gallini, L., Bonifacio, E., 2002. 137Cs contamination from Chernobyl of soils in Piemonte (North-West Italy): spatial distribution and deposition model. *Water, Air, and Soil Pollution*, *134*(1-4), 339-350.

FAO. 2015. Understanding Mountain Soils: A contribution from mountain areas to the International Year of Soils 2015 , by Romeo, R., Vita, A., Manuelli, S., Zanini, E., Freppaz, M. & Stanchi, S. Rome, Italy.

Filippa, G., Cremonese, E., Migliavacca, M., Galvagno, M., Forkel, M., Wingate, L., Tomelleri, E., Morra di Cella, U., Richardson, A.D., 2016. Phenopix: A R package for image-based vegetation phenology. Agric. For. Meteorol. 220, 141–150.

Fornes, W. L., Whiting, P. J., Wilson, C. G., & Matisoff, G., 2005. Caesium-137-derived erosion rates in an agricultural setting: the effects of model assumptions and management practices. *Earth Surface Processes and Landforms*, *30*(9), 1181-1189.

Frankenberg, P., Geier, B., Proswitz, E., Schütz, J., & Seeling, S., 1995. Untersuchungen zu Bodenerosion und Massenbewegungen im Gunzesrieder Tal/Oberallgäu. *Forstwissenschaftliches Centralblatt vereinigt mit Tharandter forstliches Jahrbuch*, *114*(1), 214-231.

Fuhrer, J., Beniston, M., Fischlin, A., Frei, C., Goyette, S., Jasper, K., & Pfister, C., 2006. Climate risks and their impact on agriculture and forests in Switzerland. In *Climate Variability, Predictability and Climate Risks* (pp. 79-102). Springer Netherlands.

Garcia-Ruiz, J.M., Lasanta, T., Ruiz-Flano, P., Ortigosa, L., White, S., Gonzalez, C., Marti, C., 1996. Land-use changes and sustainable development in mountain areas: a case study in the Spanish Pyrenees. Landscape Ecol., 11, 267-277.

Gentleman, R., 2008. R programming for bioinformatics. CRC Press.

Guo, D., Westra, S., Maier, H.R., 2016. An R package for modelling actual, potential and reference evapotranspiration. Environ. Model. Softw. 78, 216–224.

He, Q., Walling, D. E., 1996. Interpreting particle size effects in the adsorption of ^{137}Cs and unsupported ^{210}Pb by mineral soils and sediments. *Journal of Environmental Radioactivity*, *30*(2), 117-137.

Herman, F., Seward, D., Valla, P. G., Carter, A., Kohn, B., Willett, S. D., & Ehlers, T. A., 2013. Worldwide acceleration of mountain erosion under a cooling climate. *Nature*, *504*(7480), 423-426.

Hinojosa, L., Napoléone, C., Moulery, M., & Lambin, E. F. 2016. The "mountain effect" in the abandonment of grasslands: Insights from the French Southern Alps. *Agriculture, Ecosystems & Environment*, *221*, 115-124.

Hoo, W. T., Fifield, L.K., Tims, S.G., Fujioka, T., Mueller, N., 2011. Using fallout plutonium as a probe for erosion assessment. Journal of environmental radioactivity, 102(10), 937–942.

IAEA (International Atomic Energy Agency), 2014. Guidelines for using Fallout radionuclides to assess erosion and effectiveness of soil conservation strategies. IAEA-TECDOC-1741. IAEA publication. Vienna, Austria. 213 p.

Inger, R., Jackson, A., Parnell, A., Bearhop, S., 2010. SIAR v4 (Stable Isotope Analysis in R): an ecologist's guide. Zostera.

Iurian, A. R., Mabit, L., Begy, R., Cosma, C., 2013. Comparative assessment of erosion and deposition rates on cultivated land in the Transylvanian plain of Romania using ^{137}Cs and $^{210}Pb_{ex}$. *Journal of Environmental Radioactivity*, *125*, 40-49.

Iurian, A. R., Mabit, L., Cosma, C., 2014. Uncertainty related to input parameters of ^{137}Cs soil redistribution model for undisturbed fields. *Journal of environmental radioactivity*, 136, 112-120.

Kachanoski, R. G., 1987. Comparison of measured soil 137-cesium losses and erosion rates. *Canadian Journal of Soil Science*, *67*(1), 199-203.

Kachanoski, R. G., 1993. Estimating soil loss from changes in soil cesium-137. *Canadian Journal of Soil Science*, *73*(4), 629-632.

Kachanoski, R. G., & De Jong, E., 1984. Predicting the temporal relationship between soil cesium-137 and erosion rate. *Journal of Environmental Quality*, *13*(2), 301-304.

Ketterer, M.E., Hafer, K.M., Jones, V.J., Appleby, P.G., 2004. Rapid dating of recent sediments in Loch Ness: ICPMS measurements of global fallout Pu. *Science of the Total Environment, 322*, 221–229.

Kirchner, G., 2013. Establishing reference inventories of 137 Cs for soil erosion studies: methodological aspects. Geoderma 211, 107–115.

Kirchner, G., Strebl, F., Bossew, P., Ehlken, S., Gerzabek, M.H., 2009. Vertical migration of radionuclides in undisturbed grassland soils. *Journal of Environmental Radioactivity, 100,* 716–720.

Kirtman, B., Power, S. B., Adedoyin, J. A., Boer, G. J., Bojariu, R., Camilloni, I., ... & Prather, M. (2013). Near-term climate change: projections and predictability. *Climate change*, 953-1028.

Knoll-Heitz, F., 1991. Piora: Konzept für die Erhaltung einer Landschaft. Herausgeber: WWF Sezione Svizzera Italiana. pp. 303.

BIBLIOGRAPHY

Konz, N., Schaub, M., Prasuhn, V., Baenninger, D., & Alewell, C., 2009. Cesium-137-based erosion-rate determination of a steep mountainous region. Journal of plant nutrition and soil science, 172(5), 615-622.

Konz, N., Prasuhn, V., Alewell, C., 2012. On the measurement of alpine soil erosion. *Catena*, *91*, 63-71.

Lal, R., 2003. Soil erosion and the global carbon budget. Environ. Int. 29, 437–450.

Lal, R., Tims, S.G., Fifield, L.K., Wasson, R.J., Howe, D., 2013. Applicability of ^{239}Pu as a tracer for soil erosion in the wet-dry tropics of northern Australia. *Nuclear Instruments and Methods in Physics Research Section B: Beam Interactions with Materials and Atoms*, *294*, 577–583.

Lasanta, T., Gonzaléz-Hildalgo J.C., Vicente-Serrano S.M., Sferi E., 2006. Using landscape ecology to evaluate an alternative management scenario in abandoned Mediterranean mountain areas. Landscape Urban Plan. 78, 110-114.

Leisch, F., 2008. Creating R Packages: A Tutorial.

Lettner, H., Bossew, P., Hubmer, A.K., 1999. Spatial variability of fallout Caesium-137 in Austrian alpine regions. J. Environ. Radioact. 47, 71–82.

Li, S., Lobb, D. A., Kachanoski, R. G., & McConkey, B. G., 2011. Comparing the use of the traditional and repeated-sampling-approach of the 137 Cs technique in soil erosion estimation. *Geoderma*, *160*(3), 324-335.

Loughran, R. J., & Balog, R. M., 2006. Re-sampling for Soil-caesium-137 to Assess Soil Losses after a 19-year Interval in a Hunter Valley Vineyard, New South Wales, Australia. *Geographical Research*, *44*(1), 77-86.

Loughran, R.J., Pennock, D.J., Walling, D.E., 2002. Spatial distribution of caesium-137, in: Handbook for the Assessment of Soil Erosion and Sedimentation Using Environmental Radionuclides. Springer, pp. 97–109.

Mabit, L., Benmansour, M., Walling, D. E., 2008. Comparative advantages and limitations of the fallout radionuclides ^{137}Cs, $^{210}Pb_{ex}$ and ^{7}Be for assessing soil erosion and sedimentation. *Journal of Environmental Radioactivity*, *99*(12), 1799-1807.

Mabit, L., Bernard, C., Wicherek, S., Laverdière, M.R., 1999. Les retombées de Tchernobyl, une réalité à prendre en compte lors de l'utilisation de la méthode du Césium-137. Paysages Agraires Environ. Principes Écologiques Gest. En Eur. Au Can. CNRS 285–292.

Mabit, L., Chhem-Kieth, S., Toloza, A., Vanwalleghem, T., Bernard, C., Amate, J.I., de Molina, M.G., Gómez, J.A., 2012. Radioisotopic and physicochemical background indicators to assess soil degradation affecting olive orchards in southern Spain. Agric. Ecosyst. Environ. 159, 70–80.

Mabit, L., Meusburger, K., Fulajtar, E., Alewell, C., 2013. The usefulness of ^{137}Cs as a tracer for soil erosion assessment: A critical reply to Parsons and Foster (2011). *Earth-Science Reviews*, 127, 300–307.

Mabit, L., Zapata, F., Dercon, G., Benmansour, M., Bernard, C., & Walling, D. E., 2014. Assessment of soil erosion and sedimentation: the role of fallout radionuclides. *IAEA TECDOC SERIES*, *3*.

MacDonald, D., Crabtree, J. R., Wiesinger, G., Dax, T., Stamou, N., Fleury, P., ... & Gibon, A., 2000. Agricultural abandonment in mountain areas of Europe: environmental consequences and policy response. *Journal of environmental management*, *59*(1), 47-69.

Mathys, N., Brochot, S., Meunier, M., & Richard, D., 2003. Erosion quantification in the small marly experimental catchments of Draix (Alpes de Haute Provence, France). Calibration of the ETC rainfall–runoff–erosion model. *Catena*, *50*(2), 527-548.

Matisoff, G., 2014. Pb-210 as a tracer of soil erosion, sediment source area identification and particle transport in the terrestrial environment. *Journal of Environmental Radioactivity*, 138, 343–354.

Meusburger, K., Alewell, C., 2008. Impacts of anthropogenic and environmental factors on the occurrence of shallow landslides in an alpine catchment (Urseren Valley, Switzerland). *Natural Hazards and Earth System Science*, *8*(3), 509–520.

Meusburger K., Alewell C. 2014: Soil Erosion in the Alps. Experience gained from case studies (2006–2013). Federal Office for the Environment, Bern. Environmental studies no. 1408: 116 pp.

Meusburger, K., Leitinger, G., Mabit, L., Mueller, M.H., Walter, A., Alewell, C., 2014. Soil erosion by snow gliding–a first quantification attempt in a subalpine area in Switzerland. *Hydrology and Earth System Sciences*, *18*(9), 3763–3775.

Meusburger, K., Mabit, L., Park, J.H., Sandor, T., Alewell, C., 2013. Combined use of stable isotopes and fallout radionuclides as soil erosion indicators in a forested mountain site, South Korea. Biogeosciences 10, 5627–5638.

Meusburger, K., Mabit, L., Ketterer, M., Park, J. H., Sandor, T., Porto, P., & Alewell, C. 2016. A multi-radionuclide approach to evaluate the suitability of 239+ 240 Pu as soil erosion tracer. *Science of The Total Environment*, *566*, 1489-1499.

Meusburger, K., Steel, A., Panagos, P., Montanarella, L., & Alewell, C., 2012. Spatial and temporal variability of rainfall erosivity factor for Switzerland. *Hydrology and Earth System Sciences*, *16*(1), 167-177.

Morgan, R. P. C., 2009. *Soil erosion and conservation*. John Wiley & Sons.

Owens, P.N., Walling, D.E., 1996. Spatial variability of caesium-137 inventories at reference sites: an example from two contrasting sites in England and Zimbabwe. Appl. Radiat. Isot. 47, 699–707.

Palmer, M.A., Menninger, H.L., Bernhardt, E., 2010. River restoration, habitat heterogeneity and biodiversity: a failure of theory or practice? Freshw. Biol. 55, 205–222.

Parsons, A.J., Foster, I.D., 2011. What can we learn about soil erosion from the use of 137 Cs? Earth-Sci. Rev. 108, 101–113.

Parsons, A. J., & Foster, I. D., 2013. The assumptions of science: A reply to Mabit *et al.*(2013). *Earth-Science Reviews*, *127*, 308-310.

Patric, J.H., 2002. Forest Erosion Rates.

Pennock, D.J., Appleby, P.G., 2002. Site selection and sampling design, in: Handbook for the Assessment of Soil Erosion and Sedimentation Using Environmental Radionuclides. Springer, pp. 15–40.

Parry, M. L. (Ed.). 2007. *Climate change 2007-impacts, adaptation and vulnerability: Working group II contribution to the fourth assessment report of the IPCC* (Vol. 4). Cambridge University Press.

Por□ba, G., Bluszcz, A., 2008. Influence of the parameters of models used to calculate soil erosion based on ^{137}Cs tracer. *Geochronometria*, *32*(1), 21–27.

Porto, P., Walling, D.E., Alewell, C., Callegari, G., Mabit, L., Mallimo, N., Meusburger, K., Zehringer, M., 2014. Use of a 137 Cs re-sampling technique to investigate temporal changes in soil erosion and sediment mobilisation for a small forested catchment in southern Italy. J. Environ. Radioact. 138, 137–148.

BIBLIOGRAPHY

Porto, P., Walling, D.E., Ferro, V., 2001. Validating the use of caesium-137 measurements to estimate soil erosion rates in a small drainage basin in Calabria, Southern Italy. *Journal of Hydrology*, *248*(1), 93-108.

Pourcelot, L., Louvat, D., Gauthier-Lafaye, F., & Stille, P. 2003. Formation of radioactivity enriched soils in mountain areas. *Journal of Environmental Radioactivity*, *68*(3), 215-233.

Ritchie, J.C., McHenry, J.R., 1990. Application of radioactive fallout cesium-137 for measuring soil erosion and sediment accumulation rates and patterns: a review. *Journal of Environmental Quality 19*, 215–233.

Ritchie, J. C., Ritchie, C. A., 2001. Bibliography of publications of Cesium-137 studies related to erosion and sediment deposition. USDA-ARS Hydrology and Remote Sensing Laboratory.

Robert, C., Casella, G., 2010. Introducing Monte Carlo Methods with R. Springer New York, New York, NY.

Schaub, M., Alewell, C., 2009. Stable carbon isotopes as an indicator for soil degradation in an alpine environment (Urseren Valley, Switzerland). Rapid Commun. Mass Spectrom. 23, 1499–1507.

Schaub, M., Konz, N., Meusburger, K., Alewell, C., 2010. Application of in-situ measurement to determine Cs-137 in the Swiss Alps. *Journal of Environmental Radioactivity*, 101, 369–376.

Schimmack, W., Auerswald, K., & Bunzl, K. 2002. Estimation of soil erosion and deposition rates at an agricultural site in Bavaria, Germany, as derived from fallout radiocesium and plutonium as tracers. *Naturwissenschaften*, *89*(1), 43-46.

Schmidli, J., & Frei, C. 2005. Trends of heavy precipitation and wet and dry spells in Switzerland during the 20th century. *International Journal of Climatology*, *25*(6), 753-771.

Schmidt, S, Alewell C., Panagos P. & Meusburger K., 2016. Regionalization of monthly rainfall erosivity patterns in Switzerland. *Hydrology and Earth System Sciences,* 20, 4359–4373.

Schwarz, G. F., Rybach, L., & Klingele, E. E. 1995. Data processing and mapping in airborne radioactivity surveys. Application of uranium exploration data and techniques in environmental studies, IAEA-TECDOC-827, IAEA, Vienna, 61-70.

Stanchi, S., Freppaz, M., Godone, D., & Zanini, E. 2013. Assessing the susceptibility of alpine soils to erosion using soil physical and site indicators. *Soil Use and Management*, *29*(4), 586-596.

Stock, B.C., Semmens, B.X., 2013. MixSIAR GUI user manual, version 1.0. Access. Online Httpconserver Iugo-Cafe Orguserbrice SemmensMixSIAR.

Stoffel, M., & Huggel, C., 2012. Effects of climate change on mass movements in mountain environments. *Progress in Physical Geography*, *36*(3), 421-439.

Sutherland, R.A., 1991. Examination of caesium-137 areal activities in control (uneroded) locations. *Soil Technology*, *4*(1), 33–50.

Sutherland, R.A., 1996. Caesium-137 soil sampling and inventory variability in reference locations: A literature survey. Hydrol. Process. 10, 43–53.

Tiessen, K. H. D., Li, S., Lobb, D. A., Mehuys, G. R., Rees, H. W., & Chow, T. L., 2009. Using repeated measurements of 137Cs and modelling to identify spatial patterns of tillage and water erosion within potato production in Atlantic Canada. *Geoderma*, *153*(1), 104-118.

Tims, S.G., Everett, S.E., Fifield, L.K., Hancock, G.J., Bartley, R., 2010. Plutonium as a tracer of soil and sediment movement in the Herbert River, Australia. *Nuclear Instruments and Methods in Physics Research Section B: Beam Interactions with Materials and Atoms*, *268*(7), 1150–1154.

Van Dijk, P. M., Auzet, A. V., & Lemmel, M., 2005. Rapid assessment of field erosion and sediment transport pathways in cultivated catchments after heavy rainfall events. *Earth Surface Processes and Landforms*, *30*(2), 169-182.

Van Pelt, R.S., Zobeck, T.M., Ritchie, J.C., Gill, T.E., 2007. Validating the use of ^{137}Cs measurements to estimate rates of soil redistribution by wind. *Catena*, *70*(3), 455–464.

Venables, W.N., Ripley, B.D., 2013. Modern applied statistics with S-PLUS. Springer Science & Business Media.

Vermeesch, P., Resentini, A., Garzanti, E., 2016a. An R package for statistical provenance analysis. Sediment. Geol. 336, 14–25.

Vrieling, A., 2006. Satellite remote sensing for water erosion assessment: A review. CATENA 65, 2–18.

Walling, D.E., He, Q., 1997. Models for converting ^{137}Cs measurements to estimates of soil redistribution rates on cultivated and uncultivated soils (including software for model implementation). *Report to IAEA, University of Exeter, UK*, 315–341.

Walling, D.E., He, Q., Appleby, P.G., 2002. Conversion models for use in soil-erosion, soil-redistribution and sedimentation investigations. In: Zapata, F. (Ed.) *Handbook for the assessment of soil erosion and sedimentation using environmental radionuclides*. Kluwer, Dordrecht. Netherlands. pp. 111–164.

Walling, D.E., Quine, T.A., 1990. Calibration of caesium-137 measurements to provide quantitative erosion rate data. *Land Degradation & Development*, *2*(3), 161–175.

Walling, D. E., & Quine, T. A., 1993. *Use of caesium-137 as a tracer of erosion and sedimentation: Handbook for the application of the caesium-137 technique. UK Overseas Development Administration research scheme R4579* (No. INIS-XA-N--179). Department of Geography.

Walling, D.E., Schuller, P., Zhang, Y., Iroumé, A., 2009. Extending the timescale for using beryllium 7 measurements to document soil redistribution by erosion: 7 Be MEASUREMENTS TO DOCUMENT SOIL REDISTRIBUTION. Water Resour. Res. 45, n/a-n/a.

Walling, D.E., Zhang, Y., He. Q., 2011. Models for deriving estimates of erosion and deposition rates from fallout radionuclide (caesium-137, excess lead-210, and beryllium-7) measurements and the development of user-friendly software for model implementation. In: Impact of soil conservation measures on erosion control and soil quality. IAEA-TECDOC-1665. International Atomic Energy Agency Publication. pp. 11–33.

Walling, D.E., Zhang, Y., He, Q., 2014. Conversion models and related software. In: Guidelines for using Fallout radionuclides to assess erosion and effectiveness of soil conservation strategies. IAEA-TECDOC-1741. International Atomic Energy Agency Publication. pp. 125–148.

Wildhaber, Y. S., Michel, C., Epting, J., Wildhaber, R. A., Huber, E., Huggenberger, P., Burkhardt-Holm, P & Alewell, C., 2014. Effects of river morphology, hydraulic gradients, and sediment deposition on water exchange and oxygen dynamics in salmonid redds. *Science of the Total Environment*, *470*, 488-500.

Wischmeier, W. H., & Smith, D. D., 1978. Predicting rainfall erosion losses-A guide to conservation planning. *Predicting rainfall erosion losses-A guide to conservation planning*.

Xu, Y., Qiao, J., Hou, X., Pan, S., 2013. Plutonium in soils from northeast China and its potential application for evaluation of soil erosion. *Scientific reports*, 3.

Xu, Y., Qiao, J., Pan, S., Hou, X., Roos, P., Cao, L., 2015. Plutonium as a tracer for soil erosion assessment in northeast China. *Science of the Total Environment*, 511, 176–185.

Zapata, F. (Ed.), 2002. Handbook for the assessment of soil erosion and sedimentation using environmental radionuclides (Vol. 219). Dordrecht: Kluwer Academic Publishers.

Zollinger, B., Alewell, C., Kneisel, C., Meusburger, K., Brandová, D., Kubik, P., Schaller M., Ketterer M., Egli, M., 2014. The effect of permafrost on time-split soil erosion using radionuclides (^{137}Cs, $^{239+240}$Pu, meteoric ^{10}Be) and stable isotopes (^{13}C) in the eastern Swiss Alps. *Journal of Soils and Sediments*, 15(6), 1400–1419.